ADVANCES IN ARCHAEOLOGICAL GEOPHYSICS: CASE STUDIES FROM HISTORICAL ARCHAEOLOGY

A Dissertation

by

TIMOTHY SCOTT DESMET

Submitted to the Office of Graduate and Professional Studies of
Texas A&M University
in partial fulfillment of the requirements for the degree of

DOCTOR OF PHILOSOPHY

Chair of Committee,	D. Bruce Dickson
Committee Members,	Suzanne L. Eckert
	Mark E. Everett
	Robert R. Warden
	Michael R. Waters
Head of Department,	Cynthia Werner

August 2016

Major Subject: Anthropology

ABSTRACT

This dissertation presents advanced methods in data processing, statistical analyses, integration, and visualization of archaeogeophysical data to increase the accuracy of archaeological remote sensing interpretation and predictions. Three case studies are presented from an experimental controlled archaeological test site and two nineteenth century historic military archaeology sites at Paint Rock, Texas and Alcatraz Island, California. I demonstrate the ability of the Geonics EM-63 time-domain electromagnetic-induction metal detector to detect and localize historical metal artifacts at an experimental site and Paint Rock. Moreover, point pattern analysis spatial autocorrelation statistics were used to detect statistically significant patterns that spatially compacted the amplitude response of the data to improve the localization of artifacts of archaeological significance. The archaeological data was used to determine the spatial and temporal extent of the military camp at Paint Rock and conforms well with the historic record. A virtual ground-truthing was conducted at Alcatraz Island, where the results of a quantitative attribute analysis of ground-penetrating radar data was tested against the georectification of historic maps in order to determine the location, extent, and integrity of historic military features without excavation. These studies increased the information content of archaeogeophysical data via feedback with statistics, quantitative attributes, controlled experiments, excavation, and georectification modeling in order to increase the predictive capabilities of the methods to answer the most questions with the least amount of costly excavations.

DEDICATION

To my friends, family, and felix.

ACKNOWLEDGEMENTS

TABLE OF CONTENTS

LIST OF FIGURES

LIST OF TABLES

CHAPTER I

INTRODUCTION

Since the 1990s a series of advances in computing and electrical engineering have led to the production of less costly, less bulky, more sensitive and efficient geophysical data acquisition instruments and access to greater data processing power via smaller and faster personal computers (Conyers 2013; Gaffney2008; Linford 2006). By the twenty-first century (Figure 1) near surface geophysical techniques had gained widespread use and acceptance as yet another important methodological implement in the archaeologists toolkit (Agapiou and Lysandrou 2015). In a recent review of geophysical techniques in archaeology, Gaffney (2008) predicted that advancements in data analyses were likely to be significant research subjects in the next decade of archaeological geophysics (or archaeogeophysics). The following research illustrates various methods to increase the accuracy of archaeological remote sensing interpretation and prediction via advanced processing, integration, visualization, and statistical analysis.
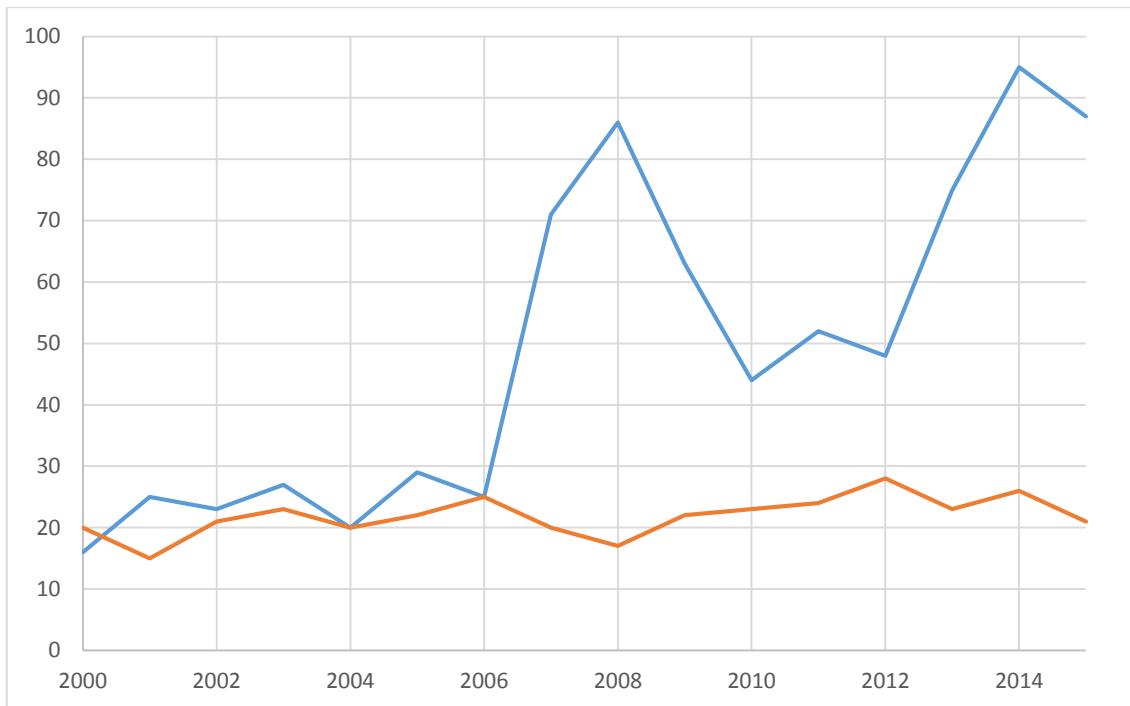
Figure 1. Archaeological geophysics papers in the flagship journal of archaeogeophysics *Archaeological Prospection* **(in red, n=350) and from numerous journals in a Science Direct search for "archaeology geophysics" (in blue, n=768) between 2000-2015. Note, the drop in papers during the Great Recession, which began in December 2007. Generally, however, the trend (r^2=0.7) of more archaeological geophysics research should continue in the decades to come.**

Advances in the integration of archaeogeophysics data generally takes two forms. In the first multiple geophysical methods are quantitatively or qualitatively integrated in an attempt to better interpret features of interest (Ernenwein 2008, 2099; Kvamme 2006a, 2007). In the second multiple data sets are presented in a single visual image to aid interpretation. This research expands upon the visualization of multiple geophysical data sets via the integration of ground-penetrating radar (GPR) and lidar data with 2D

and 3D historical models. Presenting the GPR past in the context of the 3D lidar point cloud present increases the interpretability of GPR data (Goodman and Piro 2013).

Advanced processing of GPR data via attribute analysis began in the geophysics research community in the 1990s as an offshoot of seismic attribute analysis processing methods. These advances are only possible due to the ability to digitally store data for subsequent processing with smaller, faster, less expensive personal computers (Conyers 2013). Attribute analysis methods quantify the GPR data signal to extract more information from the data, which relates to subsurface physical processes such as dielectric permitivity contrasts, permeability, stratigraphic interfaces and thickness (Zhao 2013a, 2013b). By the early 2010s the use of GPR attribute analysis methods spread to the archaeology research community (Böniger and Tronicke 2010a, b; Creasman et al. 2010; Khwanmuang and Udphuay 2012; Udphuay et al. 2014; Urban et al. 2014; Zhao et al. 2012, 2013a, 2013b, 2015a, 2015b). This research adds to a growing body of literature that seeks to increase the accuracy of archaeological interpretation via advanced processing, which better visualize and quantify patterns related to subsurface physical properties.

The visual presentation of integrated data holds great potential for community outreach and the public dissemination of complex data in both an appealing and accurate way. Tax based funding often supports archaeogeophysical research; however, public stakeholder do not always get to see the results of their investment. Rather, the results are often disseminated by scientist to scientists at professional conferences, in technical journals, and buried in the gray literature of compliance permit reports – all of which are

generally unintelligible and non-accessible to the public at large. Moreover, presenting the results and interpretation of geophysical research to the public is particularly difficult because GPR profiles look like a Rorschach test to those untrained in geology and geophysics. Therefore, the role of advanced data processing and visualization to aid interpretation for public education and outreach efforts cannot be under stressed; here the challenge is to explain the layout of archaeological artifacts and features with interpretive illustrations and geophysical data.

Statistical analyses of single or multiple methods archaeogeophysical surveys seeks to quantify significant patterns in data sets to reduce errors cause by unsystematic qualitative anomaly hunting. Interpretational errors are costly in terms of time and labor and therefore money, but also in terms of destructive excavations. Statistical analyses of archaeogeophysical data can reduce the time, labor, and monetary costs of research. Most importantly, however, increasing the confidence of interpretation and predictive capabilities of archaegeophysical data via statistical analyses holds the greatest potential for the advancement of preservation archaeology and the stewardship of the archaeological record.

Despite the recent advances in archaeological geophysics (Gaffney 2008; Linford 2006), great skepticism of the methods abounds (Jordan 2009), particularly in the United States where the application of geophysics in archaeology lags behind Europe (Johnson 2006; Thompson 2015). Remote sensing is often assumed to be highly quantitative because the methods are based in the 'hard' science; however, the interpretation of these data is often no more than qualitative X marks the spot 'anomaly' hunting (Conyers 2013;

Gaffney 2008; Jordan 2009), a situation that can lead to erroneous interpretations and a lack of confidence in the discipline. This research proposes to increase the reliability of archaeological geophysics interpretations in three key ways: (1) through the use of control experimental sites and georectification of historic maps at historical archaeology sites to create middle-range analogies to test cultural and natural processes; via (2) the application of rigorous quantitative analysis of geophysical data through geostatistics and various mathematical data filtering methods (attribute analysis); and via (3) ground-truthing excavations, which provides feedback to iteratively improve predictions.

These goals were accomplished by examining three case study sites: (1) the experimental controlled historical archeology test site in College Station, Texas; (2) the Paint Rock, Texas, battlefield and historical military camp sites (41CC1, 290, 295); and (3) the historic fortifications on Alcatraz Island, California.

In Chapter II results are presented from the Tran experimental control archaeology site where I conducted time-domain electromagnetic induction (EMI) surveys with the Geonics EM-63 before and after emplacing replica historical artifacts. The spatial structure of the EMI data was assessed with global and local point-pattern analysis (PPA) autocorrelation statistics, namely the global K-function and local Getis-Ord $G_i^*(d)$ statistics. Results suggest that the Geonics EM-63 can be used to locate historical metal artifacts and that the PPA statistics can determine significant clustering of artifacts while also compacting the spatial footprint of the EMI amplitude response.

I then tested the real world application of EMI and PPA at the Paint Rock historical archaeological battlefield and camp site discussed in Chapter III. In order to

better understand the landscape scale turnover in artifact assemblages during the mid-nineteenth century at historical military archaeology sites the theoretical perspective of 'eventful sociology' (Sewell 2005:100) was employed. Eventful sociology was operationalized for archaeology by Beck and colleagues (2007) and utilizes both structuration (Giddens 1984; Sewell 1992) and practice/agency theory (Bourdieu 1977, 1984). Results suggest that the military presence at the site dates to the 1850s to 1870s and extends between the springs and first terrace on the north side of the Concho River. The results of the EMI and PPA statistics are applicable in a real world archaeological context.

In Chapter IV, I use geographical information systems (GIS) software to georectify historic maps to create testable hypotheses as to the possible location of historic military fortifications on Alcatraz Island, California. GPR data were used to physically test the georectification model, to virtually ground-truth (VGT) the site, without excavation. A quantitative attribute analysis of the GPR data was used to better determine the true location, extent, and integrity of subsurface archaeological remains from the late 1800s. Results suggest that the advanced processing techniques of migration and attribute analysis are able to detect the location, extent, and integrity of subsurface archaeological features that date to the military earthwork fortification period on the island.

As physical anomalies may not be represented materially, archaeological excavation is the only way to definitively asses and validate the interpretations of near-surface applied geophysics data (Hargrave 2006); however, excavations are inherently

destructive and permanently remove buried artifacts from their primary context. It is sometimes said that "archaeology is the only branch of anthropology where we kill our informants in the process of studying them" (Flannery 1982:275). Excavation is not only invasive and destructive, but it is also time consuming and labor intensive, and therefore expensive (Johnson and Haley 2006). Moreover, at many cultural heritage sites excavations may not be desirable or possible. An ideal archaeological investigation of the subsurface based mainly upon interpretations of remote sensing data would be accurate enough to require minimal excavations, answering the most anthropological research questions with limited excavations, thereby preserving as much of the valuable non-renewable *in situ* cultural resources as possible for future generations (Doelle and Huntley 2012). The potential of geophysical methods for preservation archaeology is the foundation for the future of the ethic of stewardship of the archaeological record, for we cannot protect our cultural resources if we do not know what they are and where they are located.

CHAPTER II

ELECTROMAGNETIC INDUCTION IN SUBSURFACE METAL TARGETS:

CLUSTER ANALYSIS USING LOCAL POINT-PATTERN SPATIAL STATISTICS*

Introduction

Clustering of subsurface metal targets is important in near-surface geophysical application areas such as unexploded ordnance (UXO) remediation, mineral exploration, environmental or geotechnical site assessment, and historical or industrial archaeology. The spatial distribution of metallic targets can reveal information about the natural or anthropogenic spatiotemporal processes which led to the emplacement of objects that are now of historical, cultural, environmental, economic, geotechnical, or archaeological significance. Electromagnetic geophysical measurements offer a powerful noninvasive probe of subsurface metal distribution. The data, carefully analyzed, can be used to test and discriminate hypotheses about the underlying site formation processes. Spatial cluster analysis is relevant to archaeological reconstructions or site assessments since artifacts that are associated with a past event such as a battle, or past industrial use such as a foundry or railyard, tend to be found in close proximity (Schwarz and Mount 2006). At brownfields sites scheduled for reclamation or re-

development, due to past land-use patterns there often develops clustering of targets of interest, such as underground pipes, drums, or storage tanks or the buried remnants of reinforced concrete foundations.

A wide variety of methods are available to discern patterns in spatial data (Perry et al. 2002), including self-organizing maps (Benavides et al. 2009), various clustering algorithms (Paasche and Eberle 2009, 2011), and numerous global and local point pattern analysis (PPA) techniques (Getis and Ord 1996). Global PPA of geophysical responses discriminated UXO from clutter at a practice bombing range in which the UXO was deposited according to known aircraft flight patterns while the clutter was randomly distributed (MacDonald and Small 2009).

Paasche and Eberle (2009, 2011) in the context of mineral exploration have recently discussed and utilized numerous clustering algorithms like k-means, fuzzy c-means, and the Gustafson-Kessel method. One major drawback of these techniques is that the number of clusters must be chosen prior to analysis, regardless of whether clustering is actually present in the data set. As such the usefulness of these clusters must be verified against external criteria. With local statistical measures of spatial autocorrelation, as used in this paper, no a priori assumptions are made about the number of clusters.

The preferred geophysical technique for detecting subsurface metal items is transient electromagnetic induction (EMI). The EMI data analyzed in this paper were collected with a Geonics EM-63 metal detector (www.geonics.com). The EM-63 records

a time-decaying voltage at the receiver (RX) coil after a sudden switch-off in the magnetic field generated by the transmitter (TX) coil. The RX voltage decay is due to the dissipation of eddy currents that are induced in the host geology along with any subsurface metal targets of sufficient inductance (Everett 2005) that are buried within several m of the surface. The RX voltage is digitized at 26 time gates, or channels, that are logarithmically spaced from $t_0=180$ μs to $t_1=25$ ms after TX switch-off.

The EM-63 normally detects targets whose characteristic size a, magnetic permeability μ, and electrical conductivity σ are such that the eddy-current diffusion time satisfies $\tau>t_0$ where $\tau\sim\mu\sigma a^2$ (Pasion 2007; Benavides et al. 2009). The shape of the RX voltage waveform is indicative of target characteristics. The amplitude of the early-time RX voltage response, for instance, reads higher than background geological noise levels for all detectable metal artifacts whether small or large, shallow or deeply-buried. The late-time RX voltage response remains high, however, only for the larger objects for which $\tau>>t_0$. An important diagnostic of such large objects, therefore, is the lengthy time that is required for the induced eddy currents, and hence the RX voltage, to decay to the instrument noise level. As the amplitude response is measured at 26 time gates, the initial response and shape of the decay curve could be used to roughly classify the depth, orientation, and size of specific anomalies.

In this paper we consider two features of the EM63 response: (*a*) the magnitude of the early-time RX voltage response [mV] (hereinafter called the *channel-1 response*); and (*b*) the time gate at which the RX voltage decays to the instrument noise level (hereinafter called the *decay time*). The channel-1 response reads high for all detectable

metal targets while a lengthy decay time can be used to preferentially select the larger ones.

Local PPA is used herein to detect and locate target clustering. The precise identification and location of target clusters helps stakeholders to better comprehend site formation processes and to develop an efficient excavation strategy. We weight points according to their EM63 channel-1 response and decay time. The location of the most interesting clusters is identified using the *local G_i^** statistic (Getis and Ord 1992, 1996; Ord and Getis 1995).

The plan of the paper is as follows. First, we suggest an EM63 acquisition technique that ensures a high quality data set. We then review elements of the point pattern statistical methodology. EM-63 data are presented from a controlled test site seeded with a known spatial distribution of common metal artifacts, and from a historical archaeological site, the Robert E. Lee camp at Paint Rock, Texas. The latter site, centrally located between Fort Mason and Fort Chadbourne, c.1851-1874 was utilized by the US Second Cavalry and many other troops, most notably then Colonel Robert E. Lee in 1856 (Freeman 1934). At both sites we show how point pattern spatial statistics can be used to describe and locate the clustering of subsurface metal targets identified by EM-63 responses. Excavation results from Paint Rock are analyzed. The results demonstrate the utility of the approach for archaeological site formation hypothesis testing.

Methods

EMI data were acquired with the Geonics EM-63 at a controlled test site and an active archaeological site in Texas (Figure 2). The Tran experimental site is located in College Station, Brazos County, about 7 km east of Texas A&M University (TAMU). The Robert E. Lee campsite (U.S. registered archaeological site no. 41CC295) is located in the town of Paint Rock in Concho County on a terrace of the Concho River near a series of natural fords. Both sites are flat grassy pastures characterized by floodplain deposits of clays, silts, and clayey sands.

Figure 2. Location of the controlled test site at College Station and Robert E. Lee Campsite archaeological site at Paint Rock. The major rivers of Texas and some large cities are included to aid orientation.

The Geonics EM-63 is a transient controlled-source electromagnetic induction instrument arrayed in the central-loop configuration. The transmitted current, which generates a primary magnetic field, is suddenly switched off, inducing a secondary magnetic field which decays slowly in subsurface ferrous and non-ferrous metal targets. After the primary field is switched off, the secondary magnetic field is recorded at 26

13

logarithmically-spaced time gates. The eddy currents induced in metal objects of different size, shape, strike, and orientation decay at characteristic rates, thus enabling a rudimentary target classification prior to excavation. The transient EM response amplitude, measured in mV, and its time rate of decay, measured in mV/s, can generally be used to predict the size and depth of subsurface anomalies. For instance, a small channel-1 response exhibiting a slow decay time typically indicates a large metal object at depth, whereas a higher channel-1 response accompanied by a brief decay time suggests a shallower burial.

Data Acquisition

An improved data acquisition protocol was developed to provide accurate sensor navigation, as required by the spatial statistics methods used in this study. Slight irregularities in the terrain causes loss of control of the EM-63 when it is deployed in the conventional cart-mounted configuration. The EM-63 was mounted on a sled and pulled along the survey lines. Data on an accurate rectilinear grid are straightforward to acquire in this fashion, with consistent positional accuracy to within a few cm, using manual data triggering. Data acquisition times using the cart and sled systems are similar.

The improved acquisition protocol was used to evaluate the performance of the

EM-63 for spatial cluster analysis at a controlled test site seeded with metal artifacts. For

this purpose, a clean site on private land was selected. The landowner Mr. S. Tran stated

that the site is used for agricultural purposes and that subsurface metal objects are not

expected. The site was seeded by a number of common metal items in the spatial pattern

shown in Figure 3. In order to test the ability of the statistics to discriminate between

clustering and random spatial patterning, we purposely buried 32 of these items in four

clusters (these are called "artifacts") and another 18 at randomly chosen locations (these

are called "clutter"). A background EM-63 data set was acquired prior to the seeding

(Figure 4*a*), in which minor and widely scattered EM-63 signals are observed. The line

spacing and the station spacing are both 0.5 m for the 20 x 20 m survey area, for a total

of 1681 data points. A second EM-63 data set was then acquired after seeding. The

resulting EM63 channel-1 response of the seeded site (Figure 4*b*) clearly reflects the

spatial distribution of the shallow buried items.

A third data set was acquired at the site using the Geometrics G-858 cesium-

vapor magnetometer (www.geometrics.com) in order to compare the capabilities of EMI

and magnetometry for target cluster analysis (Figure 5). Magnetometry is widely used

in archaeological prospection (Conyers and Leckebusch 2010; Kvamme 2006b; Perttula

et al. 2008) and UXO mapping and detection (Beard et al. 2008; Doll et al. 2008),

sometimes in conjunction with EMI (Beard et al. 2008; Pétronille et al. 2010). The G-

858 magnetometer is a passive device that measures the intensity of the sum of the background geomagnetic field and the much smaller magnetic field due to any nearby ferrous objects.
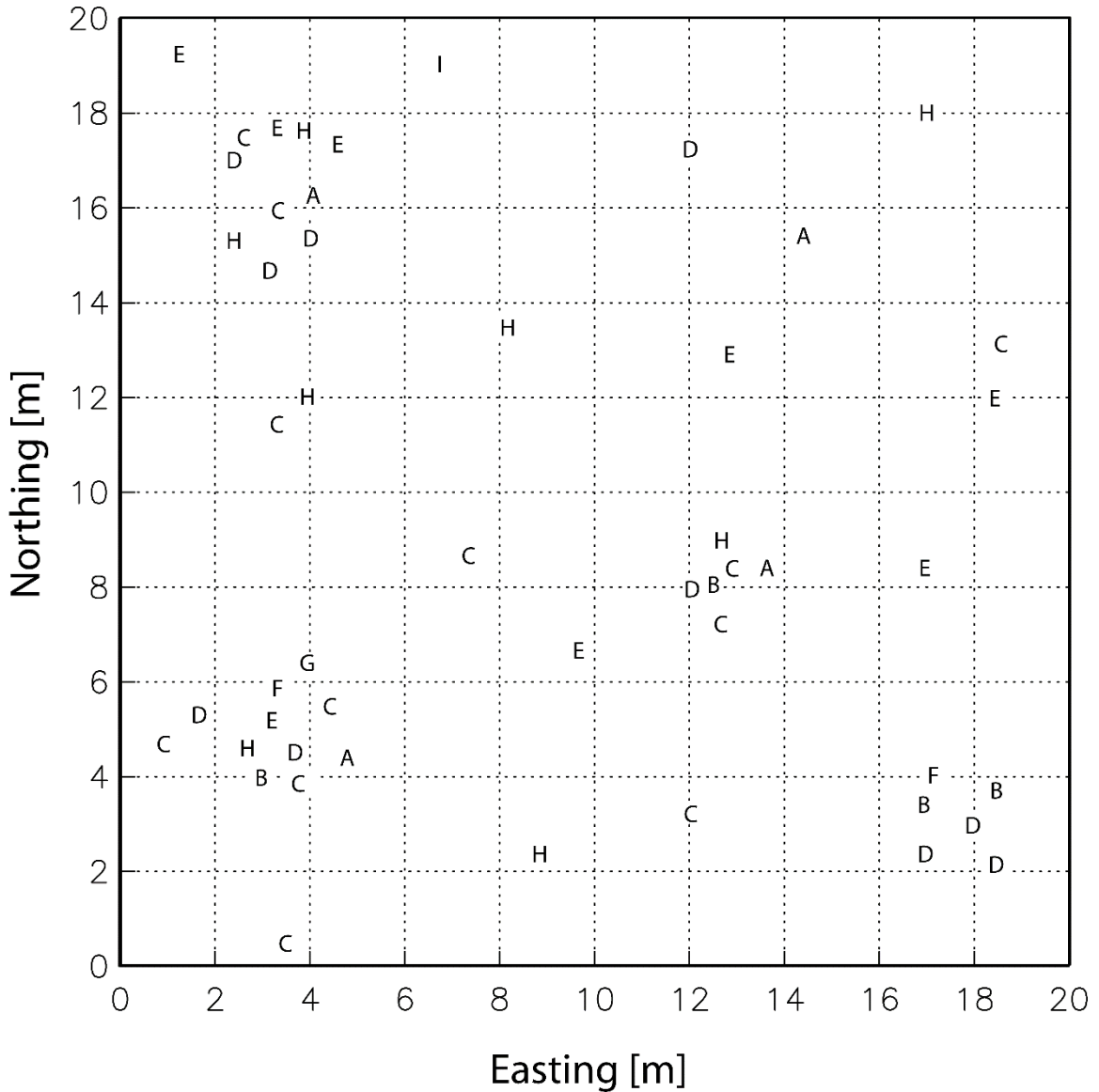
Figure 3. Distribution of seeded artifacts, symbol-coded by type, at the Tran test site: (a) bolt, (b) washer, (c) cylinder, (d) bottle cap, (e) coke can, (f) bullet, (g) license plate, (h) rebar, (i) musket ball. Plot dimensions in m.
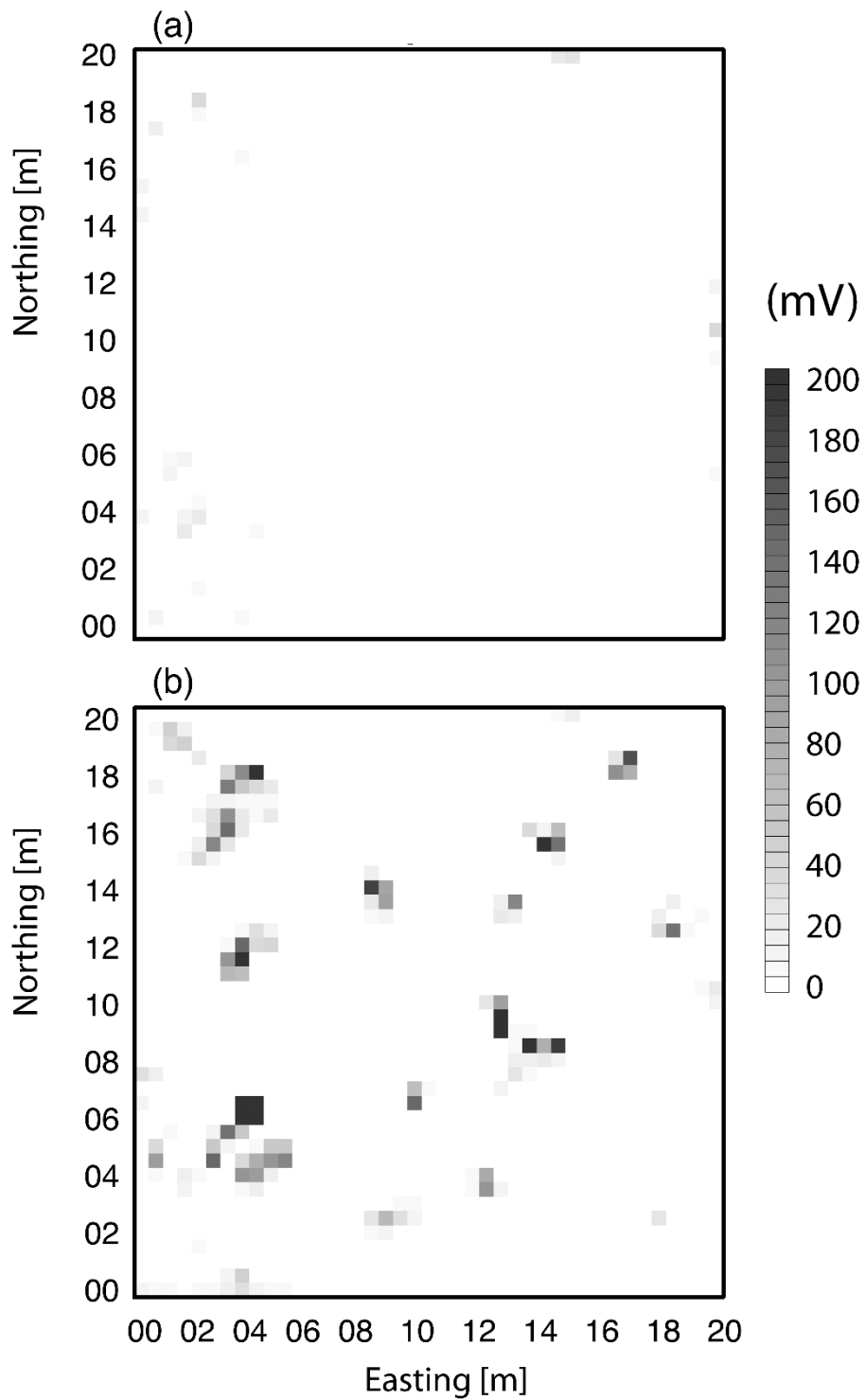
Figure 4. EM-63 channel-1 data acquired at the Tran test site: (a) before; and (b) after seeding with artifacts.
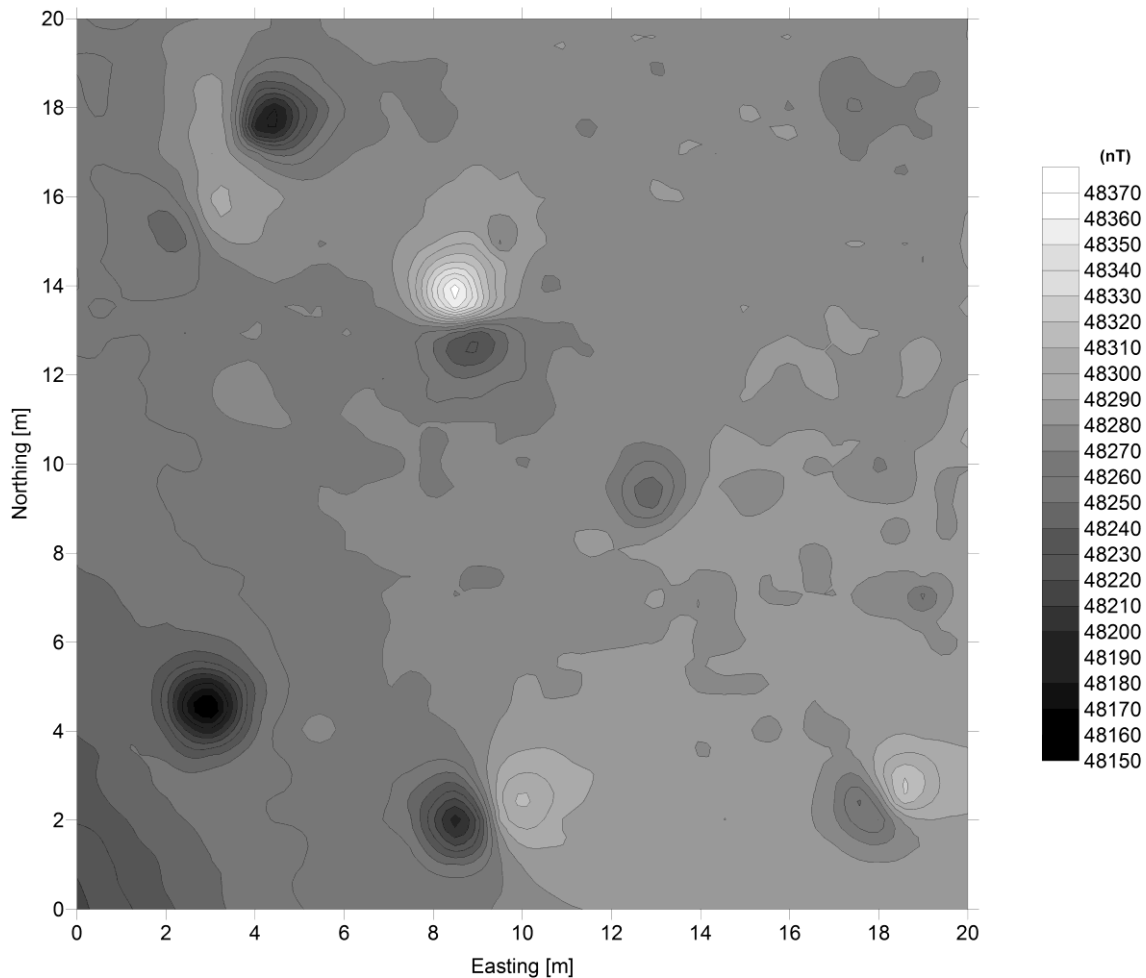
Figure 5. G-858 magnetometer total field data set from the Tran site.

The G-858 and EM-63 instruments have complementary capabilities. The EM-63 responds to *all* conductive metal objects, whereas the G-858 detects *only ferrous* targets. A G-858 data set does indicate, however, the background spatial variation of magnetic soils and sediments. The G-858 yields a spatially distributed pattern of dipole anomalies, rather than a discrete point set, since the magnetic signature of a buried target is dipolar and often merges with neighboring signatures. Spatial filtering by methods such as reduction-to-pole, analytic signal, or regional subtraction are *required* to better

18

isolate the magnetic signatures, whereas virtually no processing is necessary with EM data. For this reason, the G-858 data set is not as amenable as the EM-63 data set to target cluster analysis using point-pattern spatial statistics. A qualitative visual inspection of Figure's 4 and 5 demonstrates that EM-63 anomalies are more compact than their G-858 counterparts - note especially the isolated rebar at coordinates (2, 9) and (8, 13).

Archaeological Case Study at Paint Rock

An EM-63 data set was acquired at the Robert E. Lee campsite (Figure 6) over a 20 x 20 m grid with 0.5 m line and station spacing, for a total of 1681 measurements. The site was previously scanned with hand held metal detectors by the local avocational archaeological society (Ashmore, 2010) to identify subareas most likely to yield historic metal artifacts. This is standard archaeological practice (Bevan 2006; Connor and Scott 1998). The EM-63 data sets were analyzed using point pattern statistical methods, which are described in the next section of this paper. The PPA program (Aldstadt et al. 2002) is a statistical toolbox designed for spatial analysis applications, including cluster analysis.
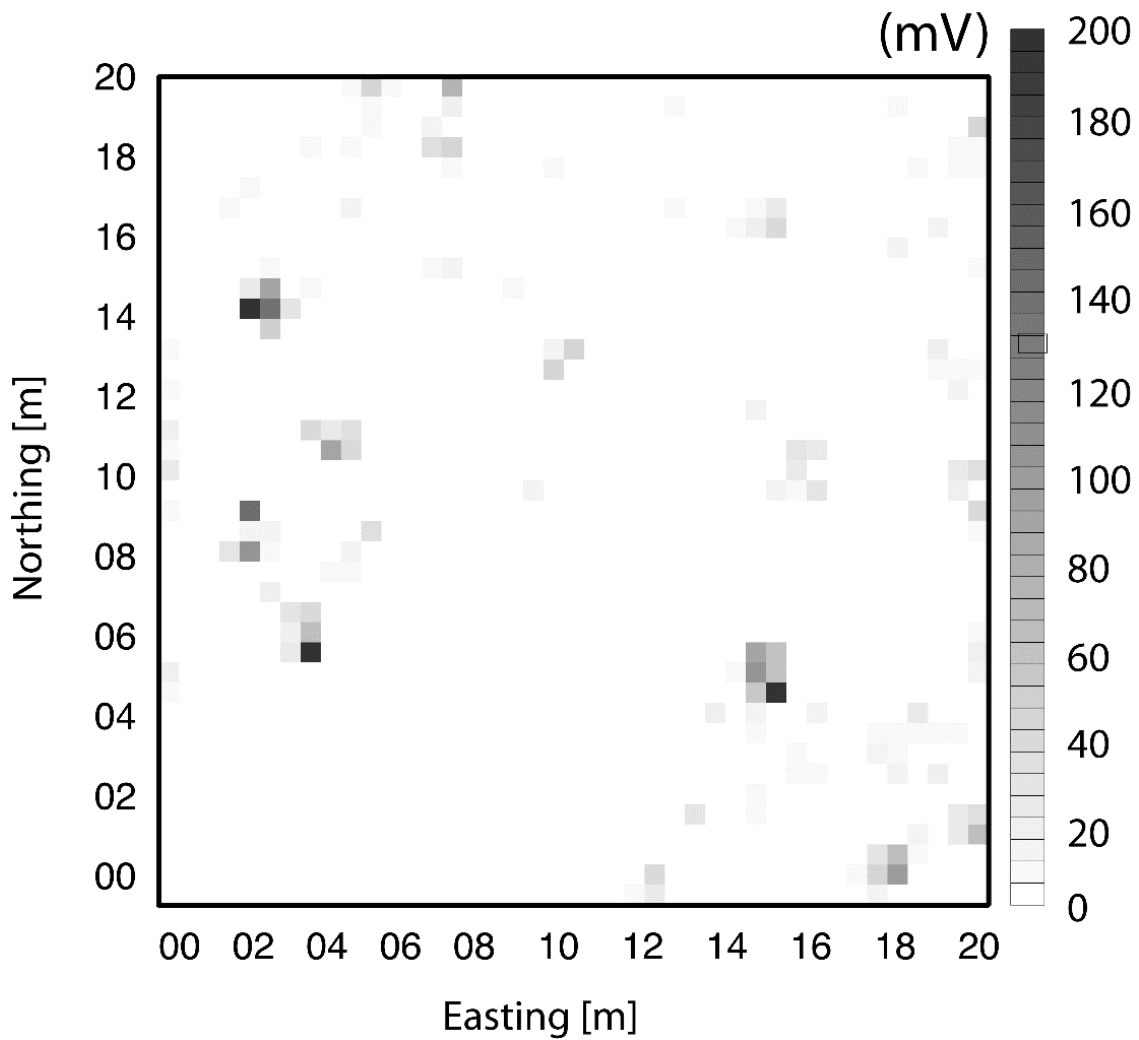
Figure 6. **EM-63 channel-1 data acquired at Robert E. Lee campsite.**

Point Pattern Analysis Statistics

Geostatistics has long been used by geoscientists to study continuous natural or anthropogenic spatiotemporal processes and is based on interpolating observations made at a number of discrete locations and times. Geostatistics was developed originally

20

(Krige 1951; Matheron 1963) within the mining industry as a method for determining the grade of recoverable ore. The most important geostatistical technique is kriging, which estimates an unknown process over a continuous region by interpolating between its measured values at discrete locations, taking into account spatial correlations within the observations. Geostatistical and related spatial techniques are best reserved for geophysical applications in which the target of interest, such as a zone of groundwater contamination or oil and gas accumulation, is distributed more or less continuously throughout the subsurface.

PPA differs from geostatistics in that the key analyzed variable is the location of a specified event, rather than the size or the probability of an event as a continuous function of its location. PPA is broadly applicable to UXO remediation, archaeological prospection, brownfields rehabilitation, or civil infrastructure assessment, since ordnance items, metal artifacts, and buried engineered structures are typically found or concentrated at discrete locations in the subsurface (Ostrouchov et al. 2003).

A local analysis of the autocorrelation structure of a spatial variable (Anselin 1995) can be used to detect clustering. A spatial cluster is characterized by the occurrence of a larger number of points within a specified distance of a given reference location than the number that would be expected under complete spatial randomness (CSR; Diggle 2003). A "point" is defined as a location at which the EM-63 responds significantly above the instrument noise level, indicating the presence of an underlying metal target. Points may take binary (0/1, or hit/miss) values or they may be weighted (Getis 1984) based on the value of the channel-1 response (in mV) or decay time (in

mV/s). In addition to simply detecting the presence of clustering by analyzing binary or weighted point distributions, we can also pinpoint the location of clusters using the techniques originally described by Getis and Ord (1992).

The standard *K*-function statistic (Ripley 1976, 1977, 1981; Schwarz and Mount 2006) detects spatial clustering of events with respect to some length scale *d*. An illustration of spatial clustering, with respect to a random distribution for which the expected number of events increases by one for each unit increase in radius around a specified event, is given in Figure 7. A *K*-function tests the observed distribution of event locations against the null hypothesis of complete spatial randomness (CSR). A set of events scattered randomly throughout a studied region is statistically equivalent to a homogeneous Poisson distribution (Cressie 1993). The model of CSR is always approximate since it rests on a largely untenable assumption that the investigated site contains a distribution of targets that is statistically equivalent to that of surrounding areas. Generally however, an archaeological, environmental, or UXO site is expected to contain a statistically distinct target distribution compared to the surrounding areas that have not been subject to the same set of natural processes and past land uses.
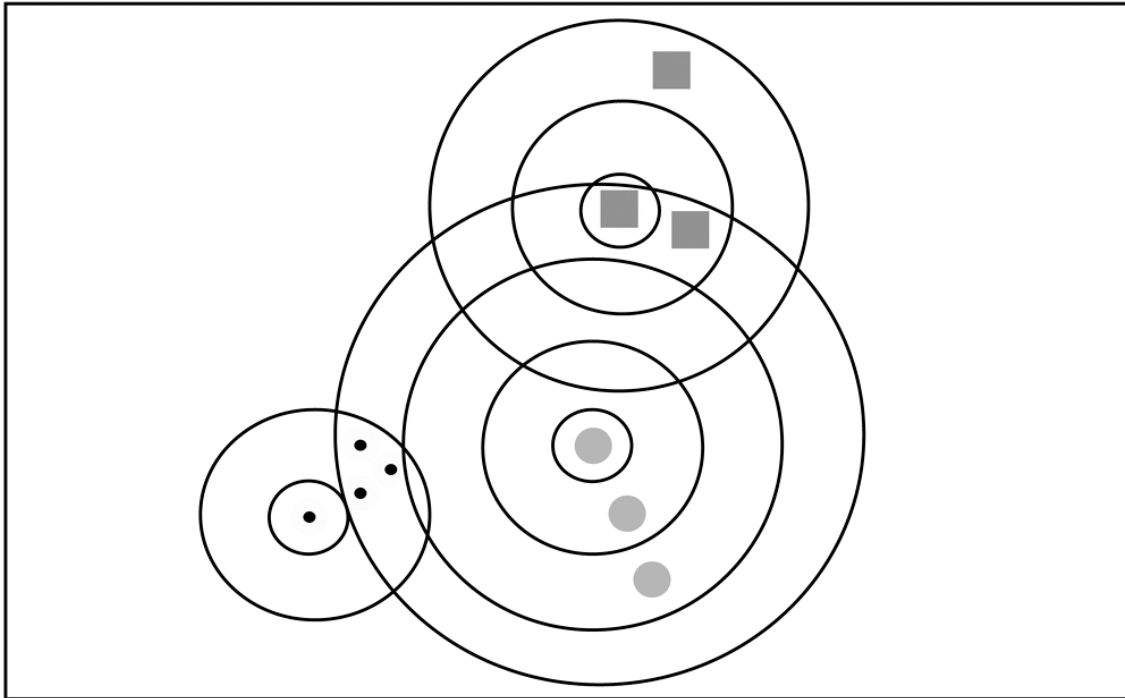
Figure 7. Illustration of spatial clustering. Circles with integer radius are drawn about three specified events: black circle, grey circle, and grey square. There is clustering around the black circle event at radii 1<*d*<2. The same clustering is recorded at 3<*d*<4 around the grey circle event. The grey circle event, like the grey square event, shows no clustering at small radii 1<*d*<3.

A global *K*-function analysis uses simulations to determine the statistical significance of clustering. For instance, *M*=95 permutations tests the null hypothesis of CSR at the α=0.05 level, such that values of *L*(*d*) outside the confidence envelope are interpreted to be significant, thereby rejecting the null hypothesis of CSR. Previous geophysical research utilizing the *K*-function to detect subsurface metal target clusters was carried out on airborne helicopter magnetometer data acquired over two former precision bombing ranges (MacDonald and Small 2009). Spatial clustering of the magnetic anomalies caused by buried UXO and clutter could not be determined by

visual inspection. Point pattern analysis was required to distinguish statistically significant clustering patterns from apparent clustering of randomly distributed targets.

The *K*-function is a *global* statistic that simply detects the presence or absence of significant clustering and dispersal at a given length scale. The G_i^* function (Getis and Ord 1992; Ord and Getis 1995), on the other hand, is a *local* statistic that can characterize and pinpoint individual clusters. We use the *K*-function to determine whether a dataset is significantly clustered, or completely spatially random, or significantly dispersed. Then we apply the local G_i^* statistic to determine the locations and length scales of individual clusters.

Local $G_i^*(d)$ statistic: 'Hot Spot' Analysis

The purpose of the $G_i^*(d)$ statistic is to identify "hot spots," or locations that are surrounded by a cluster of events carrying anomalous weight. Positive values $G_i^*(d)>0$ indicate spatial clustering of events with large weight whereas negative values $G_i^*(d)<0$ correspond to clustering of low-weighted events. The formula is

$$G_i^*(d) = \frac{\sum_j k_{ij}(x_j - \bar{x})}{s\sqrt{\dfrac{N\sum_{j \neq i} k_{ij}^2 - (\sum_j k_{ij})^2}{N-1}}} \tag{1}$$

where $\bar{x}$ is the mean of the weights, s is the variance of the weights, N is the total number of events (or sample size), and k_{ij} is the number of events within distance d of point i. The variables $\bar{x}$ and s are the same for all distance scales d as they represent the global mean and variance.

The null $G_i^*(d)$ hypothesis is that there is no association between the weight x_i at point i and the weights of its neighbors x_j that lie within radius d. Therefore, the null hypothesis can be restated as: the sum of the weights of the j points (including point i) that lie within radius d of point i is not more than the sum that would be expected by chance for a population of mean $\bar{x}$ and variance s (Getis and Ord 1996). In this paper the distance d is taken to be a multiple of 0.5 m. It is important to note that the expected number of neighbors for short distance scales is small (Table 1). Accordingly, the $G_i^*(d)$ statistic may be biased at short distance scales by the weight x_i at point i itself and by the small number of neighbors.

Table 1. Number of neighbors calculated by the *local* $G_i^*(d)$ statistic.

Distance (meters)	Number of Neighbors Calculated
0.5	5
1	13
1.5	29
2	49
2.5	81
3	113
3.5	149
4	197
4.5	253
5	317

It can be shown that the $G_i^*(d)$ statistic is asymptotically normally distributed as d increases. Thus, under the null hypothesis, the expected value of the $G_i^*(d)$ statistic is 0 and its variance is 1. As such, the $G_i^*(d)$ statistic is a standard variate, and its value is equivalent to a *z*-score at each point. The *z*-scores can be used to assess significance of clustering at various length scales about point *i*. However, the weights x_j of the neighbors *j* around point *i* are often correlated, in violation of assumptions of independence. Because of this dependence, a Bonnferroni-type correction can be used to control for a false positive, or Type I error (Ord and Getis 1995; Getis and Ord 1996). To determine significance values (Table 2) we prefer instead to use the Šidàk correction

(Šidàk 1967) since it is more powerful against a false negative, or Type II error (Abidi 2007).

Table 2. Significance Values of the *local Gi*(d)* statistic at the 90, 95, 99, and 99.9[th] percentiles for various sample sizes (α=0.10, 0.05, 0.01, and 0.001 respectively).

N	90th percentile	95th percentile	99th percentile	99.9[th] percentile
1	1.282	1.645	2.326	3.09
10	2.309	2.568	3.089	3.719
25	2.635	2.870	3.351	3.944
50	2.862	3.083	3.539	4.107
100	3.075	3.283	3.718	4.265
1000	3.706	3.884	4.264	4.753
1500	3.807	3.982	4.353	4.834
1681	3.835	4.009	4.378	4.856

The *local G_i^** statistic is an improvement over a global statistic such as the *K*-function insofar as it indicates the *locations* of individual clusters. For the case in which the observed events are weighted by the EM-63 decay time, for example, a high value of $G_i^*(d)$ implies that large buried metal targets are clustered about the specified point *i*. On the other hand, a low value of $G_i^*(d)$ indicates that such targets are relatively dispersed about point *i*. For the case of the channel-1 response, the value of $G_i^*(d)$ indicates the relative concentration or dispersal of all detectable metal targets. Since different EM-63

response features could be used as weights, the $G_i^*(d)$ statistic enables the geophysicist

to examine the spatial distribution of targets with specific attributes. In this way the

$G_i^*(d)$ statistic provides a powerful method of testing hypotheses about site formation

processes based on geophysical data.

Results

Tran Control Site

The $G_i^*(d)$ local statistic was analyzed at specific coordinate points to explore

clustering about those points. The coordinates (3.5, 6.5) and (3.5, 11.5) were selected

since both correspond high-amplitude EM-63 responses, one is a member of a cluster

and the other is a clutter item, respectively. The former is an automobile license plate

with a 675 mV channel-1 response, which was the largest in the survey area, while the

latter is a piece of rebar with a 272 mV channel-1 response. We first explored the effect

of sample size on the $G_i^*(d)$ statistic. The effect of decreasing the sample size by

counting only events with channel-1 response values greater than thresholds of 5 mV

($n=159$) and 50 mV ($n=52$) is to decrease significance, even after adjusting the z-scores.

There are two reasons for this: 1) a larger sample size implies many more neighbors

within radius d of a point i, most of which are below the threshold levels; 2) the mean

and variance increase as the sample size is decreased. These factors both contribute to

lower the $G_i^*(d)$ statistic, as shown in Figure 8a,b. We therefore use the entire data set ($n=1681$) to maintain the highest possible significance.

The EM-63 channel-1 target responses from the license plate and the rebar are both statistically significantly clustered at the 1 m distance scale (Figure 8c). The rebar EM-63 response shifts to non-clustered at greater distance, reflecting the fact that the rebar was purposely seeded as isolated clutter. However, the license plate EM-63 response is significantly clustered to a distance of 7 m, because the license plate belongs to a purposely seeded cluster, which at large ranges merges with other clusters.

Maps of the $G_i^*(d)$ statistic at the Tran site are shown in Figure 9 for various distances $d=1$—4 m. The maps are formed by calculating the $G_i^*(d)$ statistic at each grid coordinate, and plotting the results. It is apparent that the EM-63 responses of the artifacts maintain significant clustering at greater distances than the clutter responses. Of the latter, only the previously analyzed rebar shows any significant clustering. It is also apparent that only three of the four artifact clusters are identified. The cluster of small artifacts at the lower right corner of the Tran site (Figure 3) is missed by the G_i^* analysis because these artifacts are too small and/or deeply buried to be detected by the EM-63. These results are similar to those of Beard and colleagues (2008) in that small buried objects were missed, as they fall below a threshold of EM-63 detection. This cluster was detected by the magnetometer, however, as a dipolar anomaly (Figure 5). There are four large dipolar anomalies in the magnetometry data set and two single poles; two dipoles are due to artifact clusters while the other two are caused by isolated rebar. The isolated rebar, emplaced as clutter at (2, 9) and (8, 13) generate the largest dipolar anomalies in

the magnetic data set, but they appear as much more compact anomalies in the EM-63 maps. The two other dipolar anomalies and two single poles in the magnetic data set, which correspond to clusters, are actually more compact than the isolated rebar. This is possibly because the magnetization directions of the various artifacts within the clusters are not aligned. While a magnetics data set is always a useful complement to EM-63 data, magnetic anomalies are spatially extended relative to EM, as mentioned, and not as amenable to application of point pattern statistics.

The Tran site provided a useful testbed for local $Gi*(d)$ statistical analysis of EM-63 responses generated by subsurface metal distributions. The $G_i*(d)$ significance value maps (Figure 9) provide valuable graphical representations of clustering, which can be used to guide excavations and constrain archaeological site formation theories. Our attention now turns to the archaeological site.
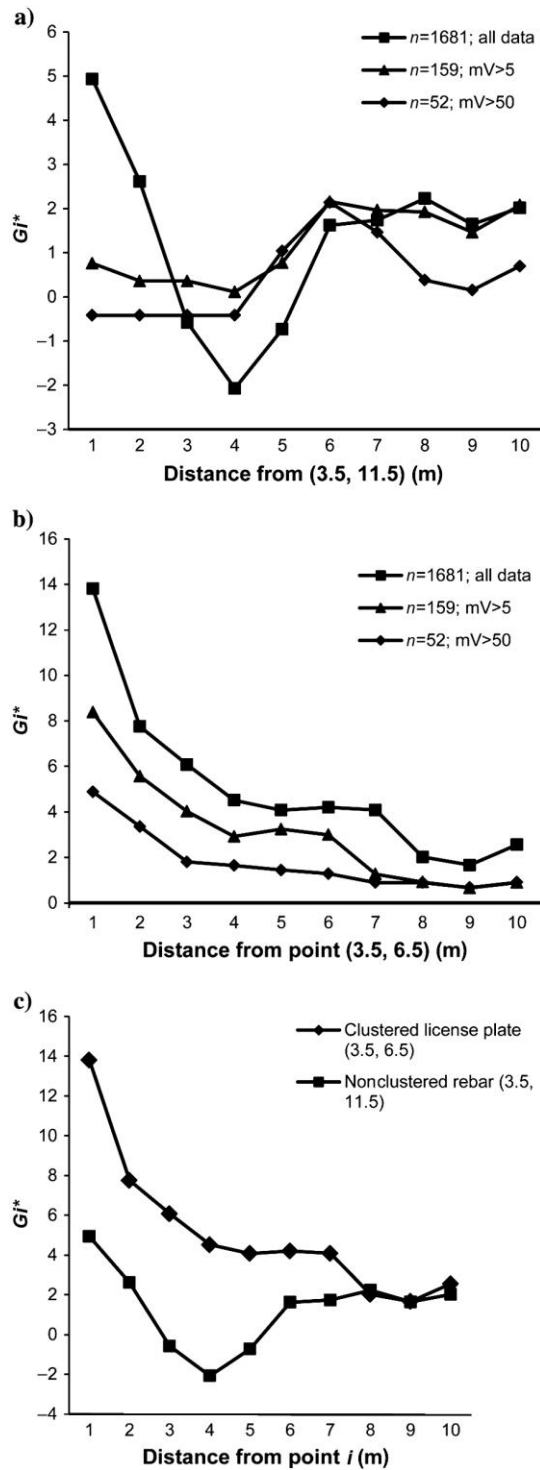
Figure 8. *Gi*(d)* **statistic for stratified datasets at Tran Site:** (*a*) **'clustered' license plate at (3.5, 6.5);** (*b*) **'clutter' rebar at (3.5, 11.5);** (*c*) **comparison of** (*a*) **and** (*b*) **for the entire dataset.**
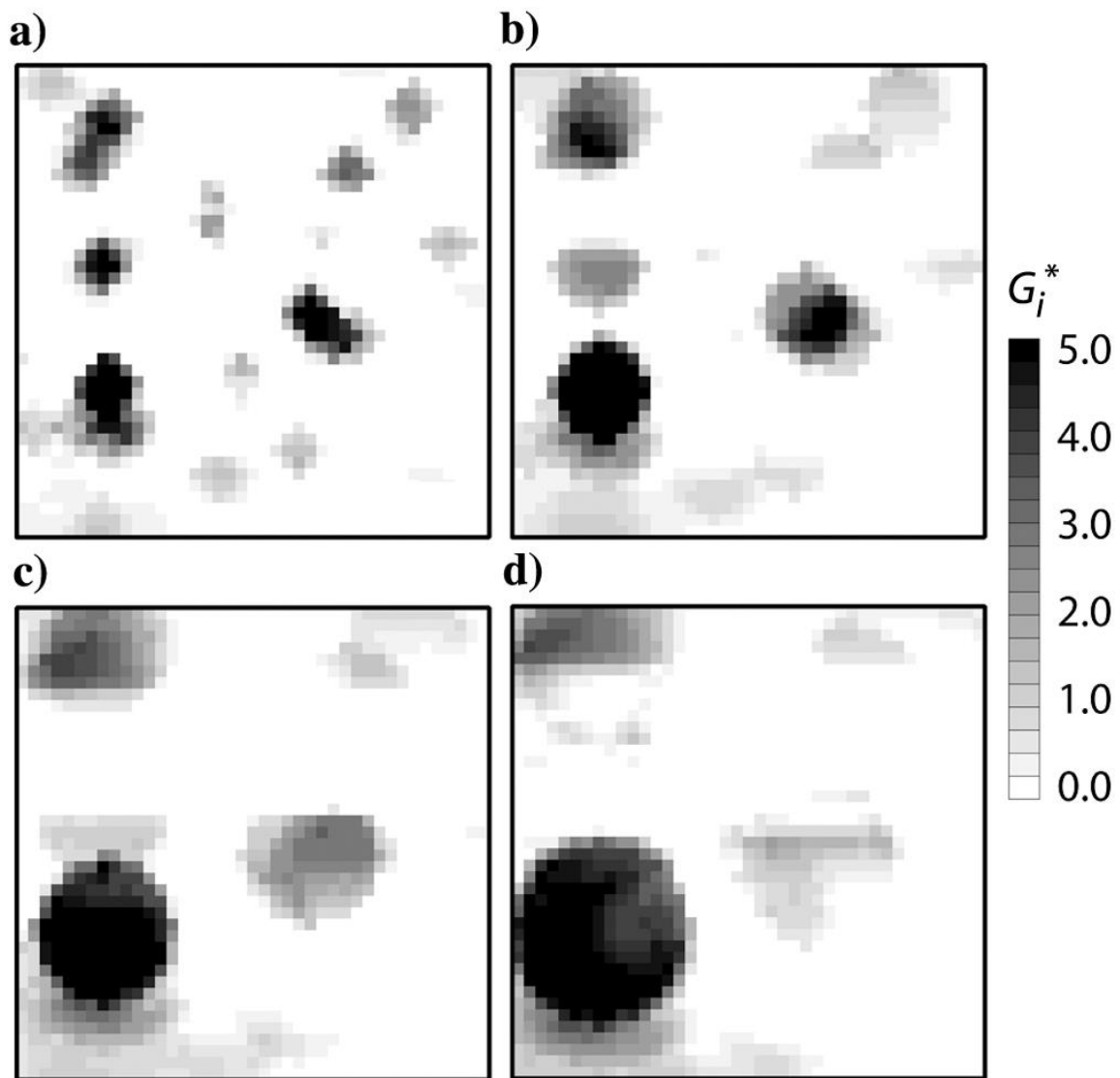
Figure 9. *Gi*(d)* significance maps, Tran Site: (a) *d*=1.0; (b) 2.0; (c) 3.0; and (d) 4.0 m.

Robert E. Lee Campsite

In the summer of 2010 and spring of 2011 archaeological excavations at the

Robert E. Lee campsite were undertaken according to standard archaeological

conventions. Thirty-three 1 x 1 m units were carefully excavated with hand troweling in precise 5 cm depth increments, measured with respect to a Topcon RL-H3C laser level calibrated daily. The excavation strategy was informed by the results of point pattern statistical analysis of the EM-63 dataset. We followed the same protocol as at the Tran site with $Gi^*(d)$ analyses of the complete channel-1 response data set.

Maps of the local $Gi^*(d)$ statistic at the Lee campsite are shown in Figure 10. There are three clusters of significant Gi^* values, based upon α=0.10 (Gi^* values > 3.835) as in Table 2, at scale d=1 m, two clusters at d=2 m, and only one at d=4 m. This suggests that the single cluster toward the bottom left of the maps (3, 7) corresponds to an isolated target with a high channel-1 response, analogous to the aforementioned rebar at the Tran Site. Subsequent excavation confirmed that the target was in fact a large piece of saw-tooth barbed wire patented in the 1880s (Clifton 1970). A second area of high Gi^* values in the upper left indicates clustering at the 1 m distance scale, persisting through the 2 m scale, then falling off (2, 15). This suggests the presence of neighboring items with high response values in the vicinity. Excavations confirmed this, as a horse shoe was found *in situ*, while present in adjacent units were a nail belonging to this horse shoe, fragmentary metal, and a shotgun shell. A third cluster in the bottom right (6, 15) is significantly clustered up to 2 m, but then falls off. Excavations revealed unidentifiable barbed wire along with nails and other fragmentary metal suggestive of fence remnants.

Discussion

Reduction of false positives is important in UXO remediation (Butler 2004) and archaeology as both disciplines work with budgetary and temporal constraints. The EM-63 performance at the Lee campsite gives encouraging results in this direction. We excavated 10 units characterized by EM-63 'hits' along with 23 adjacent EM 'barren' units. Hits were defined as $G_i*(d=1$ m$)$ values >3.835 ($n=26$), which represents a p-value of 0.10, or a one in ten chance of Type I Error, as can be seen in Table 2; while barren is everything below this threshold.

I report seven false negatives, as the statistics failed to predict the presence of metal in 7 of the 16 units which contained metal upon excavation; although some units labeled 'barren' were rather close to the $G_i*(d)$ values deemed significant, as there are 18 G_i* values between 3 and 3.835. Moreover, some of the metal in these units was quite fragmentary. If we relax the significance threshold of G_i* values to include all those >3, we reduce the amount of false negatives to just three. This is expected as Ord and Getis (1995) believe the corrected p-values for multiple comparisons is overly cautious against Type I Error, therefore inflating Type II Error, or false negatives. By exploring the relationship between these two sources of error we are able to examine more patterns in the data. There was, however, only one false positive, which was near the detection threshold and probably the result of an overlapping footprint from larger channel-1 responses in adjacent units. Interestingly, one false positive - or Type I Error - is expected from the ten EM 'hits' at the $\alpha = 0.10$ level.
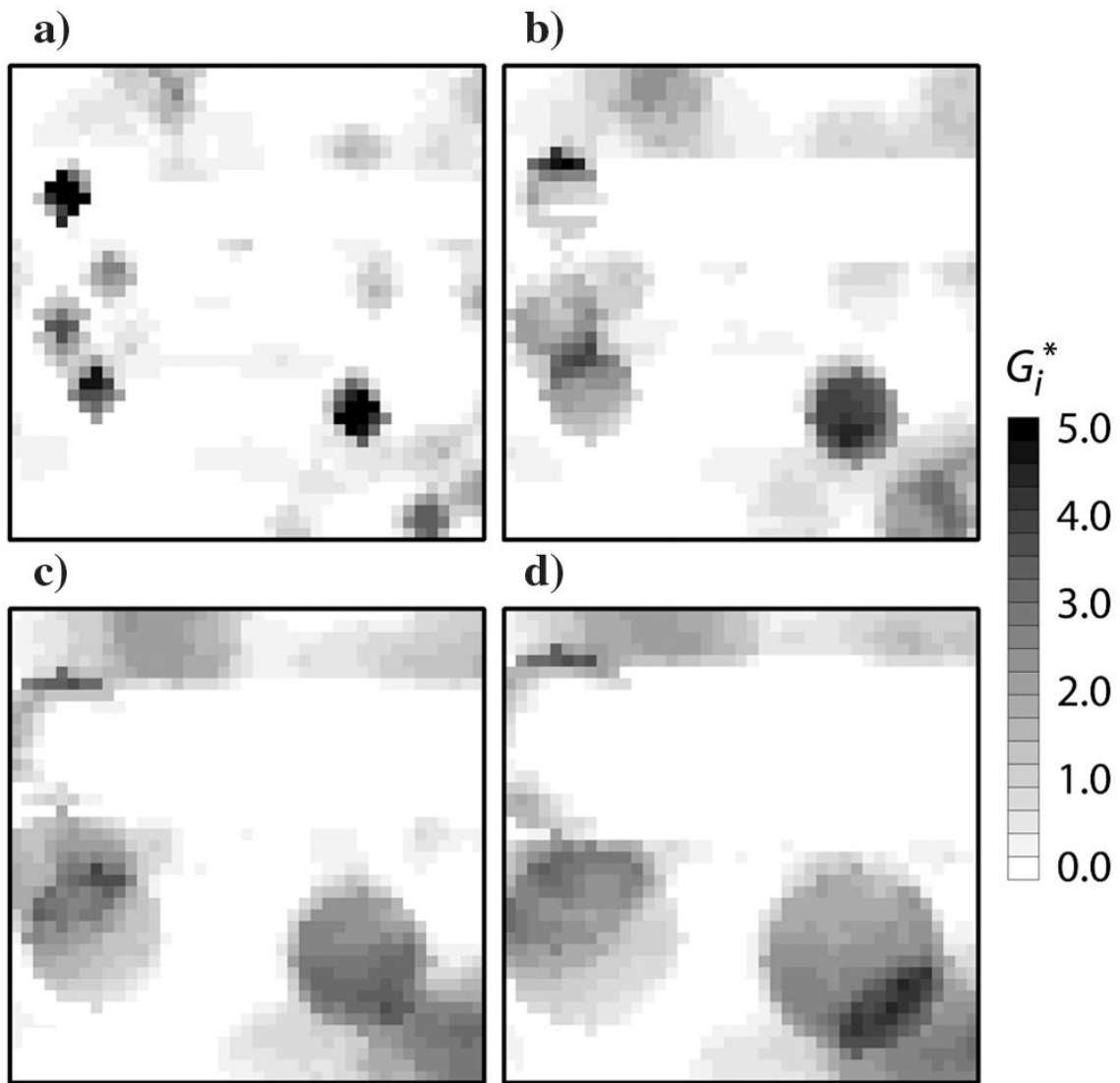
Figure 10. *Gi*(d)* **significance maps, Lee campsite: (a)** *d=*1.0; (*b*) 2.0; (*c*) 3.0; and (*d*) 4.0 m.

A Pearson's Chi-squared test of the 76% correct predictions $((9 + 16)/(9 + 7 + 1 + 16))$ gives a p-value of 0.001652 (Table 3). The odds of such a distribution occurring by chance are small (Drennan 2010). When this is compared to a traditional approach, where EM channel-1 response values greater than one standard deviation above the mean are considered (>21 mV, n=51), the results are striking (Table 4). There are nearly identical false negatives. The percentage of correct predictions drops to just 55% $((10+12)/(10+6+5+12))$. The chi-squared value for the traditional approach in not significant at the α=0.05 level, whereas the statistical approach is significant at the α=0.01 level. Most noticeable, however, is the sharp increase in false positives, as the spatial extension of EM signals from large anomalies causes false positives in adjacent units. The $G_i^*(d)$ is better than the traditional approach, because it takes into account both the large nearby channel-1 responses and the smaller background signals from the surrounding area, thereby increasing the G_i^* value and compacting the EM anomalies, resulting in less false positives. It is clear that the $G_i^*(d)$ analysis of the EM-63 dataset acquired at the Lee campsite proved very valuable as a guide to the archaeological excavations.

Table 3. Chi-squared test for the *local Gi*(d)* statistical predictions based upon excavations at Paint Rock, where threshold is *Gi*(d)* values >3.835 (*n*=26). X^2 = 9.9005, df = 1, p-value = 0.001652.

	Metal found during excavations (n=16)	No metal found during excavations (n=17)	Total
EM hits (n=10)	9 (true positive)	1 (false positive)	10
EM barren (n=23)	7 (false negative)	16 (true negative)	23
Total	16	17	33

Table 4. Chi-squared test for the predictions based upon traditional measures, herein defined as one standard deviation above the mean (channel-1 responses >21 mV, *n*=51), based upon excavations at Paint Rock. X^2 = 3.6397, df = 1, p-value = 0.05642.

	Metal found during excavations (n=16)	No metal found during excavations (n=17)	Total
EM hits (n=15)	10 (true positive)	5 (false positive)	15
EM barren (n=18)	6 (false negative)	12 (true negative)	18
Total	16	17	33

Conclusions

The application of PPA spatial statistics to EM-63 data can be used to detect significant clustering of subsurface metal objects of historical, cultural, environmental, geotechnical, or archaeological significance. However, a high quality dataset is necessary before global and local spatial statistical analyses are attempted. We recommend the sled-mounted data acquisition protocol employed herein, although any acquisition method can be used if the navigation is accurate. EM-63 responses include both the initial amplitude and the subsequent decay time. Both features can be used as weighting factors. Our results at the Tran experimental site indicate that the *local $G_i*(d)$* statistic can be used to *locate* clusters of artifacts, even when clutter is present. These results were confirmed at the Lee campsite, where local statistics were used to successfully guide our excavation strategy, greatly reducing false positives.

Both global and local PPA techniques provide valuable information regarding the length scales of clustering and dispersal. Although useful, global approaches like *K*-function analysis can be used only to determine the presence or absence of significant clustering or dispersal at a given length scale. The $G_i*(d)$ statistical analysis, however, can be used to locate 'hot-spots' in the dataset. The use of multivariate significance values while analyzing the G_i* values is necessary in order to guard against Type II error, or false negatives; this precaution is necessary to avoid missing significant clustering patterns that may be hidden in the data.

CHAPTER III

THE BATTLE THAT WAS AND THE BATTLE THAT WASN'T: HISTORICAL AND

ARCHAEOLOGICAL INVESTIGATIONS ON THE CONCHO RIVER NEAR PAINT

ROCK, TEXAS*

A rattling drove of arrows passed through the company and men tottered and

dropped from their mounts. Horses were rearing and plunging and the mongol

hordes swung up along their flanks and turned and rode full upon them with

lances…Everywhere there were horses down and men scrambling…and he saw

men lanced through and caught up by the hair and scalped standing and he saw

the horses of war trample down the fallen…They had circled the company and

cut their ranks in two…riding down the unhorsed Saxons and spearing and

clubbing them and leaping from their mounts with knives and running about on

the ground…and stripping the clothes from the dead and seizing them up by the

hair and passing their blades about the skulls on the living and the dead alike and

snatching aloft the bloody wigs…everywhere the dying groaned and gibbered

and horses lay screaming. [McCarthy 1985:55-57]

Cormac McCarthy's vision of a Comanche attack on Anglo filibusters is violent. But, is it historically accurate or just another exaggerated work of historical fiction? Modern revisionist scholarship tells us that the nineteenth century American West "frontier was not a particularly dangerous place to live – unless, of course, [if] you were an Indian" (West 1995:2). The Hollywood vision of the West has been written off in academic circles as myth; however, most myths contain kernels of truth (Anderson 2005; Calloway 2003). McCarthy's fiction is probably more accurate than the pervasive academic myth that the Western frontier was only a violent place for Indians, when in fact it was an arena of conflict between *both* groups. Both sides were active participants in the fray, the Comanche actively "raiding and kidnapping on a large scale" (Anderson 2005:7) and the Texas Rangers and Federal Government committing men and money to expel and replace them with Anglo settlers (Campbell 2003; DeLay 2008; Hämäläinen 2008; Smith 1999).

Books like John Wesley Wilbarger's (1889) *Indian Depredations in Texas* and John Henry Brown's (1893) *History of Texas from 1685 to 1892*, have been called "racist and biased," but they cannot be ignored as they provide some of the earliest primary accounts (Anderson 2005:10). The Comanches did raid ranches and farms, and they did kidnap Anglo women and children, such that "the raids on the Parker, Lockhart, and Webster families between 1836 and 1838 resulted in eighteen deaths and the carrying into captivity of a dozen women and children." (Anderson 2005:10; Hämäläinen 2008). The real problem academics seem to have is not with Indians

40

perpetrating violent acts against Anglos, but with the idea that this in some way justifies

subsequent actions, like the removal of Native Americans to reservations. Anderson is

correct in asserting that "the Texas story can no longer be depicted as righteous conquest

by a courageous few bringing civilization to a 'wild' land (Anderson 2005:17). This

phenomenon of landscape turnover is often described as the shift from wild and

uncultivated to domestic and cultivated (à la Lévi-Strauss [1983] raw and cooked). In

this perspective Native Americans are viewed as just another part of the natural

landscape that needs to be tamed, pacified, and domesticated. This is a picture which

demands critical academic scrutiny.

It has been said in archaeology "that a spurious idea, once introduced into the

literature and left unexamined, has a half-life of at least 10 years (Ezzo 1994:606). This

is particularly apt when the idea is one which resonates with the political and academic

climate within anthropology. This myth reduces interethnic relations to a binary

opposition, with a victim and a villain, where villainous Anglos are active agents and

Native American groups like the Comanche are passive victims. Native Americans have

recently been pacified by a history that has often conflated the end result – of an Anglo

dominated West - with the story itself. Recent scholarship has demonstrated that the

Comanche were an active group with diverse motives, goals, and methods to achieve

their ends (DeLay 2008; Hämäläinen 2008). The truth lies somewhere in between the

myths, and must be examined critically in order to bring the past into focus. Luckily,

archaeologists and historians have a toolbox with which to critically examine the past

from an anthropological perspective with great temporal depth. Conflict event theory

(CET) can be used to understand the material culture shift at Paint Rock as part of a broader trend of landscape scale social interaction between the Comanche and Anglo frontiers. This site has multiple archaeological components and histories, which did not end with the deposition of artifacts, but rather with their continual adaptation and (re)interpretation up to this very day. The archaeology here augments and adds but another layer of meaning to the historical record. With this in mind, let us now turn to our case study, an arena of conflict on the Texas frontier along the Concho River near Paint Rock.

Introduction and Site Setting

The town of Paint Rock is located in west-central Texas some 50 miles east of San Angelo. The town is named for the >1,500 Native American pictographs (41CC1), which reside on the Permian limestone bluffs overlooking the Concho River (Kirkland and Newcomb 1967:146-158). There are also a number of historic period archaeological sites located near the pictographs, like the 1856 Robert E. Lee camp site (41CC295) and spring (41CC290), which reside on the first terrace (T_0) north of the Concho River (Figure 11). This is also the site where, in either 1842 or 1846, Captain John 'Jack' Coffee Hays and Lieutenant Benjamin McCulloch famously fought the Comanche (Cutrer 1993:48). The bluffs provide a strategic high point in the river valley, and there is also excellent graze for horses and abundant spring water in the area, making it an ideal stopping point. Moreover, there are a series of natural fords at this point of the Concho

and it has been described as the "Concho crossing…of the Chadbourne-Mason road" (Freeman 1934:367) and "crossing of the trail from Fort Chadbourne to fort Mason" (Rister 1946:50-51) The site is also only 15 miles south of the Colorado River.
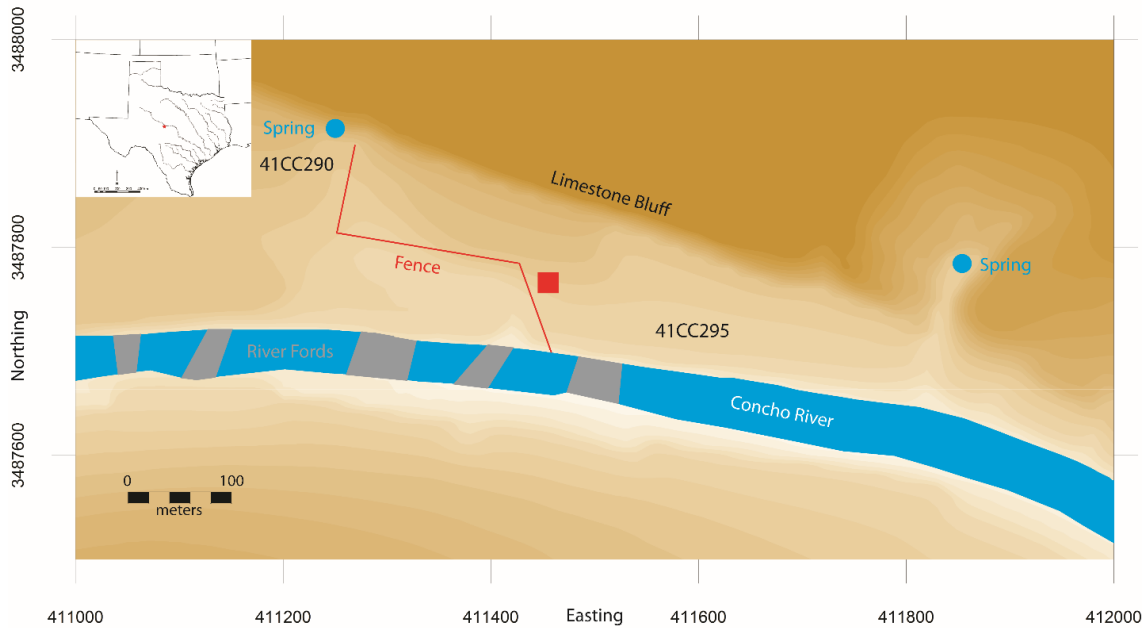
Figure 11. Map of Paint Rock sites 41CC290 and 41CC295. Fords are in grey. Springs and Concho River are in blue. Fence line and 20 x 20 m geophysical survey block in red. Contour interval 1 m. The pictographs were painted, penciled, and incised on the steep limestone bluff, which has many shallow rock shelters. Grid in UTM northing and eastings, 1.0 x 0.5 km.

Two significant events occurred near Paint Rock, Texas, during the 1840s and 1850s, where the governments of Texas and the United States military forces against the Comanche. In the 1840s a series of battles between the Texas Rangers and the Comanche culminated at Paint Rock. In the course of these skirmishes the Comanche utilized similar tactics to those described by McCarthy, but with dissimilar results. The second encounter occurred in 1856, when then Col. Robert E. Lee led the U.S. Second

43

Cavalry on an expedition to engage and punish the Comanche. The expedition achieved neither end.

In the 1840s Indian policy often involved signing treaties to determine land claims, but by the 1850s policy had shifted to removal. CET, originally elaborated upon by Sewell (2005) and operationalized for archaeology by Beck and colleagues (2007), offers a powerful tool to aid the analysis of the historic events which comprise the archaeological record - especially as structural transformations are manifest materially at archaeological sites. The archaeological record at Paint Rock was transformed between the 1840s and 1870s: from arrows to musket balls and cartridge casings, Apache and Comanche pictographs to English graffiti signatures, Native to English Staffordshire white earthenware, and Indians to Anglos.

Our project at Paint Rock consisted of geophysical and archaeological work carried out in 2010 and 2011 and had three goals. First, we tested the ability of the Geonics EM-63 time-domain electromagnetic-induction metal detector to predict the nature of the subsurface of the site through systematic archaeological excavation. Second, our ground-truthing experiment tested the utility of point-pattern analysis spatial statistics by comparing its predictions against the actual materials revealed by excavation. Third, we sought to determine the spatial and temporal extent of the military presence at a multi-component campsite from a significant period in history by analyzing the pictographs and artifacts at the site. These data, combined with archival research, provide us with a more nuanced understanding of the site and Anglo-Indian relations during the period.

Historical Background

The First Event: The Texas Rangers Campaign against the Comanche in the 1840s

During the 1840s a little known battle between the Comanche and Texas Rangers occurred at Paint Rock. There is little primary documentation of this battle because the Texas State Archives, which were housed in the State Capitol, were destroyed in a fire in 1881, along with the official report of the battle (Affleck 1911). Even the year of the battle is difficult to ascertain. A newspaper article from the *San Antonio Express* entitled "The Battle Lost to History" places the battle around June 1846 (Affleck 1911); however, Ben McCulloch biographer Thomas W. Cutrer (1993:48) places the battle at 1842. The year of the battle is no arbitrary distinction. In 1842, Texas was a Republic (1836-1845), but in June 1846 was part of the United States, which was then at war with Mexico.

The Republic of Texas Indian policy shifted erratically and was dependent on the President in power and upon the perception of recent Indian raiding activities. In 1842, Sam Houston was President of the Republic of Texas and he implemented an Indian policy based upon treaties and territorial boundaries. U.S. government policy in 1846 under James Polk was to negotiate treaties in order to determine land claims (Campbell 1993:93; Campbell 2003). Therefore, it seems that this battle was possibly unsanctioned in either case, which is much different from the actions of Robert E. Lee's Second Cavalry just one decade later.

The description of the battle in the *San Antonio Express* was given by a former Texas Ranger, F.M. Harrison, who described the battle between 40 Rangers and 600 Comanche as a 3 day struggle. In Harrison's narrative the Texas Rangers took up a fixed defensive position along the tree line near the Concho River due to their numeric inferiority. This position was advantageous and he noted that, "Although thousands of arrows were discharged at them they were harmless otherwise, because the men and horses were sheltered by the trees and undergrowth where they could not be seen and which the Indians failed to penetrate. Thus protected, the rangers had greatly the advantage and the arrows were wasted" (Affleck 1911:9).

The "forting up" strategy employed at Paint Rock by the Rangers mimics that of Jim Bowie and James W. Fannin during the Texas Revolution at the October 28, 1835, Battle of Conceptión on the outskirts of San Antonio de Bexar near the Conceptión Mission (Campbell 2004:134-136; Ramos 2008:147). Outnumbered by the Mexican cavalry and infantry, the Texan Army took up a position along the steep tree lined riverbank in order to use it as a breastwork. Mexican General Cos should have ordered his soldiers to flank them, but because the Mexican army was used to open country and cavalry tactics they attempted a frontal assault. The Texans army was comprised mostly of Eastern Americans accustomed to woodland fighting tactics. The Texans were able to suppress and eventually repulse the Mexican charge because the Texans had excellent cover and long rifles with a greater effective range than Mexican arms. Mexican cavalry tactics emphasized sabers and lancers, while Comanche tactics employed the bow-and-arrow; however, on open ground both utilized speed to their advantage to close on and

directly engage the enemy in close quarter hand-to-hand combat (DeLay 2008; Hämäläinen 2008) - resulting in numerous Comanche victories like the aforementioned McCarthy quote.

Although firearms might be expected, Harrison states that the Comanche shot "thousands of arrows" at the Rangers. In an analysis of artifacts from the 1874-75 Red River War, Cruse concluded that Indians possessed far fewer firearms than previously supposed and many metal arrow points were discovered at the battlefield sites (Cruse 2008). Johnson recently examined a 1854 battle in New Mexico by 60 men of the U.S. First Dragoon against the Apache and found 40 metal points at the battlefield; metal debitage was also found at the site, which he interprets as metal point manufacture areas (Johnson 2007:240-241). By the mid nineteenth century metal had replaced stone as predominant material for arrow point manufacture in the Upper Missouri and amongst the Navajo and Comanche considerably earlier in the 18th century (Hanson 1972; Kluckholn et al. 1971:34; Thompson 1980). Wallace and Hoebel (1986:104) state that Comanche "war point[s] were barbed and loosely attached to the shaft" so that they were difficult to extract from wounds. The purpose of this production technique is to make the arrows break or fall off easily upon impact so that they cannot be reused against them, much like the Roman pilum (Boatwright et al. 2004:171). Archaeologically the location of these points should be very near their intended target if little subsequent taphonomic processes have affected their initial point of impact (Schiffer 1987).

If Harrison's account is accurate, archaeologically, we should expect concentrations of artifacts related to the battle near the limestone bluff and tree lined

river. Metal arrows should be associated with the Comanche charges and cluster near the tree lined Concho River. Rangers provided their own horses and weapons, and "after 1840, no self-respecting ranger would ever be caught without a Colt five- or six- shot revolver strapped to his side, a most effective weapon that dramatically changed Indian warfare on the plains" (Anderson 2005:8). Since the Rangers would have had a variety of revolvers and rifles, both bullets and musket balls are expected and should be clustered along the bluff. This event was the beginning of a shift at Paint Rock and a rupture with the past as predicted by CET. The archaeological assemblage within just a few short years was transformed at the site.

The Second Event: Robert E. Lee Leads the Second Cavalry through West-Central Texas

In July, 1856, then Colonel Robert E. Lee led four companies – nearly two hundred men - of the U.S. Second Cavalry on a sweep of the Concho River in search of Comanche Indians Indians (Anderson 2005:286; Freeman 1934:367; Rister 1946:50-51). Lee describes this action in his journal, noting that on July 16th and 17th his men camped at a series of natural fords along the Concho River between Forts Mason and Chadbourne, near modern Paint Rock, Texas. Anderson (2005:286) describes the orders and purpose of Lee's expedition thusly:

General Johnston, who commanded the Second Cavalry in May

1856...confidently ordered a gifted officer, Colonel Robert E. Lee, to mount the

first expedition designed to cleanse the plains west of the   reserves of

Indians…Colonel Johnston's orders to Lee were clear. There was to be little

quarter in dealing with the Indians. The Comanches' 'continued rejection of the

privilege of settling on the Reservation under the protection of the government,'

Johnston said, 'will be considered sufficient evidence of their unfriendliness.'

Lee was to search for them and destroy them!

In total, Lee's expedition is reported to have covered about 1,600 miles in 40 days, or

about 40 miles a day (Freeman 1934:367). The mission was considered a failure because

they only encountered four Yamparika Indians, of which two men were killed, one man

escaped, and one woman was captured (Freeman 1934:367; Rister 1946:48-50).

Although the expedition failed to achieve the desired results, the orders Lee received in

1856 were significant, as they signaled a *shift in policy* that would eventually lead to the

expulsion of Native Americans from Texas. Moreover, Lee's command of this

expedition and his time in Texas were formative in his military career.

Lee's efforts were a small part of a larger campaign by the Republic of Texas and

later the United States of America to remove Native Americans from the state (Anderson

2005). Native Americans were seen as a threat to incoming Anglos who wanted to settle

the land free from the fear of raids. The population of Texas ballooned from less than

40,000 to more than 600,000 between 1836 and 1860. Two-thirds of these settlers were

Anglos and the other third largely black slaves (Campbell 1989:55). Approximately 75%

were from the Southern U.S. (Campbell 2003:207). This influx resulted in a steady

advance of the civilian settlement frontier. The fort system and its attendant military/commercial complex accompanied the settlement frontier north and west, and exacerbated prolonged conflict along border (Figure 12). The fort system presaged the attendant civilian frontier and moved north and west as it expanded (Smith 1999).

Paint Rock was used as a winter camp ground by the Comanches, who aggregated in the winter instead of splitting into small dispersed bands like the Sioux and other High Plains Indians groups (Hämäläinen 2008:284). The pictographs were probably created during these times and thus date to the last few hundred years and can be attributed to the Apaches and Comanches. This is supported by pictographs depicting horses and Spanish Missions (Figure 13). The spot was also frequently used by soldiers moving between Forts Mason and Chadbourne, because its fords and springs are ideally geographically situated at approximately 43 miles from Fort Chadbourne and 72 miles from Fort Mason. This is approximately one and two days ride, respectively, if we recall the rate of 40 miles per day by the Lee expedition.
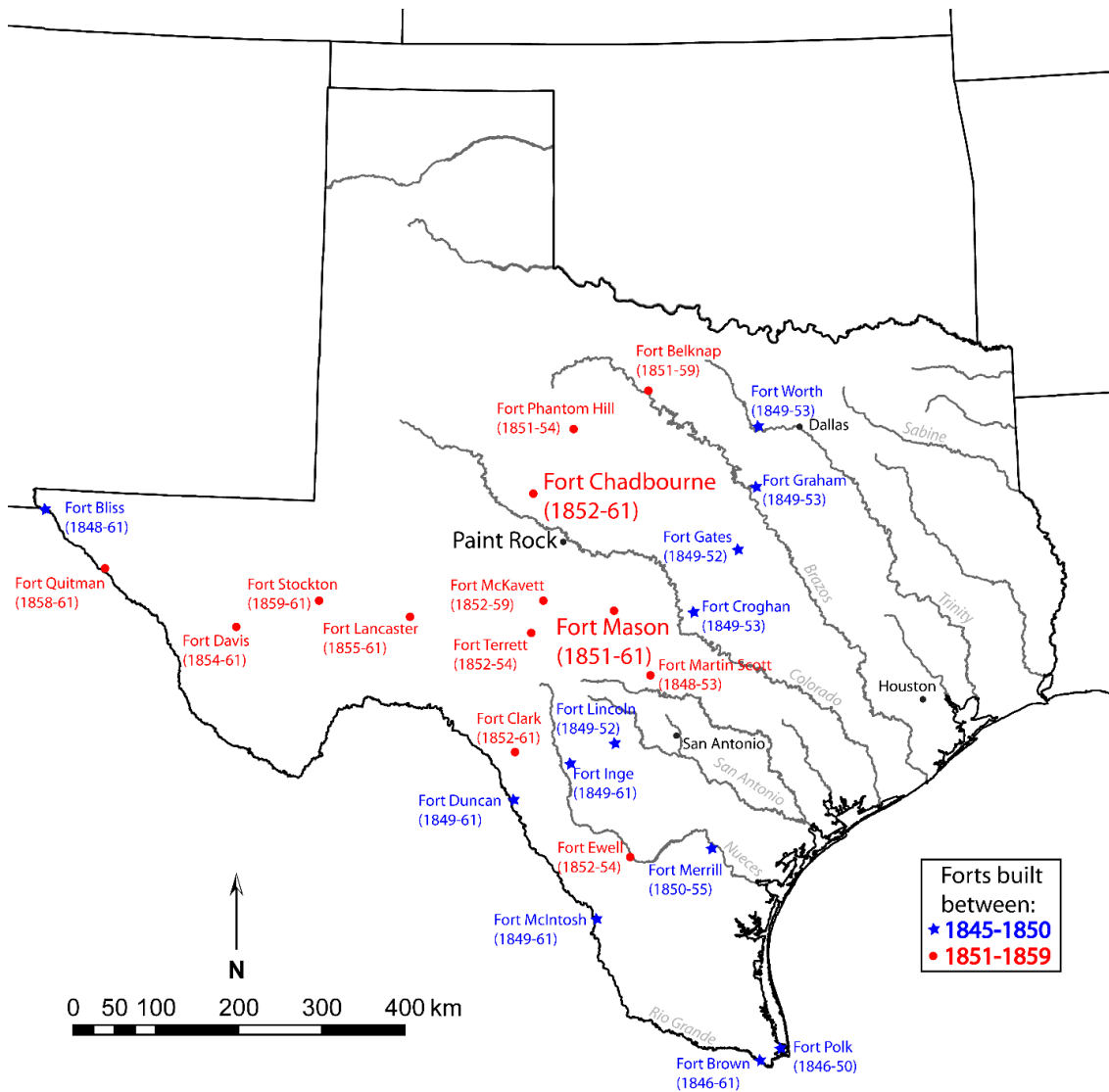
Figure 12. Texas forts built during the Statehood Period (1845-1861) and their dates of use prior to the Civil War in parentheses. The blue stars are forts founded between 1845 and 1850, while the red dots are forts constructed after 1850. After 1850 the civilian settler frontier and military fort systems spread to the west. Paint Rock, Fort Mason, and Fort Chadbourne are in larger font in west-central Texas. Major rivers and modern cities are included to aid orientation.

Figure 13. (a) Historic graffiti at Paint Rock. 'HOBAN 1856' is faded, but was painted over probable Comanche and/or Apache pictographs. Scale is 10 x 2 cm. (b) Spanish Mission with incised graffiti name 'L.C. Gibson Aug 1880.' Perhaps nowhere at the site more clearly demonstrates the shift from a Native American site and assemblage to an Anglo dominated one. The Native American pictographs are literally written over, but not completely erased.

Native Americans were not the only ones to record their passage on the Paint Rock limestone, Anglo soldiers and later settlers wrote their names over the Native American pictographs. The earliest known recorded signature was by a person named Hoban in 1856, the same year Lee camped at Paint Rock (Figure 13); however, there are two unreadable signatures that have dates of 1854. At least two Privates, Davis and Henninger from the 8th and 3rd Infantry respectively, who were stationed at Fort Chadbourne also left their names as graffiti on the limestone bluff at Paint Rock (Pate 2010:294, 296). Thus far we have recorded 21 painted, penciled, or incised names which date to the military period between 1852 and 1875 at the conclusion of the Red River

War. It is expected that as more records from Forts Mason and Chadbourne are cross referenced with the graffiti names on the bluffs that more soldiers stationed at these forts will be confirmed. The graffiti is a testament to the landscape scale turnover at Paint Rock, as the area moved from the Comanche sphere into the modern Anglo dominated one that remains to this day. The pictographs were literally written over, but not erased.

Robert E. Lee decided to camp at Paint Rock in 1856 because it was a midway camp spot for detachments heading to-and-from Forts Mason and Chadbourne and a known camping spot for the Comanche. He was hoping to find Sanaco's Penatekas ("honey eaters') Southern Comanche band. Lee's expedition was not the only one to make use of this camp spot. Many detachments of soldiers did likewise between 1852 and 1875 when the forts were in use (see Figure 12). During the Civil War (1861-1865) the frontier forts were largely abandoned and Comanche attacks caused the frontier to regress between 50 and 100 miles (Campbell 2003:266). Wallace and Hoebel (1986:301) note a direct correlation between the number of troops and the frequency of Comanche raiding; more Federal troops resulted in less raiding and vice versa. This retreat was no doubt inevitable. Moreover, many homesteads were abandoned as majority of the white male population between the ages of 18 and 45 left to fight with the Confederacy during the Civil War (Wooster 1995). After the Civil War, many of these forts were briefly garrisoned again. At the onset of the Red River War in 1874 eight companies of the 4th Cavalry under the command of Col. Ranald S. Mackenzie left Fort Concho in San Angelo, only about 50 miles west of Paint Rock (Cruse 2008:18). At the conclusion of the Red River War in 1875 these forts were largely abandoned.

Archaeologically, we expect the assemblage of the military camp period to have a wide variety of artifact classes from the mid nineteenth century. Because of the heavy cavalry presence we expect equestrian related artifacts like horseshoes, stirrups, spurs, buckles, saddle rings, and various other saddle gear. We also expect metal military buttons, firearm parts, bullets, cartridge casings, cooking equipment and utensils, bottles shards, ceramic sherds, and various other artifacts. Our survey and excavations seek to determine the spatial and temporal extent of the military presence at this multi-component campsite.

Archaeological Background

Our initial work at the site began in 2010, after avocational archaeologists from the Concho Valley Archeological Society (CVAS) found graniteware sherds (Figure 14) bearing Anthony Shaw's makers mark (Ashmore 2010), which dates to between 1850 and 1882 (Gooden 1964:571). Lee complained in his journal of the expense of purchasing ceramics in San Antonio, saying that "it cost more than French Chinaware in Baltimore" (Rister1946:38). Fine ceramics are an odd luxury so far out on the frontier, especially at a stopover site for cavalry heading to-and-from forts. Therefore, we hypothesized that these sherds might indeed be from Lee's service. This is a particularly tantalizing hypothesis because some of Lee's dishes were destroyed by the time he returned to Camp Cooper in April 1857 (Rister 1946:83).

Figure 14. Graniteware sherds with Anthony Shaw's maker's mark, which dates to between 1850-1882. These are possibly from then Col. Robert E. Lee's service.

Archaeological work at the Paint Rock sites has been limited. Avocational CVAS metal detecting and excavation has been mostly limited to the area around the natural springs in 2009 and 2010 (Ashmore 2010). Professional work has been conducted by Solveig Turpin and colleagues (2002) in 1999 and 2000. Because of the potential significance of this site for historical military archaeology we decided to investigate further using state of the art methods in interdisciplinary research, drawing from geophysics, archaeology, and statistics.

Methods

Time-Domain Electromagnetic-Induction

Electromagnetic (EM) methods have been described as one of the four main techniques used in geophysical archaeological prospection, along with ground penetrating radar (GPR), magnetometry, and resisitivity (Conyers and Leckebusch 2010). Unfortunately, the full potential of EM prospection has yet to be realized in archaeology, as it has chiefly been used to define subsurface structural features, like walls and earthworks (Bevan 2006; Pétronille et al. 2010; Simpson et al. 2009; Thiesson et al. 2009). This, however, does not exhaust the potential uses of EM for archaeology. The underuse of time-domain EM is odd when one considers the fact that it is widely used in near-surface applied geophysics for unexploded ordnance (UXO) remediation (Benavides et al. 2009), and to detect and classify other anthropogenic targets such as

pipes and underground structures (Benavides and Everett 2005). A body of theory and standards already exists within the geophysical community as to the use and interpretation of EM methods and data such that archaeology need only operationalize the technique for historical archaeology (Everett 2013; Reynolds 2011).

In comparing EM with traditional hand-held metal detecting for archaeological prospection, one should consider the positives and negatives of each method. The traditional "mag-and-flag" method used in gridded surveys with hand-held metal detectors is relatively time and cost efficient (Connor and Scott 1998). Learning to use a metal detector is straight forward and the detectors themselves inexpensive, relatively speaking; however, interpretation of the beeping noise emitted by a metal detector is subjective and there is limited predictability – and thus replicability - of the type or depth of targets. Little quantitative work has been done to determine the rate of false positives and negatives encountered during a typical mag-and-flag survey. As such, the time efficiency in prospection may be lost during subsequent excavations. This is in stark contrast to UXO remediation where false alarm rates (FAR) are of paramount importance (Lee et al. 2007).

The EM-63 time-domain electromagnetic-induction metal detector, by contrast, is more objective in that it records the millivolt (mV) amplitude response of the subsurface at 26 geometrically spaced time gates from 0.177 to 25.010 milliseconds (Geonics 2002). The currents induced in metal objects of different size, shape, strike, and orientation have different EM response amplitudes measured in millivolts (mV) and decay rates in mV per second (mV/s). Because of these differences a prediction of size

and depth may be made, and a target classification is possible. The EM method is

described in great detail in Chapter 2, such that further discussion is unnecessary here. It

must be noted, however, that the large upfront costs of the equipment (~ $70,000 U.S.)

and the learning curve of data processing are prohibitive to non-specialists. Moreover,

data interpretation can be difficult. To avoid subjectivity in data interpretation we

employ point-pattern analysis spatial statistics to detect *significant* clustering patterns

within the data sets. Our excavations tested the ability of the Geonics EM-63 time-

domain electromagnetic-induction metal detector to predict the nature of the subsurface

of the site.

Point-Pattern Analysis: Global and Local Spatial Statistics

MacDonald and Small (2009) have used point pattern analysis (PPA) statistics to

examine clustering at UXO remediation sites, namely the *k*-function analysis. The

authors were able to detect significant clustering where a visual inspection of the data

could not. Kvamme (1990) and Whitley and Clark (1985) have used global PPA to

analyze the spatial autocorrelation of terminal Maya long-count dates and more recently

Premo (2004) used local PPA to interpret regional trends within terminal long-count

dates from the Classic Maya Lowlands area. Ciminale and colleagues (2009) used local

spatial autocorrelation statistics to enhance archaeological and paleoenvironmental

features from satellite data over a Neolithic village site in Italy. Recent applications of

PPA to archaeology by Hill et al. (2011) and Miller (2011) have attempted to use

measures of local spatial autocorrelation to define site structure, activity organization, and site occupation span. PPA was used by Schwarz and Mount (2006) to model site location. Both local and global PPA spatial statistics have a wide variety of applications in archaeology. Here we expand their use to archaeological geophysical data analysis.

K-function analysis is a global spatial statistic, which can be used to determine the presence or absence of clustering at various distance scales (Getis 1984). The null hypothesis of the k-function is complete spatial randomness (CSR). Distributions that are greater than would be expected by chance are considered non-random, or clustered. In order to determine the significance of the k-function statistic from a data set we use the online software developed by Aldstadt and colleagues (2002). This program randomly generates N points (the number of observations) across the study area M times (the number of permutations). From these permutations a confidence envelope is created, which testes the null hypothesis (H_0) of CSR based upon the number of permutations, such that M=95 permutations tests the H_0 at the α=0.05 level; while M=99 permutations tests the H_0 at the α=0.01 level, etc. Values within the confidence envelope fail to reject the null hypothesis and are considered spatially random. Values above the confidence envelope are significantly clustered at that distance scale. Values below the confidence envelope are significantly dispersed, which may also indicate human behavior, as it is also non-random, but are beyond the topic of this paper. The equation for the weighted K-function is:

$$L_w(d) = \frac{\sqrt{A\sum_{\substack{i=1}}^{N}\sum_{\substack{j=1\\j\neq i}}^{N} z_i z_j k_{ij}}}{\sqrt{\pi\sum_{\substack{i=1}}^{N}\sum_{\substack{j=1\\j\neq i}}^{N} z_i z_j}} \qquad (2)$$

where A is the size of the study area, N is the sample size, d is the inter-event distance, z_i is the weight of point i itself, neighbors z_j are the points that lie within radius d of point i, and k_{ij} is the border correction for edge boundaries. The weighted K-function adds a Z component to the analysis, which is the channel-1 mV response in this study. This is an improvement over the simple unweighted K-function in that a third Z variable and location are used to define the confidence envelope. For the weighted K-function the Z variable is randomly generated to N points for M iterations in order to determine significance.

The global k-function, however, cannot be used to determine the location of clustering. Therefore we used the local $G_i^*(d)$ statistic developed by Arthur Getis and J. Keith Ord in order to *locate* significant clustering - or 'hot-spots' - within the data sets (Getis and Ord 1992, 1996; Ord and Getis 1995). The null hypothesis of the $G_i^*(d)$ statistic is that there is no association between the value of an individual point (x_i) and its neighbors (js) that lie within radius d of point i itself. Since the *local* weights within this radius are compared to the *global* mean $\overline{x}$ and variance s within the entire data set, this is considered a *local* statistic. Basically, the statistic measures whether or not the sum of the weights within the *local* search radii are greater than would be expected by chance when compared to the *global* mean and variance. The $G_i^*(d)$ in equation (1) differs from

the *K*-function (2) in that k_{ij} is the number of data points within distance *d* of point *i*,

otherwise, all variables are the same. The $G_i^*(d)$ statistic is a standard variate, which

means the output values at each point are analogous to *z*-scores, which we use to asses

significance about point *i* at various distances. The $G_i^*(d)$ statistic, however, often

violates the assumption of independence. Ord and Getis suggest using the Bonferroni

correction for multiple tests to control for this dependence and correct the Type I error,

or false positive, for the desired alpha. Although, with large sample sizes (*n*) Bonferroni

critical values for G_i^* may be too conservative (Getis and Ord 1996; Ord and Getis

1995:297-298). Therefore, we prefer the Šidàk correction:

$$1 - (1 - \alpha)^{1/n} \tag{3}$$

where *n* is the sample size and α is our probability of a Type I error, because this

correction is more powerful against Type II error, or false negatives (Abidi 2007; Šidàk

1967). This equation gives p-values, which must then be converted to critical values in

order to determine the significance of the $G_i^*(d)$.

   Interpretation of EM data sets can be difficult. Humans are excellent at finding

patterns in data whether such patterns exist or not. The use of these statistics was meant

to provide objective quantitative measures with which to assess significant patterns in

the data, free from the problems associated with subjective qualitative assessment.

Although it must be admitted that a qualitative approach to data interpretation must also

be used, especially in early stages of data processing. We used PPA statistics in order to

determine the *presence* and *location* of significant clusters within the EM data, namely a global weighted *k*-function and local $G_i^*(d)$ statistical analysis. The global *k*-function statistic was used to determine the presence or absence of significant clustering at various length scales. These length scales were then used to determine the location of clustering with the local $G_i^*(d)$ statistic, keeping with Anselin's (1995:112) recommendation that global measures of spatial autocorrelation "should precede the assessment of significant local spatial clustering." The last phase of this work was to test the utility of PPA spatial statistics by comparing their predictions against the actual site structure revealed by systematic archaeological excavation.

Archaeological Methods at Paint Rock

In 2009 and 2010 the Concho Valley Archeological Society (CVAS) used hand held metal detectors to identify subareas most likely to yield historic metal artifacts (Ashmore 2010), as is standard archaeological practice (Bevan 2006; Connor and Scott 1998). Use of handheld metal detection reduces the size and cost of more intensive geophysical surveys. In 2010 we built upon the work of the CVAS by surveying one of the subareas with a Geonics EM-63 transient controlled-source EM induction instrument. The EM data were acquired at a line and station spacing of 0.5 m over a 20 x 20 m grid for a total of 1,681 data points. The data was processed with typical drift corrections to account for the decline in battery voltage and diurnal variation throughout the survey. The data mean is -2.64 mV with a standard deviation of 23.80 mV and a

range of -109 to 484 mV. Statistical analyses of these data were then run in order to select locations with high probability of significantly clustered artifacts. From these areas we selected and excavated thirty-three 1 x 1 meter units in five centimeter increments, measured with respect to a Topcon RL-H3C laser level, which was calibrated daily to ensure the highest accuracy and precision. A greater elaboration of our methods is described in de Smet and colleagues (2012).

Results and Discussion

We acquired an EM data set in the summer of 2010 over a 20 x 20 m grid. The channel-1 mV response amplitude is mapped in Figure 15 along with the location of our 33 one-by-one meter excavation units as well. A weighted *k*-function on the mV response amplitude data from the EM-63 channel-1 receiver suggests clustering at all length scales at the Lee campsite when then entire data set is analyzed (Figure 16b). This result is expected at the site, since metal items related to various human activities have been discarded here for many years. We also analyzed a stratified sample of the data with a threshold of amplitude response values > 25 mV. Here (Figure 16a) the data were significantly clustered up to 2 meters and were spatially random at distances greater than 2 m. The reason for this drop in clustering length scales is due to two factors: (1) smaller samples have fewer neighbors within distance *d* of point *i*, and (2) these neighbors are greater in amplitude response because of the 25 mV threshold and therefore have a greater mean and variance. Essentially, smaller more subtle responses are only

statistically significant when there are many background responses, but less so when

they are compared with only the right tailed responses greater than one standard

deviation above the mean. This is similar to other statistics - like the chi-squared test –

where sample size affects the significance of the results.
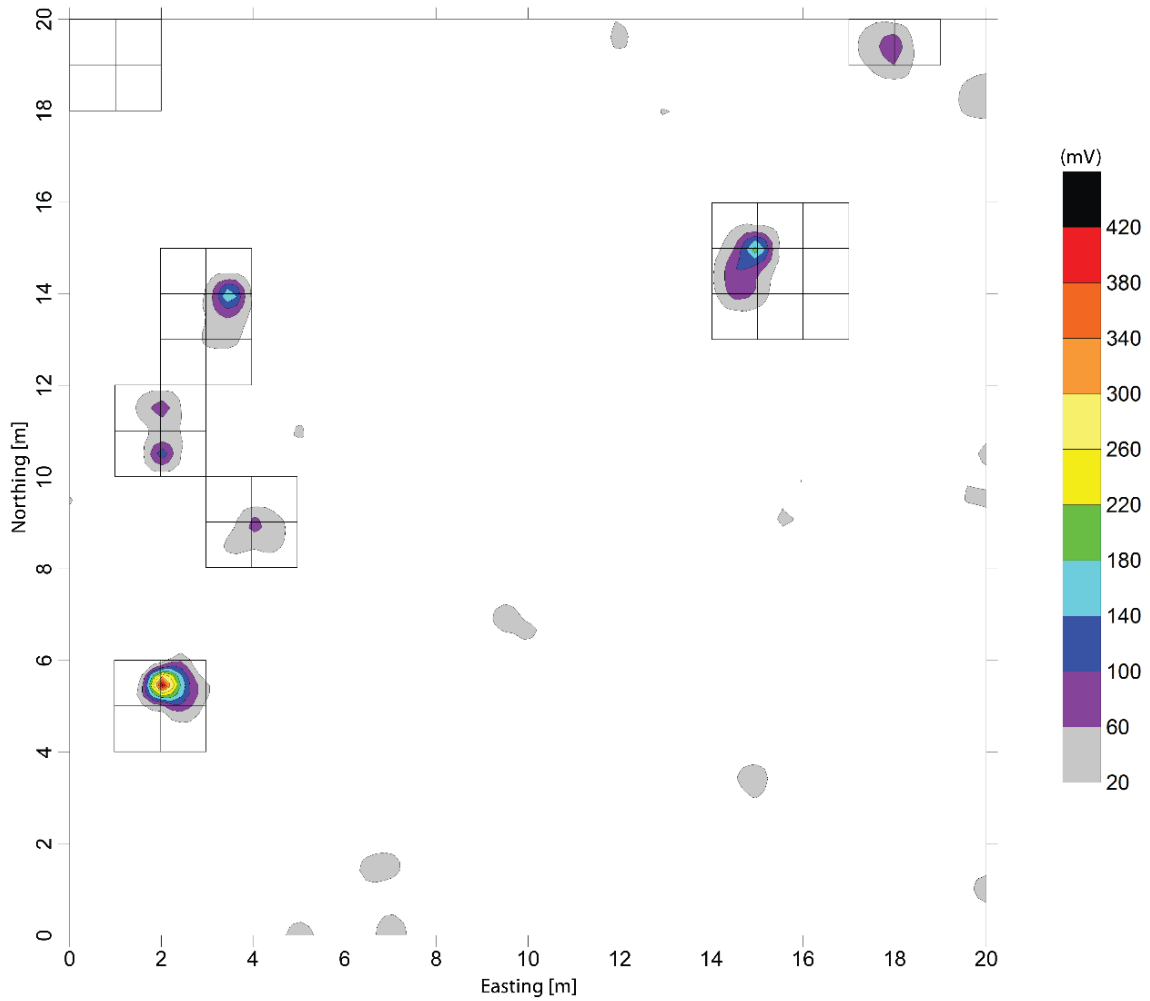
Figure 15. Geonics EM-63 time-domain electromagnetic-induction channel-1 data at 41CC295, in mV. Grid oriented north in m. For grid location at Paint Rock see Figure 11. Location of the thirty-three 1 x 1 m excavation units are overlain on the contour map.
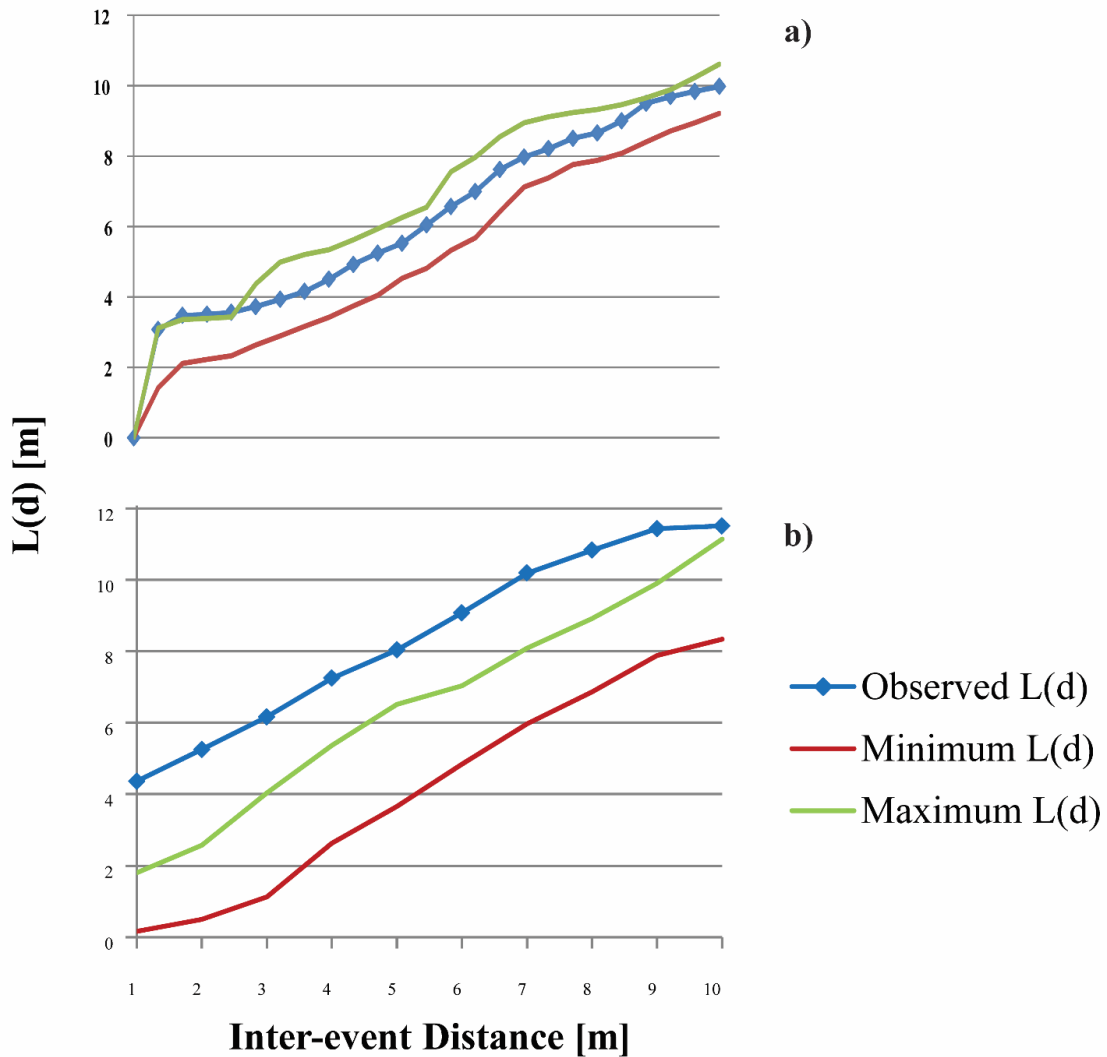
Figure 16. Weighted K-function of Geonics EM-63time-domain electromagnetic-induction channel-1 response at 41CC295 over (a) a threshold stratified dataset of response > 25 mV where *n*=58 and (b) over the entire dataset where *n*=1,681. The observed L(d) is greater than the maximum L(d) because the data are significantly clustered at all distance scales in (b) while significant clustering falls off to spatial random at distances > 2 m in (a).

We created a map of the $G_i*(d)$ values for every data point from the same data set. The local $G_i*(d)$ statistic values in Figure 17 indicate that there are a larger number of significant clusters at small distance scales like *d*=1 m, but fewer at large distance

65

scales like d=4 m. This is expected, since an increase in the number of neighbors

included increases as the search radius increases, such that at smaller distance scales

solitary large mV response values may appear to be clustered, when in fact they are just

lone, large objects. However, these lone large objects will exhibit a quick fall off from

clustered to non-clustered as more background values from the larger search area are

included in the statistic, thus driving down their G_i^* value. For instance, in 2011 we

found a horseshoe in situ in unit N5E2 (see Figure 15), and in adjacent units we found a

shotgun shell and nails belonging to the same horseshoe. The G_i^* significance values

indicated significant clustering of a distance < 2 m, which was confirmed by our

excavations. Even with the more liberal Šidàk correction the G_i^* significance value of

3.835, which corresponds to α=0.1 or a Type I error probability of 10%, is too

conservative. If instead we relax the G_i^* significance value threshold to those >3.0 our

correct prediction percentage is 85% [(13+15)/(13+3+2+15)], and the predictions are

significant at the α<0.0001 level (Table 5). The odds of such a distribution occurring by

chance are less than 99.99% (Drennan 2010; Shennan 1997).

Although excavations and analyses are still ongoing, numerous artifacts from the

military period have been found at the site (Figure 18). Temporally the assemblage at

Paint Rock, both the pictographs and artifacts encompass, then entire military period, pre

and post civil War, and those prior to and after as well (Table 6). Spatially, the artifacts

tend to cluster at the spring (41CC290) and along the still visible trail near the river fords

(41CC295). General service military buttons and musket balls are evidence of the

cavalry's presence at the site. The aforementioned whiteware and some cartridge casings also date to the period. Dark bottle glass is also is indicative of the military period.

Table 5. Chi-squared test for the local $G_i*(d)$ statistic based upon excavations at Paint Rock, where threshold is $G_i* >3.0$ (n=44) at $d=1$ m; $\chi^2=16.05$, df=1, p-value significant at $\alpha <0.0001$.

	Metal found during excavations (n=16)	No metal found during excavations (n=17)	Total
EM hits (n=15)	13	2	15
	true positive	false positive	
EM barren (n=18)	3	15	18
	false negative	true negative	
Total	16	17	33
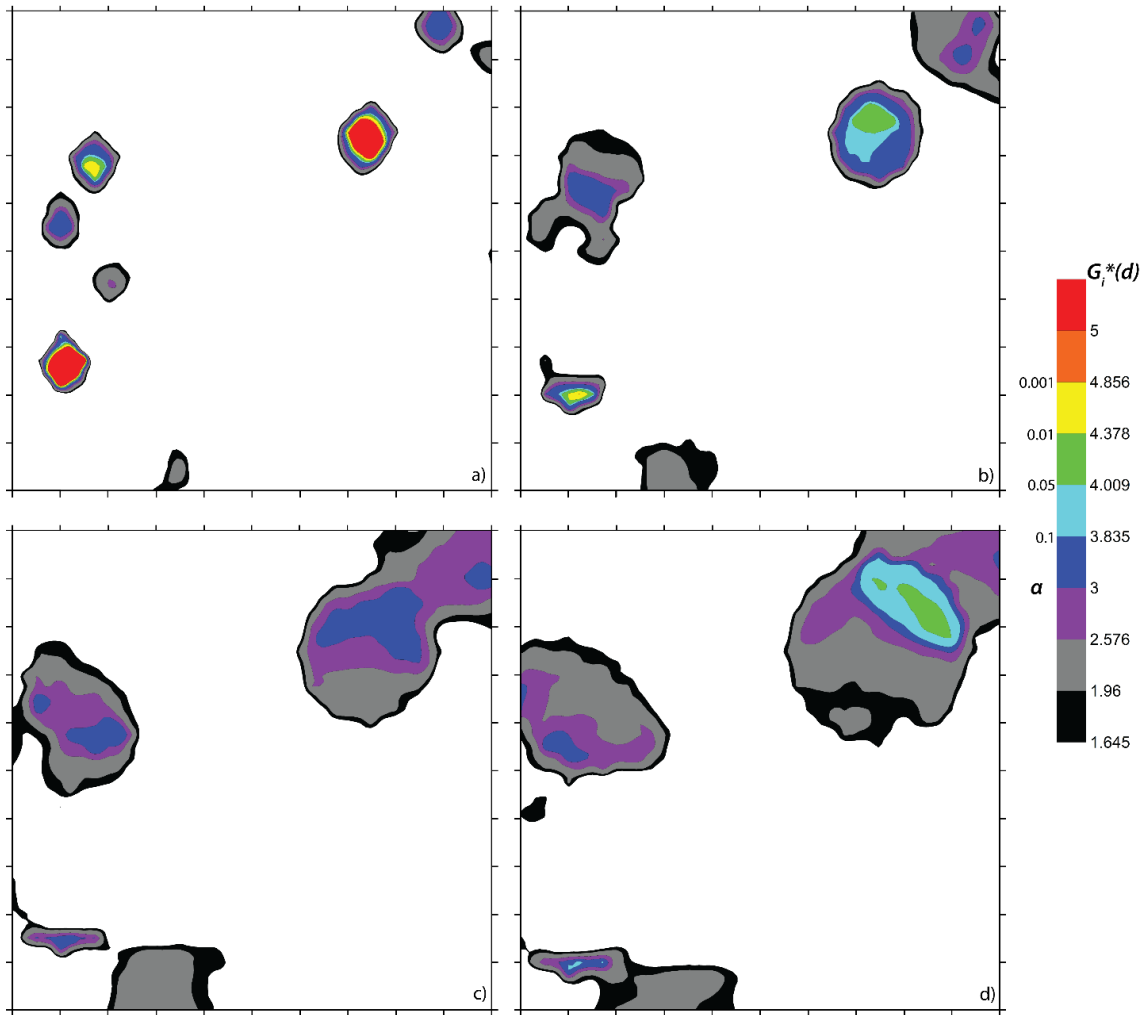
Figure 17. $G_i^*(d)$ **significance map at 41CC295: (a)** d **= 1.0; (b) 2.0; (c) 3.0; and (d) 4.0 m. Same 20 x 20 m grid as Figure 15, oriented north. The** α **is on the left side of the scale bar to illustrate this relationship between the** $G_i^*(d)$ **statistic values, p-values, and statistical confidence. Since the** $G_i^*(d)$ **values of 3.835, 4.009, 4.378, and 4.836 for** n**=1681 are equivalent to statistical p-values of** α**=0.1, 0.05, 0.01, and 0.001 respectively, the odds of a Type I error, or false positive, are 10, 5, 1, and 0.1%.**

Table 6. Select representative and diagnostic artifact assemblage at Paint Rock from sites 41CC290 and 41CC295.

Artifact Class	Count	Period	Comments
White earthenware	39 sherds	1840s or later	Few makers marks
Bottle Glass	51 shards	1915 or earlier	Black to purple
Toe-clip rim horseshoes	5	19th-20th centuries	An additional 11 horseshoe nails
Barbed wire	4	1880s or earlier	Saw-toothed
Shotgun shells	31	1880s or later	UMC; Peters; Western; Winchester
Musket balls/bullets	30	1870s or earlier	.69 cal musket; .58 cal Minie balls
Cartridge casings	78	1860s or later	50-70; .22 short
Metal military buttons	4	1840s to 1865	General Service Coat
Cut nails	121	1810s to 1890s	At least 11 horse shoes nails
Grafitti	21	1854-1875	Earliest date 1854 has no associated signature

Figure 18. Select diagnostic and representative artifacts from Paint Rock sites 41CC290 and 41CC295: (a) pistol frame and barrel, (b) picket pin, (c) three-tine forks, (d) .69 caliber musket balls, (e) toe-clip rim horseshoe, (f) decorative saddle skirt ornament, (g) Eagle and Stars powder flask, (h) saddle rings, (i) 3 Merry widows condom case, (j) flattened federal eagle buttons (k) federal eagle great coat buttons, (l) .58 caliber Minié balls, (m) spur.

Conclusions and Future Research

The use of electromagnetic induction and point pattern analysis statistics greatly enhanced our excavation strategy, resulting in a more time a cost effective project. The archaeological excavations revealed that the EM-63 precisely predicted the location of historic metal artifacts at the site. Further, there was a significant correspondence between the PPA statistics predictions and the actual pattern and distribution of archaeological remains reveal by systematic archaeological excavation. The dateable artifacts at site cluster around the decades prior to and after the Civil War and are located between the spring and terrace near the river.

The events that precipitated the Texas Rangers and U.S. Second Cavalry to pursue the Comanche with the intent to kill at Paint Rock were part of a policy shift which can be better explained by conflict event theory. This theory is a powerful analytical tool to explain not just history, but also the transformation of the archaeological record at Paint Rock from an Indian to Anglo dominated assemblage, as demonstrated by a dramatic shift in the material culture at the site in specific and on the landscape within just a few mere decades.

Our next phase of work is to analyze the firing pin signatures on the cartridge casings to identify the type and minimum number of firearms used at the site. We will also continue to identify more historic graffiti from the military period and ascertain the identity of the individuals who wrote them. We also plan further research into the little know battle between the Comanche and Texas rangers at Paint Rock in the 1840s. First,

a thorough historical background analysis - including primary and secondary sources - will be undertaken in order to ascertain the actual year of the battle. Then, we will search for the location of the battle with techniques similar to those utilized in this research.

CHAPTER IV

FATE OF THE HISTORIC FORTIFICATIONS AT ALCATRAZ ISLAND BASED

ON VIRTUAL GROUND TRUTHING OF GROUND-PENETRATING RADAR

INTERPRETATIONS FROM THE RECREATION YARD

Introduction

The interpretation of ground-penetrating radar (GPR) data is one of the primary

means by which archaeologists visualize and comprehend the significance of shallow

subsurface targets of interest such as historical remains (Conyers 2012, 2013; Goodman

and Piro 2013) – preferably this work in close collaboration with other specialists

including geophysicists, architects, and historians. GPR data can provide the basis for

three dimensional (3D) reconstructions of historic or prehistoric architecture

(Leckebusch 2003; Neubauer et al. 2002; 2014). While GPR interpretations are often

used, sometimes in conjunction with other geophysical or remotely sensed information

such as lidar, simply to guide archaeological excavations (Conyers and Leckebusch

2010; Hargrave 2006), they are more powerfully employed as scientific evidence that

can be used to support or weigh against hypotheses about site formation. Perhaps the

best interpretations of GPR data are those for which the archaeologist and the allied

skilled team discern the same patterns and come to consensus about their significance.

Archaeological excavations are inherently destructive and permanently remove

buried artifacts from their primary context. It is sometimes said that archaeologists are

like doctors who kill their patients in order to make a diagnosis! Ground-truthing by excavation, which can include drilling, trenching and tunneling, is certainly the most reliable method to assess, validate and refine archaeological hypotheses that are based upon interpretations of geophysical data. However, apart from being destructive, ground-truthing is time consuming and labor intensive. Moreover, for many important historical structures excavations may not be desirable or even feasible. An ideal archaeological investigation of the subsurface based significantly upon an interpretation of geophysical data would be accurate and reliable enough to require minimal excavations, thereby preserving valuable non-renewable cultural resources *in situ* for future generations.

We describe herein a virtual ground-truth (VGT) approach based on GPR data and interpretations as a means of creating and testing archaeological hypotheses about the construction, use, and eventual fate of the 19th century military fortifications on Alcatraz island in California. This is accomplished without disturbing the subsurface and perchance compromising extant buried cultural resources. The main objectives of this paper are twofold: 1) to conduct VGT by employing interpretations of attributes of GPR data acquired within the recreation yard at Alcatraz to enhance site formation models generated from prior information such as historic map georectifications and photographs; and 2) to demonstrate that integration of geophysical interpretations with remote sensing data, in this case lidar scans, is a viable method to practice historical preservation and enhance cultural studies that explore the developmental history of iconic landmarks such as Alcatraz.

Figure 19. Map of San Francisco Bay showing Alcatraz island and Fort Point. Red on the state of California inset map is the location of San Francisco county.

Alcatraz Island

The study area is a well-documented historic archaeological site: the recreation yard on Alcatraz island in California. Alcatraz is located in San Francisco Bay within the Golden Gate National Recreational Area (Figure 19), and is maintained under the auspices of the U.S. National Park Service. Alcatraz has become an American cultural icon and major tourist attraction. It has been the setting for numerous books, television

programs, video games, and motion pictures that contribute to the lore of the island and have captivated popular attention for decades (e.g. Abrams 2012; Bay 1996; Campbell 1964; Frankemheimer 1962; Siegel 1979). Over one million tourists visit the island annually (Wellman 2008). Much of the iconic status of Alcatraz owes to mythology built up around the prison, its notorious prisoners such as Al Capone and their various exploits, fights, riots, and escape attempts. Although much of the interest in Alcatraz may be classified as "dark tourism" (Loo and Strange 2000; Strange and Loo 2001), the site also serves as a natural laboratory for scholarly investigations into 19th century American military history. The National Park Service is currently tasked with preserving the cultural resources at Alcatraz island, a difficult and costly job exacerbated by the effects of the corrosive marine environment on the historic metal and concrete structures. For several years the Concrete Industry Management summer field school has contributed to this effort by actively training students in the scientific art of historical concrete preservation at the site.

While there is no shortage of popular historical accounts of "the Rock", Erwin N. Thompson's (1979) comprehensive history of the island is an important early study based in large part upon primary archival documents. A number of scholars have written about the penitentiary era and the subsequent 1969-1971 native American occupation (Loo and Strange 2000, Strange and Loo 2001, Ward and Kassebaum 2009), while Martini (2004) has written specifically about the history of Alcatraz as a 19th century military fortification. Recently, the consultant firm Mundus Bishop compiled an updated history of Alcatraz as part of its extensive cultural landscape report (CLR 2010).

In this research we employ GPR interpretations from 500 MHz survey data acquired at the recreation yard in December 2013 in order to illuminate an often overlooked period of the island's history, namely the epoch 1852-1907 during which the island functioned principally as a strategic harbor stronghold during the "initial military" (1847-1867) and later "earthen" (1868-1907) fortification periods. The military use of Alcatraz island has long been recognized to be of historical and archaeological significance. The location, extent, and integrity of subsurface architectural remains from this era, however, are largely unknown and many of the historic archaeological features may have been partially or completely destroyed during construction of the prison. The GPR survey provided an opportunity to image some of the remnants of the late 19th century fortifications, many of which appear on historical maps, photographs, and modern georectifications.

19th Century Historical Context

Understanding the historical context upon which the archaeological canvas is painted enables a more nuanced and thoughtful interpretation of the archaeological record. In order to properly interpret the subsurface remains of the fortifications on Alcatraz it benefits to briefly explore U.S. military technological developments during the nineteenth century. Following the War of 1812 the U.S. invested heavily in coastal fortifications to protect its major harbors along the Eastern seaboard (Kaufmann and Kaufmann 2005). In 1821 this "Third System" of coastal fortifications employed large,

77

imposing masonry constructions of stone or brick (Floyd 2010; Konstam 2003). A common element of these defensive works were seaward-facing batteries with numerous gun emplacements aimed towards the expected direction of the enemy threat. Such gun emplacements were of two types: (1) casemated employments with limited traverse protected by overhead "bombproof" roofs, and (2) barbette with 360 to 180 degree traverse but no overhead cover. The latter type were deployed at Alcatraz, as illustrated in Figure 20.
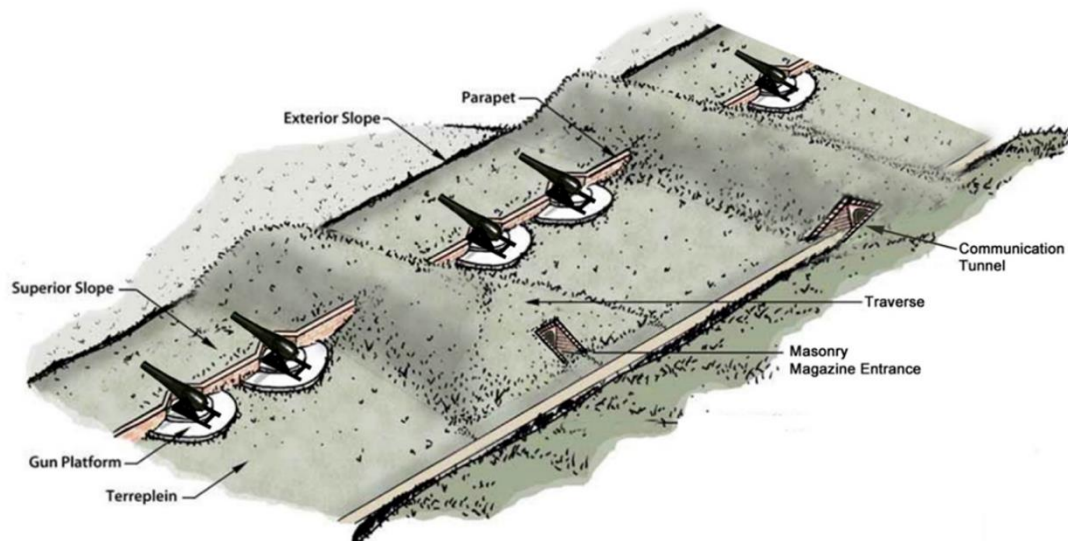
Figure 20. Illustration of common military earthwork architectural features deployed at Alcatraz [credit: Golden Gate NRA, Fort Point/GG Bridge CLR, with alterations by John Martini].

During the Polk administration (1845-1849) the doctrine of Manifest Destiny became quasi-official government policy and had brought the United States into territorial disputes with United Kingdom and Mexico involving Oregon and Texas, respectively. Diplomacy settled the Oregon question, but the U.S. and Mexico went to

war between 1846-1848 over Texas. In June 1846 Yanquis began the Bear Flag Revolt and claimed an independent California Republic after defeating Mexican forces at their army barracks in Sonoma and by July 1846 two U.S. warships had come to claim Alta California Territory for the United States by raising the U.S. flag at the customhouses in Monterey and San Francisco. During the war U.S. Major General John Charles Freemont purchased the rights to Alcatraz island because of its strategic value to protect San Francisco Bay from invasion by sea. At that time Alcatraz was a barren uninhabitable rock without freshwater or topsoil known as either La Isla de los Alcatraces (Island of the Seabirds) or more colloquially as White Island due to copious amounts of guano left behind by the eponymous seabirds.

In January 1848 gold was discovered in the Sierra Nevada mountains leading to a rush on the territory and an increase in the level of activity in San Francisco Bay. After 1850, when California achieved statehood, the population of San Francisco rose dramatically. The need for a coastal fortification to protect these assets remained evident to the U.S. government at the time. Construction of Third System fortifications began in 1853 on Alcatraz island and also at Fort Point on the southern margin of the Golden Gate strait (see Figure 19), which marks the Pacific entrance to San Francisco Bay. The fort on Alcatraz boasted seaward-facing open-air masonry batteries with guns aimed toward the Golden Gate. This emplacement (Figure 21a) became the largest fortification of its type west of the Mississippi River. On the eve of the American Civil War (1861-1865) the fort on Alcatraz island was both a physical and symbolic expression of American power and westward expansion.
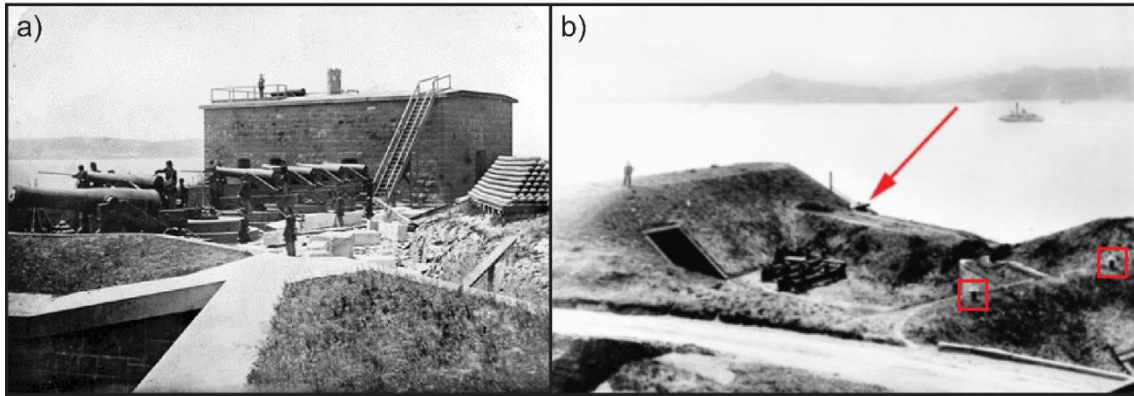
Figure 21. (a) Third System masonry [credit: National Archives] and (b) later earthwork fortifications on Alcatraz Island facing the city of San Francisco [credit: Golden Gate NRA, Park Archives, Interpretive Negative Collection, GOGA-2316]. Note the caponier, the brick building in (a), was later reduced to half its height and then buried (its location is marked by the red arrow) during the earthwork fortification period of the island's history. Also marked in red squares are ventilation ducts above the masonry magazines.

During the Civil War, Alcatraz served mainly as a deterrent to Confederate ships such as the CSS *Shenandoah*, which was known to have attacked Union commercial whaling vessels in the Pacific (Field 2011). Military technology and tactics change rapidly, however, and the heavy masonry structures erected to protect San Francisco Bay were obsolete even before their construction had finished (Field 2011; Floyd 2010; Martini 2004). During the Civil War the new rifled-cannon technology proved effective against Forts Sumter, Morgan, and Pulaski (Floyd 2010; Martini 2003), all of which were Type III masonry fortifications. Rifled cannons have a longer effective range and can fire larger projectiles faster and more accurately than the smooth-bore cannons used during earlier parts of the nineteenth century (Field 2011). Soon after the Civil War, newly built fortifications became principally of earthwork construction. Instead of collapsing into a rubble heap like masonry, earthworks can better absorb the energy of a

rifled artillery barrage. At Alcatraz starting in 1868, the existing masonry fortifications were rebuilt as earthern structures (Figure 21b). Sand and soil were brought in from the neighboring Presidio and Marin headlands and gravel from Angel island. Grasses like alfalfa were grown on the traverses, or earthen embankments, to stabilize them against erosion on the windswept and rainy island. The diminished requirement for a strategic coastal fortification, coupled with the expenses associated with its maintenance, led to the end of the military fortification era at Alcatraz. The earthworks were abandoned by the early 20th century as the island gradually transitioned from a harbor fortification to a military prison and then, from 1934-1963, into the notorious maximum-security federal penitentiary.

Recreation Yard

Construction of the military prison occurred between 1908-1912 (Figure 22a,b) and, at its completion, was reputed to be the largest concrete structure in the world. The grounds that would later become the recreation yard were originally used as a stockade. The stockade was built directly over two gun batteries labeled 6 and 7 and three earthen traverses known as I, J, and K (Figure 23). These military elements, whether left intact or partly demolished, were in any case covered with construction fill of unspecified provenance to form a level surface. The concrete bleachers on the southeast side of the recreation yard (Figure 22c) were built directly on top of outcrop bedrock in 1936 (CLR 2010; Thompson 1979). The entire recreation yard floor was covered by unreinforced concrete in 1936, save for the horseshoe pits and the baseball diamond which were left

unpaved. The shuffleboards, located just in front of the bleachers (see Figure 22d) were

one of the last additions, probably between 1956-1962, just prior to the closure of the

prison in 1963.

During the Alcatraz maximum-security federal penitentiary era (1934-1963) the

recreation yard became an outdoor facility within which prisoners in good standing

could take exercise and fresh air for a limited amount of time mostly on the weekends

(Figures 4c,d). The amenities included shuffleboards, horseshoe pits, handball courts, a

baseball diamond, and later basketball courts and a weightlifting area, as well as

bleacher seating in the form of concrete steps. Inmates also played games there such as

chess, bridge and dominoes (Ward and Kassebaum 2009). The yard is approximately 78

x 33 m in its maximum dimensions and was enclosed by a 5 m high concrete perimeter

wall and a fenced sentry walk (Martini 2004), the latter now in a state of severe

disrepair.
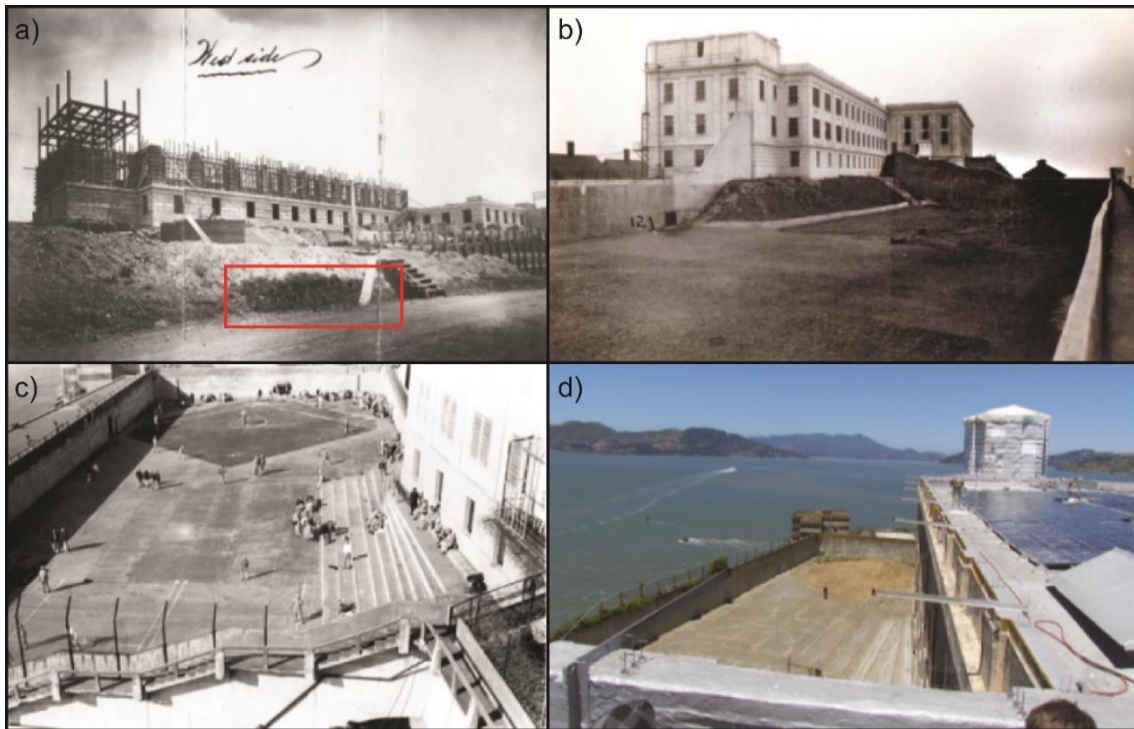
Figure 22. (a) The construction of the military prison, with stockade in the foreground [credit: National Archives]; (b) the stockade during the military prison era [credit: Golden Gate NRA, Park Archives, William Elliot Alcatraz Photographs, GOGA 40058]; (c) The recreation yard during the federal penitentiary era [credit: Golden Gate NRA, Park Archives, Betty Walker Collection, GOGA]; (d) the recreation yard today as part of the national park. Note that during the military prison era the recreation yard had a grass surface, but during the federal penitentiary era it was converted to concrete. Note the dark stains of the original soil versus the lighter colored soil fill placed during the construction highlighted in red in (a).
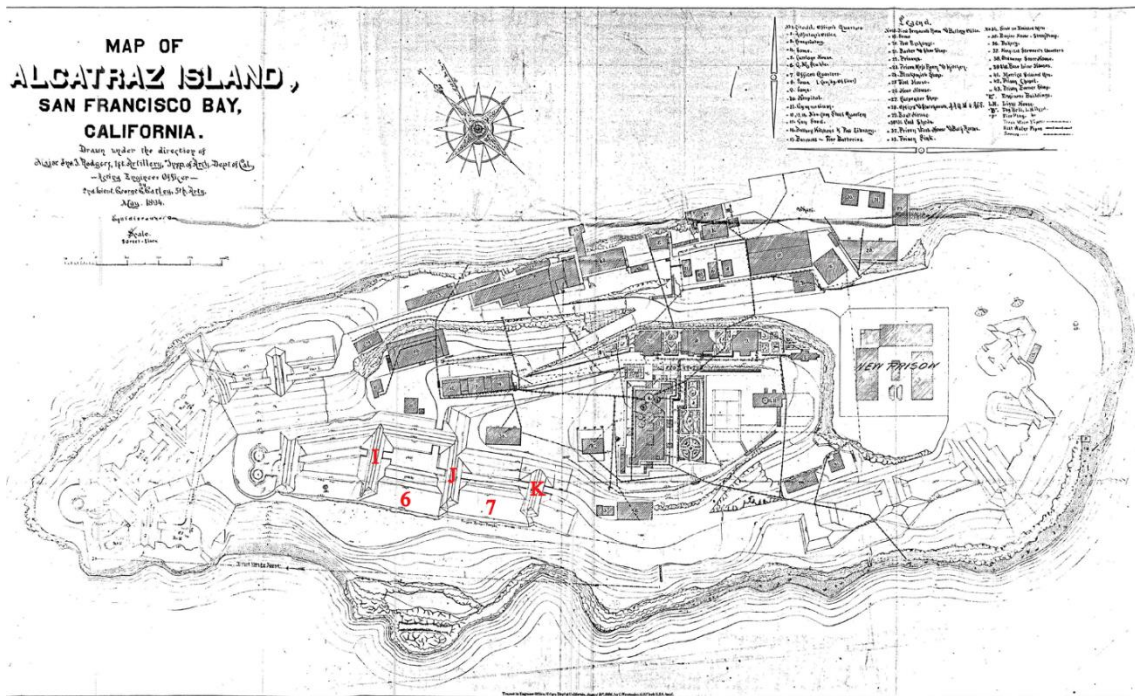
Figure 23. Historic map of Alcatraz island c.1894 with Traverses I, J, and K and batteries 6 and 7 noted in red.

Georectification Modeling

Georectification is the process by which an image is transformed or projected onto a prescribed geodetic coordinate system. In order to conduct the VGT, georectification of a historic map (c.1894; Figure 23) was performed using Esri ArcGIS software version 10.2. The locations of some of the extant structures in a modern image, like the north caponier building, were matched to their locations as they are depicted on the historic 1894 map. The resulting map was then transformed and reprojected into modern UTM coordinates (Figure 24). Georectification from historical maps is

challenging, however, due to the limited number of control points, such as the north

caponier, and the historical inaccuracy of distance scales and relative positioning.

Moreover, the 1894 map attempted to present a 3D perspective in plan view, which

always proves quite difficult. Thus, our georectified images should be viewed as GPR-

testable hypotheses of the actual locations of the now-subterranean traverses. The 2D

georectification was taken a step further by extrapolating existing 2D plans of the

fortifications (e.g. Figures 5 and 6) into 3D using SketchUp automated computer-aided

design and drafting (auto CAD) software (Figure 25) and then placing the 3D sketched

model into the context of a terrestrial laser scan (TLS), commonly referred to as lidar

scan. An exploded view (from top to bottom) of the lidar scan, a GPR data cube (to be

discussed below), the SketchUp model, and the geo-rectified map of the recreation yard

is shown in Figure 25. The green arrows in the sketch-up indicate entrance/exit points of

tunnels.
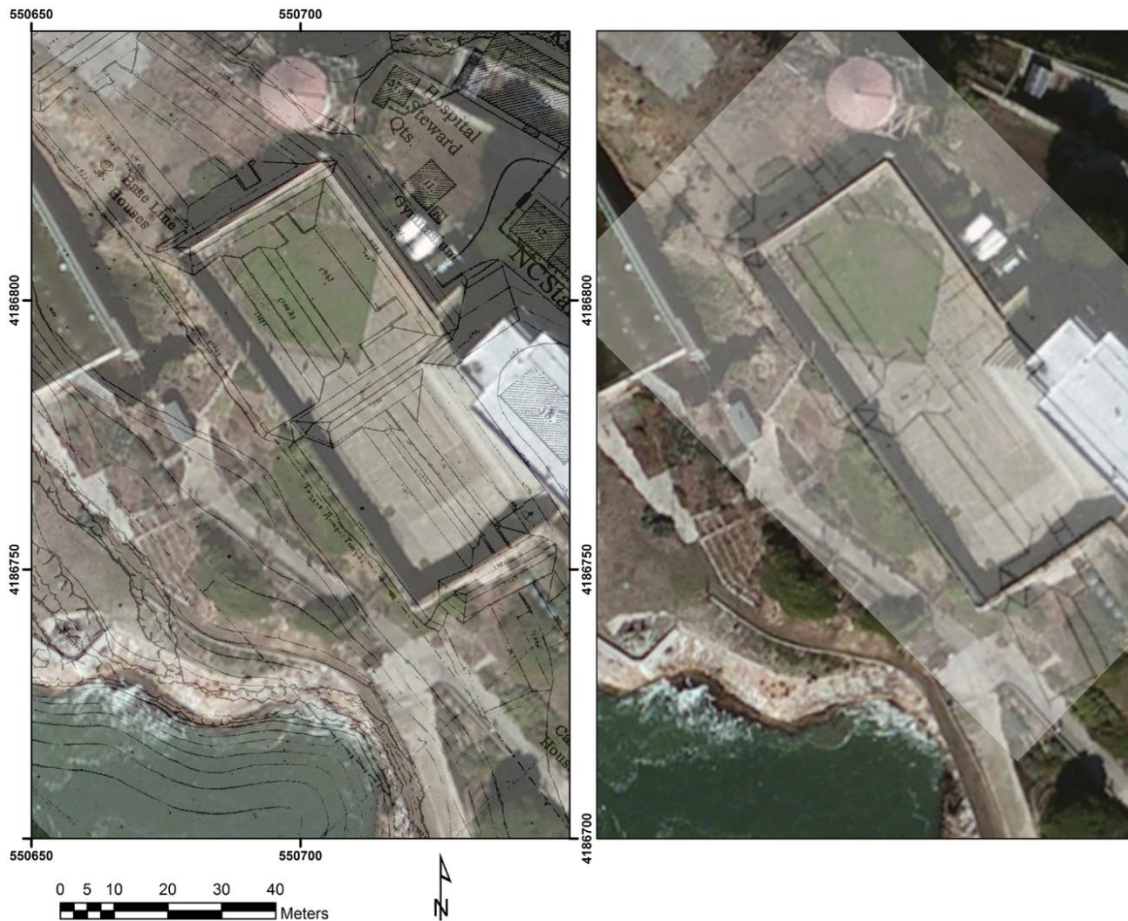
Figure 24. (left) Georectified model over the recreation yard based upon the 1894 map where Traverses I, J, and K can be seen from north to south; and (right) georectified sketch map of historic traverses I, J and K and batteries 6 and 7 based on 1892 ordnance survey map, overlain in by the approximate outline of the recreation yard walls (by Martini). The georectification on the left highlights the external architecture while the internal architecture of the masonry magazines and communication tunnels is shown on the right.

Based upon the information determined using the georectification process,

remains of cultural features associated with the "initial military fortification" (1847-

1867) were likely completely destroyed during the cutting and construction of the later

"earthen fortification" (1868-1907) period of the island's history, when the elevation of

the terreplein in the recreation yard was lowered from 39.6 to 33.2 m above sea level

(personal communication, John A. Martini). Therefore we hypothesize military features

to exist beneath the recreation yard, as mentioned above, and these include the possible

remains of traverse and bombproof tunnels I, J, and K, as well as Battery 6 and Battery

7, as indicated in Figures 6 and 7. In order to determine the location of these putative

archaeological features a GPR geophysical survey was performed at the recreation yard.
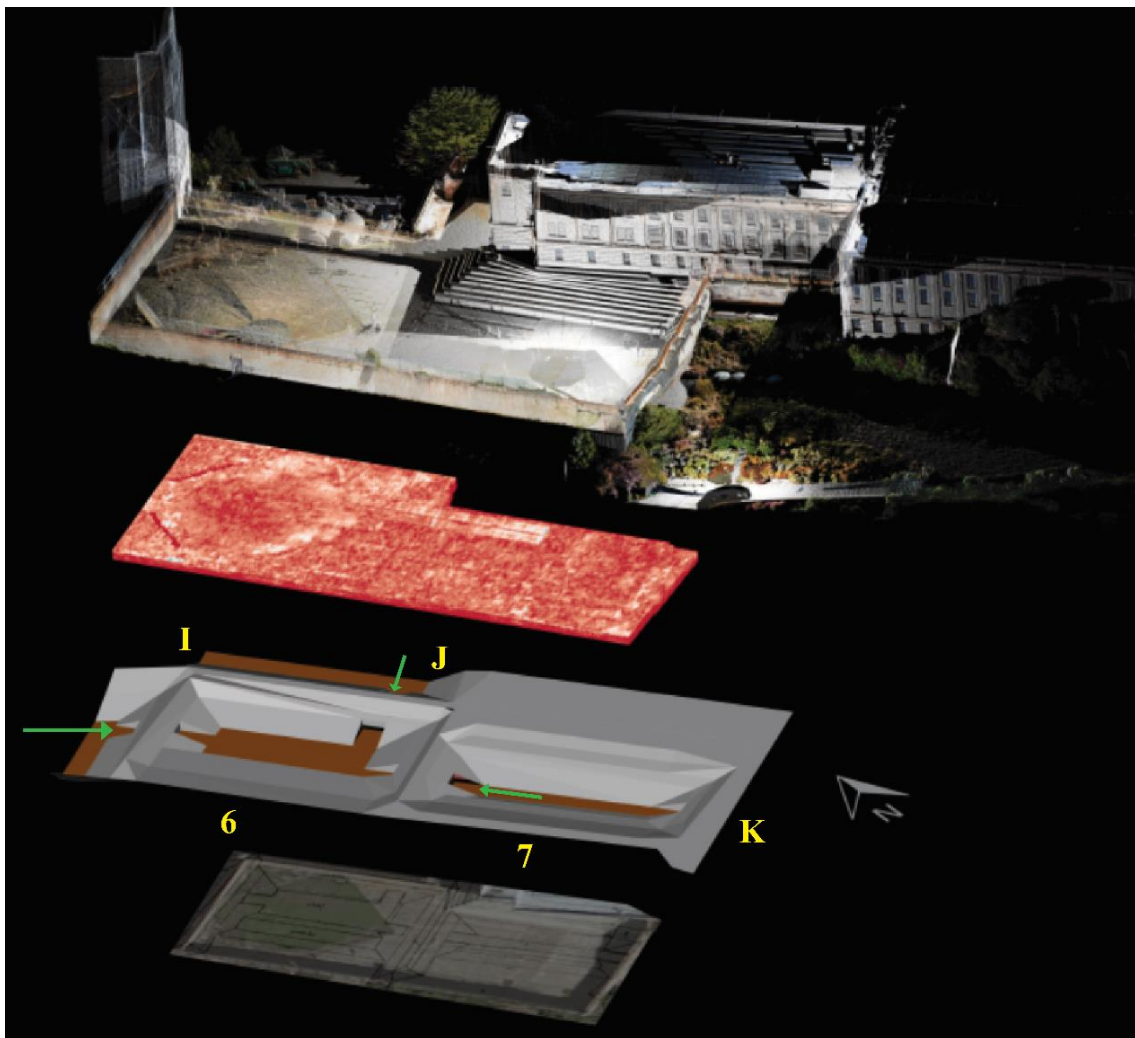
Figure 25. Exploded view (from top to bottom) of the lidar scan, a GPR data cube, the 3D SketchUp model, and the geo-rectified map of the recreation yard in 2D perspective. Green arrows point to communication tunnels between traverses. Traverses I, J, and K and batteries 6 and 7 are marked in yellow.

GPR and Laser-scan Acquisition and Processing Methods

The GPR survey using 500 MHz frequency antennas was conducted within the recreation yard in December 2013. An earlier survey at 200 MHz was performed but the resolution of subsurface targets of interest, such as traverse J, proved to be less satisfactory, as shown in Figure 26. Hereinafter we focus attention on the 500 MHz survey results. A total of 63 lines running north-south spaced at 0.5 m were acquired in a uni-directional continuous mode (triggered by a wheel odometer) of ~40 stations/m using bistatic Sensors and Software PulseEkko Pro transducers. The time window for each trace was 100 ns with sampling rate 200 ps, giving 500 samples/trace, while the in field acquisition stack number was set to 32. Preliminary editing to remove spikes and duplicate points and interpolate between dropouts was performed via visual inspection of the data. A semi-automated static correction procedure was developed and implemented in which time-zero of each trace was aligned to the first positive maximum of the radar ground-surface clutter return.
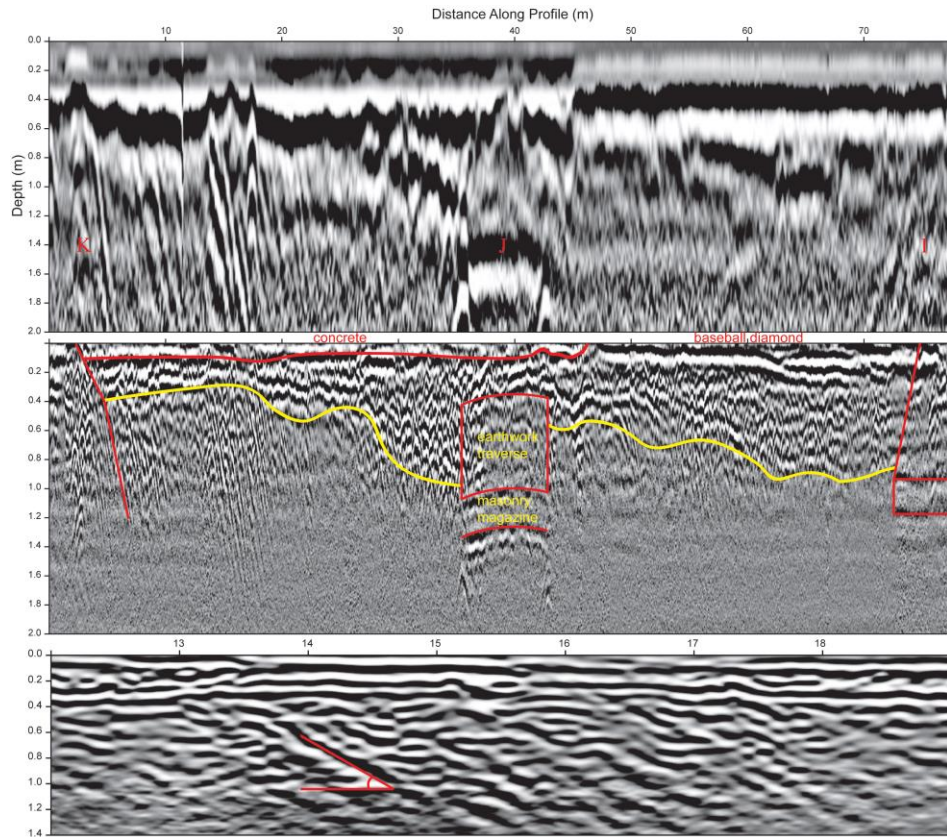
Figure 26. GPR sections showing the radar signature of buried traverse J (the prominent hyperbolic return in the middle of the sections, near the bottom at two frequencies: (top) 200 and (middle) 500 MHz data prior to migration; and (bottom) migrated close up of 12-19 m along middle 500 MHz profile with no exaggeration of vertical scale. The 200 MHz profile lacks the resolution of the 500 MHz profile due to the range-to-resolution trade-off. Architectural features associated with each of the traverses can be seen in profile from right to left I, J, and K. The thin red stratigraphic layer in the top left is the interface between the concrete added in 1936 and imported fill materials from the 1907 construction of the prison. The area in the top right is the baseball diamond, which was never overlain with concrete. The strata between the concrete and bottom of the imported fill material is demarcated with a yellow line and can also be seen in Figure 22a. The fill material below this is likely from the original traverses and slopes of the batteries. The red box in the center is the original earthwork traverse and the line below marks the reflection of the vaulted brick and concrete architecture, and dates to 1868-1907. The bottom profile demonstrates the difficulty of presenting long profiles with great vertical exaggeration. These look almost like point source reflectors in the top and middle profiles when exaggerated, but are probably analogous to – anthropogenically transported - onlap backdune deposits. Note the approximately 30 degree angle of repose of these sediments.

A comprehensive introduction to GPR is provided by Jol (2009), while the application and interpretation of GPR in archaeology can be found in Conyers (2012, 2013, 2016) and Goodman and Piro (2013). The GPR data processing sequence followed fairly standard procedures as discussed below. The Sensors and Software EkkoProject software was used to de-wow the radar traces and perform background average subtraction to ameliorate the effects of ground-surface clutter, followed by a trapezoidal bandpass filter with gates at 200-400 and 600-800 MHz. Migration was applied with a 2D FFT Stolt (1978) migration operator using a constant radar velocity 0.09 m/ns to convert time-to-depth and collapse reflections. This velocity is the mode of a number of estimations ranging from 0.064-0.101 m/ns from diffraction hyperbolae observed at varying locations throughout the survey area. The hyperbolae with the highest velocities (> 0.095) appear in the uppermost portion of the subsurface, i.e. within the surficial concrete layer, while the hyperbolae with the lowest velocities (< 0.085) appear at depth below the interface between the fill and brick architecture remains. Velocities ~0.09 m/ns are representative of the ~1.0 m thick earthwork rubble layer above the 1890's surface and it is the EM velocity used herein to migrate and transform two-way travel times to depths. Because of the decrease in velocity with depth, as indicated by the hyperbolae fitting, we might over-estimate depths below the tops of the architectural features, with a possible error of a few cm to ~10's of cm with increasing depth below ~1.2 m. Figure 27 provides an example of improperly and properly migrated diffractions showing the efficacy of our 0.09 m/ns migration velocity. Accurate archaeological interpretation of GPR data requires a migrated data volume (Böniger and Tronicke

2010a; Jacob and Urban 2015; Verdonck et al. 2015), because migration collapses diffractions and moves dipping reflections to their correct positions (Yilmaz 2001), and Zhao et al. (2013b) have demonstrated the importance of migration prior to attribute analysis. Attribute analysis if increasingly being used in advanced archaeological analysis (Zhao et al. 2015a). After migration of the GPR data at Alcatraz, the energy and instantaneous amplitude attributes were calculated. Lastly, automatic gain control (AGC) was applied to enhance the response of deeper reflectors with respect to their shallower counterparts. The attribute cube was then sliced into horizontal planes and the depth slices were displayed using the Voxler 4.0 program from Golden Software.
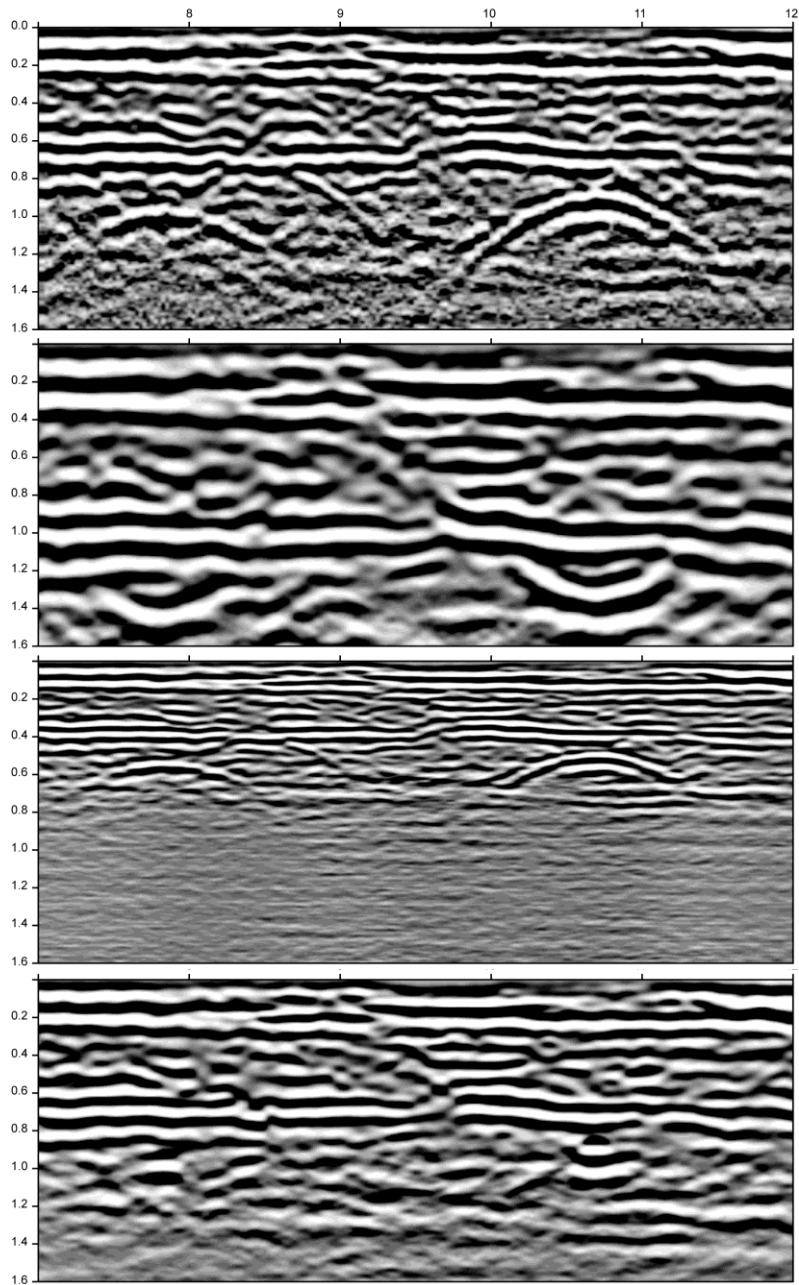
Figure 27. The efficacy of 0.09 m/ns migration: (top) profile before migration, note the two hyperbolic reflections at approximately 1.0 m depth; (second from top) data migrated at 0.13 m/ns, which is too fast, hyperbolae are not collapsed but over migrated to form smiley faces and also inaccurate depth estimates; (second from bottom) data migrated at 0.05 m/ns, which is too slow, hyperbolae are not properly collapsed by migration, and also at inaccurate shallow depths; and (bottom) data migrated at 0.09 m/ns, just right, and they are properly collapsed.

The energy attribute, which for each trace is a running average of squared sample amplitudes over a given time/depth window, is often used in archaeological prospection to detect high-energy reflections like foundations and walls (Böniger and Tronicke 2010a, 2010b; Conyers 2013, 2015; Udphuay et al. 2010). Energy attribute measures reflectivity within a specified time-gate (Zhao et al. 2012, 2013a, 2013b; Forte et al. 2012) and is positive-definite as it is a sum of squares. It can usefully highlight irregular or low amplitude reflections (Zhao et al. 2015b). The energy attribute, however, may possibly under-represent the strength of reflectors as the peak amplitudes are not connected via the Hilbert transformation, as they are with the instantaneous amplitude attribute, which calculates the amplitude envelope (Zhao et al. 2013a). The instantaneous amplitude attribute (also called "reflection strength" or "trace envelope") has recently been used in archaeology (Creasman et al. 2010; Khwanmuang and Udphuay 2012; Urban et al. 2014; Zhao et al. 2013a, 2013b, 2015b) and is an excellent indicator of variations in physical properties of materials due to impedance contrasts, stratigraphic boundaries, and porosity. Creasman et al. (2010) note that instantaneous amplitude is robust for interpretation because it removes many of the oscillations within a GPR trace. Both the energy and amplitude attributes attempt to decrease the subjectivity of an interpretation (Zhao 2013). Herein we present both attributes in order to emphasize and detect both strong and weak radar signals from subsurface architectural remains.

GPR was used in this study since contrasts in relative dielectric permittivity are presumed to exist between the different materials which comprise the subsurface beneath the recreation yard. The floor of the recreation yard is an unreinforced concrete façade

overlying unknown construction fill materials and remnants of military earthworks. The fill is likely composed of soil and sand possibly including an organic-rich Ap like soil layer (see Figure 22a,b). It is known from historical photographs that the interior tunnels and magazines of the earthworks were brick-lined in order to enable men to safely transport supplies during battle (see Figures 2 and 3b). The dielectric contrasts between concrete, soil and brick should be large enough to produce detectable GPR returns.

GPR is increasingly being used as a non-destructive testing (NDT) method and subsurface imaging technique for the evaluation of structural integrity, geometry, configuration, and physical properties of industrial transportation and civil infrastructure resources (Saarenketo 2009), geological features, and archaeology at cultural heritage structures (Pérez-Grarcia et al. 2013; Santos-Assunçao et al. 2014). Numerous recent studies, however, have used TLS and photogrammetry techniques at archaeological and architectural heritage sites to aid documentation, assessment, modeling, monitoring, management, and preservation planning (Al-kheder et al. 2009; Altunas et al. 2016; Castellazzi et al. 2015; Constanzo 2015; Domingo et al. 2013; El-Hakim 2007; Hakonen et al. 2015; Jaklič et al. 2015; Núñez et al. 2013; Pavlidis 2007; Plisson et al. 2015; Tapete et al. 2013; Yang et al. 2014 – amongst many others); but rarely in conjunction with other near-surface geophysical data (Entwistle et al. 2009; Lubowiecka 2009, 2011; Rogers 2014; Watters 2014). TLS data at the recreation yard were collected with the Riegl LMS Z390 instrument. This system can collect up to 11,000 points per second with a range of 400 m and accuracy of 2 mm, yielding 0.002^{0} angular resolution. The system includes an integrated and calibrated Nikon D200

SLR 12.3 megapixel camera, providing an RGB color value to each scanned point. To align and combine individual scans into a global point cloud, the scanner locations and several reference targets were positioned using a total station. The TLS data were then processed with Riegl's Riscan Pro Software. The scans of the recreation yard displayed in this paper represent a global point cloud of more than 20 million points. The TLS data are used herein as the foundational data set with which to integrate other information, such as GPR, and create a geometric reconstruction of the current above-ground and below-ground state of the island for historical preservation purposes. The TLS data can also be used independently to detect and locate historical markings, concrete patches and other modifications to original structures, and also cracks which can indicate potential subsidence and structural damage that may warrant mitigation.
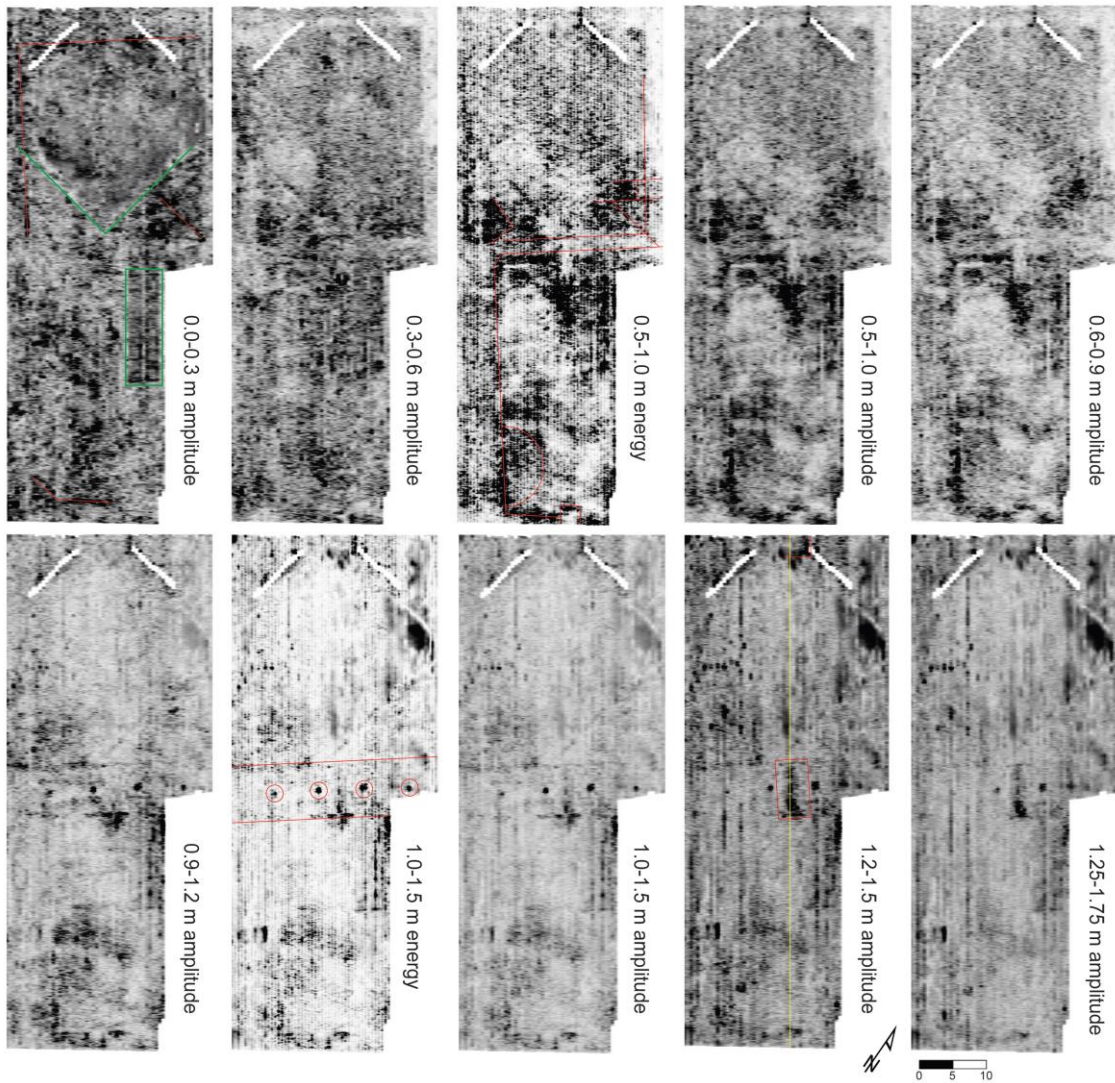
Figure 28. GPR energy and instantaneous amplitude depth slices. Red lines highlight architectural features seen in the georectifications in Figure 24 and dark (black) is high and light (white) is low amplitude. The yellow line in the instantaneous amplitude depth slice between 1.2-1.5 m is the profile seen in Figure 26. The linear white features in the north are uncollected areas due to the baseball diamond fence and the green in instantaneous amplitude depth slice 0-0.3 m are the baseball diamond and rebar reinforced shuffle boards, the last addition to the recreation yard and the only rebar in the recreation yard floor.

Presenting gridded geophysical information by projecting depth slices onto a 2D plan view is common in archaeology in order to provide context for geophysical interpretations. An example of this for the recreation yard is shown in Figure 28. While many clues can be gained as to subsurface structure, a conventional depth-slicing approach does not allow a truly immersive experience that can both enhance scientific insight and provide a compelling public dissemination of the information. Integrating above-ground lidar with subsurface GPR datasets provides a 3D real-world context of the modern built environment with which to create, view and refine interpretations of the subsurface geophysical information (Figure 29). As mentioned above, the lidar data also provide above-ground information that is useful for historical preservation purposes. The steel and concrete structures on Alcatraz, being subjected to the corrosive coastal environment, will continue to rapidly deteriorate; however, lidar/GPR documentation of the type presented herein permits the cultural resources of the island to be restored to their current state at some later date, printed in 3D, and curated in digital or traditional print format.
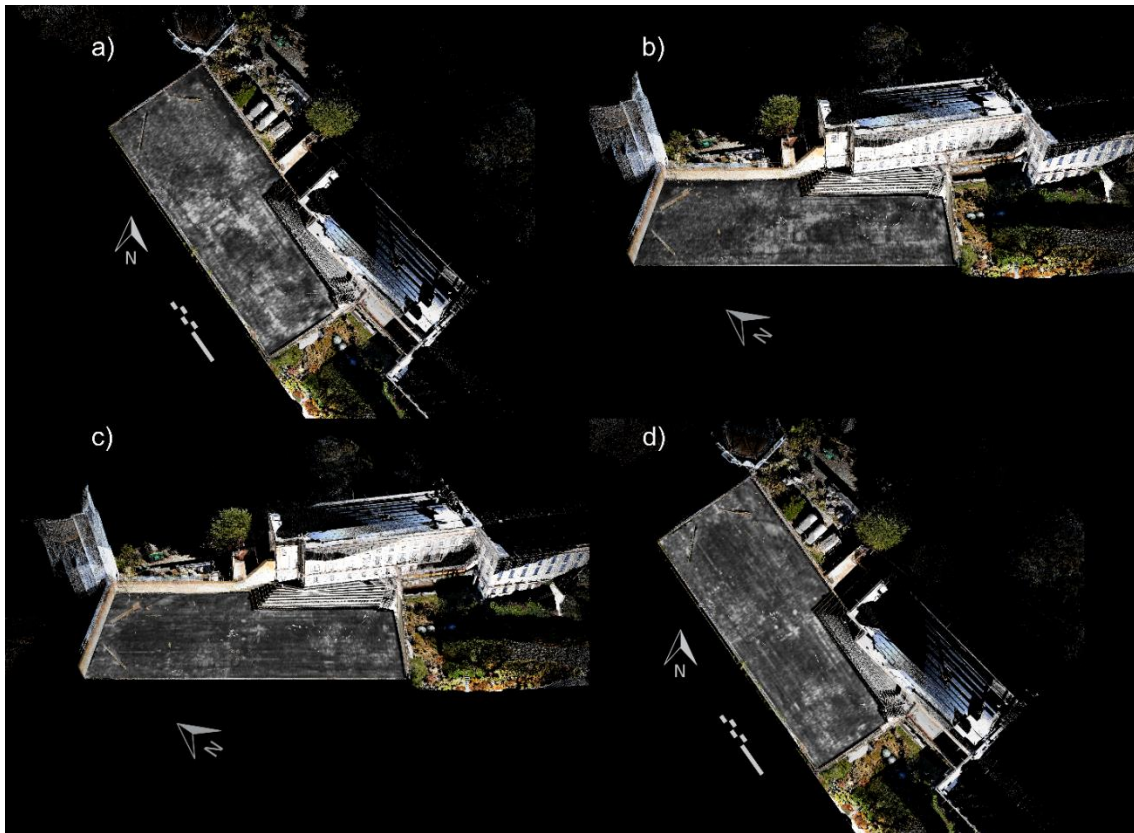
Figure 29. TLS and GPR 500 MHz instantaneous amplitude depth slices from the recreation yard, at: (a-b) 0.5-1.0 m; (c-d) 1.0-1.5 m depths. (a) and (d) show the common aerial view, while (b) and (c) show a 3D perspective view.

GPR Interpretation and Discussion

The interpretation of GPR data is always difficult, due to the complexities of electromagnetic vector wave propagation in strongly heterogeneous geological media. This is certainly the case for the task of discerning subsurface targets within the extensively anthroturbated strata underlying the Alcatraz recreation yard. Humans are remarkably proficient, however, at detecting and interpreting, or misinterpreting, subtle

patterns in data sets (Barrow and Bhavsar 1987). We constructed a georectified model of the original historic structures located beneath the present-day recreation yard to test against the GPR imagery in an attempt to lower the possibility of a poorly substantiated interpretation. Based upon the georectified historical 1894 map (Figure 24) it appears that there is a good likelihood that structural remains of portions of Traverses I, J, and K are present in the subsurface. We also utilize a quantitative attribute analysis of the GPR data in an attempt to decrease the subjectivity of our interpretations.

A qualitative visual comparison of the historical map and GPR data with the instantaneous amplitude and energy attribute depth slices between 0.5-1.0 m (compare Figures 7, 10 and 11) reveals distinctive linear patterns in the GPR images. Some of these patterns can be interpreted as the external architecture or façade of traverses; especially notable is traverse J in the center, running east-west across the width of the recreation yard. Moreover, a northwest-to-southeast trending linear feature in the energy and instantaneous amplitude depth slices between 0.5-1.0 m may be the parapet wall of battery 7. As the possible parapet wall is aligned with the direction of data acquisition, this could also represent a line leveling artifact; however, the feature does appear in several adjacent lines and is not continuous along any single line. A semi circular anomaly in the southwest also appears to abut the parapet wall and may be a signature of the gun platform (Figures 2, 11, and 12). As expected, this anomaly extends into deeper amplitude slices. The lintel of traverse K can be seen in the 0.5-1.0 m depth section to the far south, while the lintel of traverse I and J show up more clearly at greater depth as the three traverses may not have been constructed at the same elevation or had the same

amount of earthen cover, as can be seen in Figure 21b and 12b. Also notable from Figure

21b and 12b is the approximately 45 degree angle that the parapet walls abut the

traverses, which can be seen in Figure 28 between 0.5-1.0 m below surface. In the

shallowest amplitude depth slice 0.0-0.3 m, the remnants of the exterior slope of battery

6 and earthwork from traverse I are visible to the north, while the external architecture of

traverse K is visible to the south, and extant surficial features like the baseball diamond

(green lines) and rebar in the shuffleboards (green box) are clearly visible as well.

Another semi-circular low-amplitude anomaly appears to abut the exterior slope of

battery 6 in the amplitude slice 0.3-0.6 m.
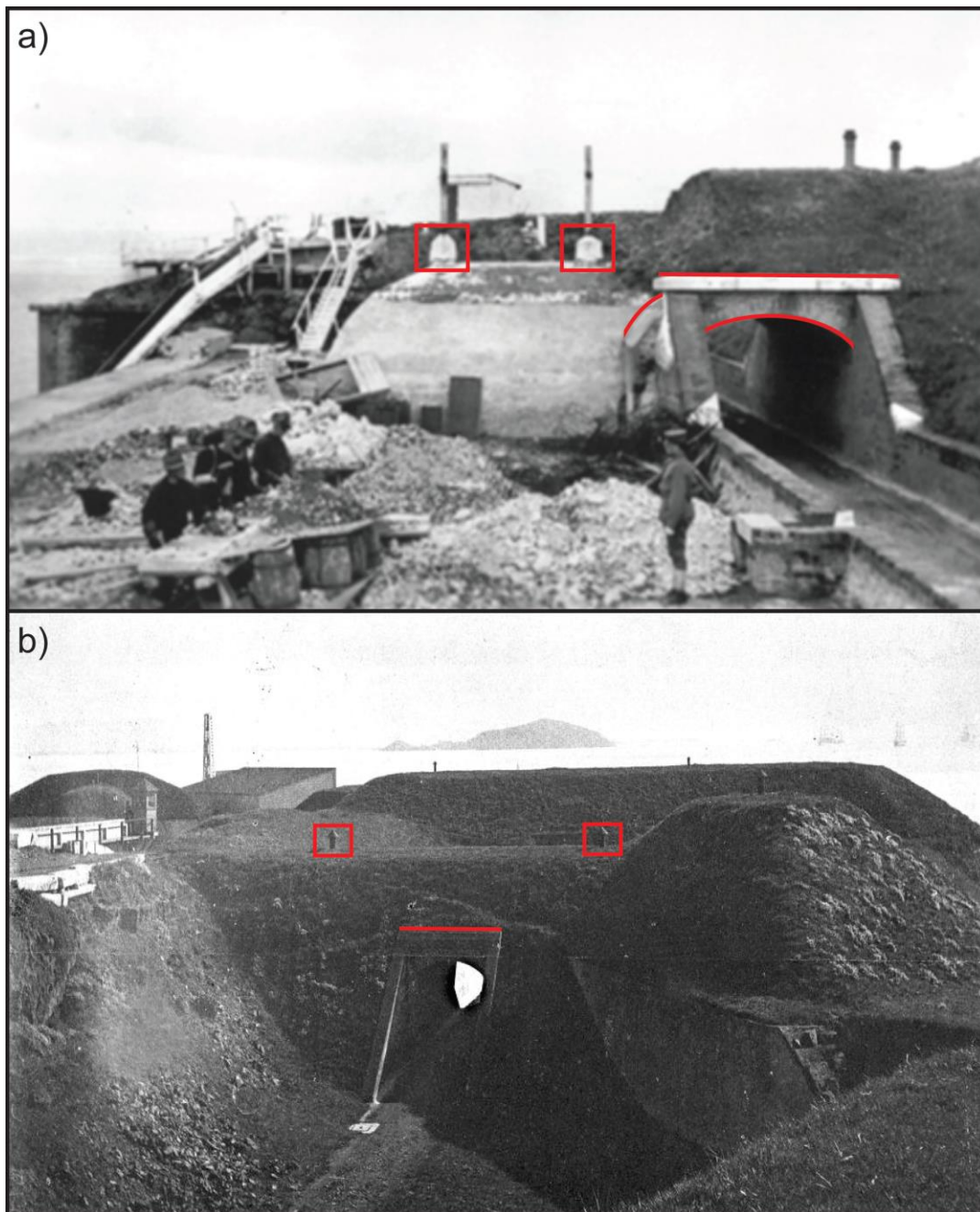
Figure 30. (a) Historical photo, taken during demolition of earthen fortifications c. 1910 on site of Battery 2, showing the ventilation ducts (two white cylindrical structures in red boxes) located at the top of the concrete magazine and vaulted brick and concrete architecture. National Archives, Record Group 92, OQMG, General Correspondence 1890-1914, Item #223810; and (b) photo showing common earthwork communication tunnel from the later 1800s with ventilation ducts and tunnel in red.

A deeper instantaneous-amplitude slice 1.0-1.5 m (Figures 10 and 11) shows four small circular high-amplitude anomalies which are aligned with traverse J as it cuts across the center of the recreation yard. These anomalies likely correspond to ventilation ducts which were located at the tops of the magazines, examples of which can be seen in the historical photograph, Figure 30. Moreover, two parallel linear features spaced ~7.5 m apart appear in red in the energy attribute depth slice 1.0-1.5 m (Figure 28). These likely indicate the interface between the facade of traverse J and the fill materials added during demolition of the batteries and traverses. The high-amplitude reflection highlighted by the red box in the instantaneous amplitude depth slice 1.2-1.5 m is likely the internal brick and concrete architecture of the vaulted communication and masonry magazine entrance tunnel of traverse J, which can also be seen in Figures 8 and 12.
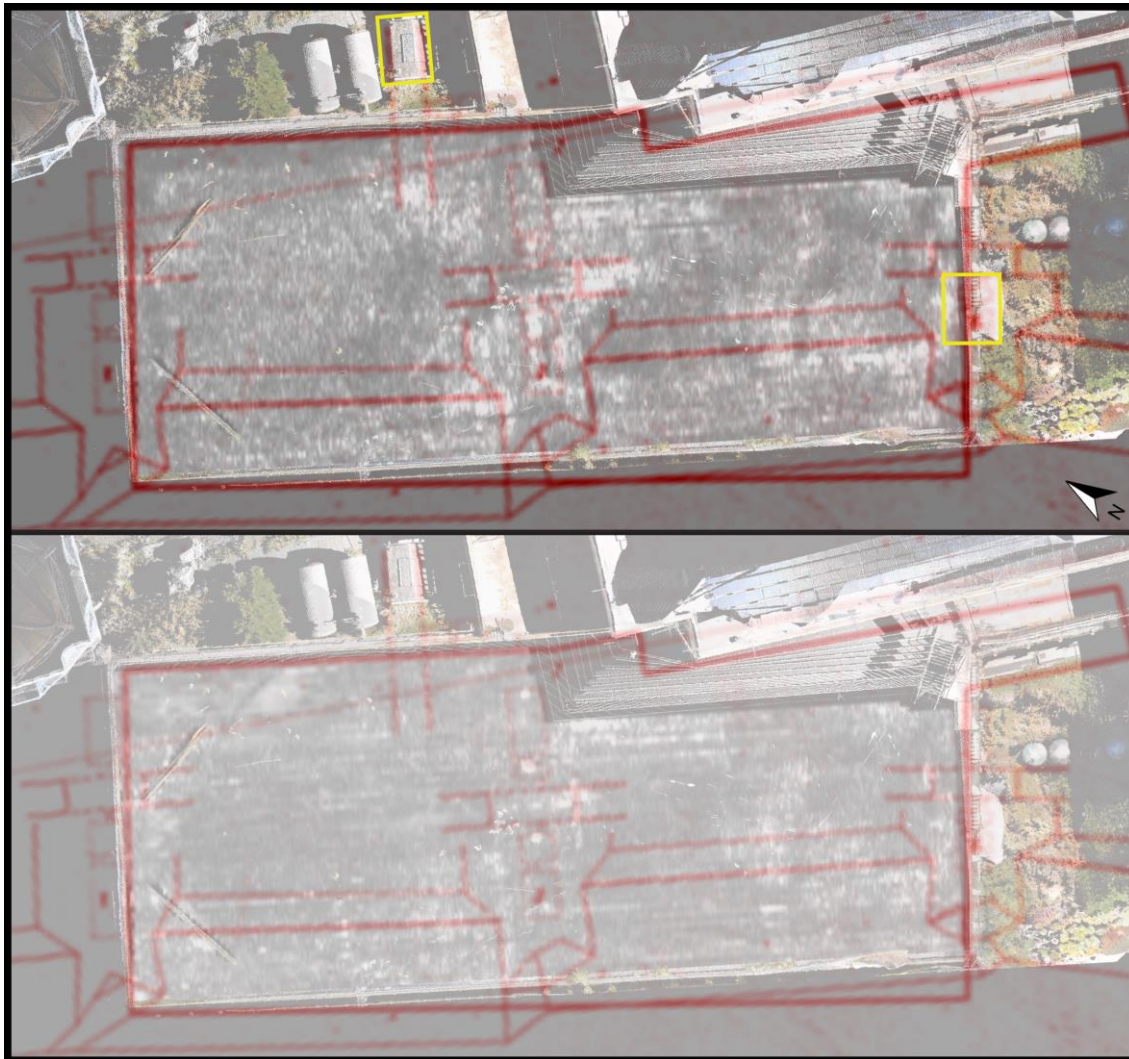
Figure 31. Improved georectification based upon GPR data at: (top) 0.5-1.0 and (bottom) 1.0-1.5 m. Yellow box on top is the morgue and yellow box on the right hand side is the remnant of Traverse K's magazine. Note the ventilation ducts align with the internal architecture at bottom.

The GPR images suggest that the georectification must be adjusted by rotating

the historic 1892 ordnance survey map slightly north and east (Figure 31). In order to

increase the accuracy of the historical model we locally georectified the model based

upon the subsurface archaeological features, rather than on extant surficial control

points. After adjustment, other archaeological features of interest become readily

apparent. The improved model is more consistent with visible extant features from the

late 1800s. The morgue (MacDonald and Nadel 2012) was built in 1910 over the

supposed location of a communication tunnel (yellow box on top in Figure 31). In Figure

24 the location of the morgue tunnel is inaccurate, but is corrected by the GPR data in

Figure 31 to line up seamlessly. The recreation yard wall was built directly over a

magazine from traverse K (yellow box on right in Figure 31) and the masonry

communication tunnel, which is also better localized based upon the model based upon

the physical GPR data. The model also agrees with the GPR data as the internal

architecture features of traverse J like the ventilation ducts are precisely where they are

predicted by the model (Figure 31 bottom). The instantaneous amplitude depth slice 1.2-

1.5 m correctly identifies the location of a high-amplitude contrast at the interface

between the vaulted masonry and concrete architecture of the communication and

magazine entrance tunnel beneath traverse J and the overlying soil of the original

traverse (red box in Figure 28); this reflection can also be seen in the GPR sections

shown in Figure 26. The architecture of the tunnels can be seen in historical photos

(Figures 12 and 3b). The historic photo in Figure 22a clearly shows the original dark soil

of the earthwork traverse overlain by a white fill material, and to the north and south of

the traverse the area had been filled in by a mix of light and dark soil, likely a mix of the

white imported materials and the tops of the battery slopes and traverses themselves,

which would have been leveled to the top of the parapet wall and used to infill the

terreplein. This can be clearly seen in profile in Figure 26, where the high-amplitude

reflections bounded by the yellow lines represent the white fill material, while the

original traverse and slope soils appear as in rubble lenses below.
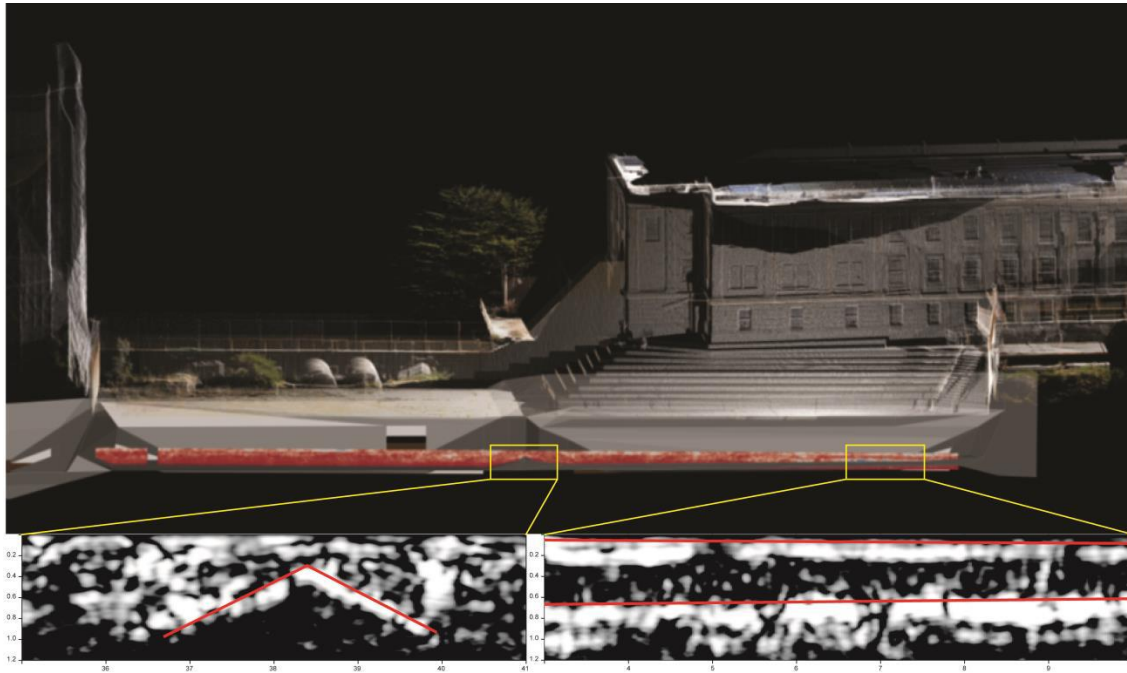
Figure 32. The 3D SketchUp model in its modern context as defined by GPR data, within context of TLS data, showing a GPR instantaneous amplitude profile with zoomed in portions of the profile highlighting the architecture of traverse J and parapet wall of battery 7 and thin concrete layer of the recreation yard floor.

The GPR sections shown in Figure 32 demonstrate the accuracy of the adjusted

model and the ability of migration and instantaneous amplitude attributes to collapse

reflections to their actual shape and place in space. The inverted-V-shaped high-

amplitude contrast in the center of the profile in the center of the recreation yard clearly

corresponds to the interface between the top of traverse J and the fill materials just ~0.3

m beneath the floor of the recreation yard. Moreover, to the south (right in Figure 32) the

105

high-amplitude contrast at depth likely signifies the interface between the parapet wall of Battery 7 and the overlying fill material. The high-amplitude contrast near the top of the profile is the interface between the concrete surface of the recreation yard floor and the subsurface fill. This is particularly interesting because it is so shallow. The unreinforced concrete veneer is only ~10 cm thick across the entire recreation yard and the historical structures appear to lie just beneath the veneer. This can also be clearly seen in Figure 26 where the concrete is evident as a thin layer. The use of migration and GPR attributes in depth slices and profiles clearly improved the detection and location of the historic military features.

Our georectification modeling and attribute analysis proved capable of detecting the precise location and extent of architectural and earthwork features; however, we were also able to determine what architectural elements were 'missing' and that large portions of the superior slope and parapet wall of battery 6 and a lintel and tunnel portion of traverse K were likely completely destroyed during the construction of the recreation yard and prison in 1907. Although absence of evidence is not evidence of absence, the absence of some features from the GPR data while others are readily apparent likely means they were partially or completely destroyed during construction activities, or outside of the range of the GPR data in the recreation yard survey. The exterior slope of batteries 6 and 7 and top earthen portions of traverses I and K were likely used to infill the terreplein until the borrow materials were exhausted and the white materials seen in Figure 22a were used instead. The white materials seen in Figure 22a may be poor quality batches of concrete from the construction of the prison and

remnants of deconstruction activates elsewhere (see Figure 30a) as other similarly colored materials like carbonates are not plentiful on the island. Although much of the top earthwork portion of traverse I was used for construction filling materials the interior masonry magazines and communication tunnel are likely intact slightly outside the area of the GPR survey in the recreation yard (Figure 31). Traverse J may have started off shorter than either I or K or with less earthen cover material, like the traverse seen in the foreground in Figure 30b. This in addition to its location at the center of the recreation yard are likely the reasons why traverse J alone of all the original earthwork traverse features from 1868-1907 remains nearly completely intact, yet buried, on the island. Knowing the location, extent, and integrity of these non-renewable archaeological resource is the first step towards preserving these invaluable in situ remains for future generations.

By using GPR interpretations to iteratively improve the georectification model and then further testing the refined georectification against GPR imagery, in a sort of feedback loop, we are able to accurately locate historically significant subsurface architecture beneath the recreation yard floor. Geophysical images can then be used to refine and possibly reproject the location of other archaeological structures on Alcatraz, beneath the recreation yard and elsewhere, which would then undergo further detailed VGT testing. Thus we suggest an iterative process to improve historical archaeological interpretations pertaining to the locations of historical architecture beneath the entire island. The methodology can be used at important cultural landmarks worldwide.

Conclusions and Future Research

A virtual ground-truth (VGT) was conducted over historic archaeological remains beneath the recreation yard on Alcatraz island. The VGT approach is flexible and recursive in that it tests historical information in the form of georectified models against geophysical data, here GPR. The georectification model is iteratively improved until the observed geophysical signatures and the georectified structures converge. The VGT approach is fast, cost and labor efficient, and it is non-destructive and accurate. The VGT approach was successfully used here to define the location, extent, and provide clues to the integrity of the subsurface archaeological remains of historical earthworks and associated military construction from a significant period in the 19th century development of a westward-expanding nation.

An attribute analysis of the GPR data provided a strong quantitative basis for the improving the accuracy of our interpretations by discerning between significant features of interest and background noise. The GPR attribute data clearly indicate the location, extent, and integrity of earthwork J, the internal architecture magazines and communication tunnel of traverse J, and portions of the parapet wall of battery 7. Partial remains of communication tunnels for traverse K, and battery 6 were also preserved, as well as the internal architecture of traverse I. However, limited evidence of tunnel lintels associated with traverses K and portions of the parapet wall of battery 6 indicate these features likely were partially or completely destroyed during construction of the

recreation yard and prison in the early 1900s. The use of energy and instantaneous amplitude attributes was instrumental in the successful results of this GPR study.

The integration of TLS and GPR information places the past into the context of the present by allowing the public to simultaneously view above-ground and below-ground aspects of the archaeological landscape. The 3D real-world context afforded by TLS greatly improves the confidence in GPR interpretations that claim to represent subsurface archaeological remains. The VGT approach is more powerful than simply mapping the historical surface and subsurface; it contributes significant new knowledge to the historical legacy of an important cultural landmark. This approach utilizes modern tools, ranging from laser scanners and ground-penetrating radar apparatus to visualization software such as AutoCad, to figuratively rather than literally dig up an otherwise inaccessible but fascinating past.

CHAPTER V

CONCLUSIONS

It might be predicted that, in the very near future, anthropological archaeologists

will view historical archaeology as one of many research strategies, like

ethnoarchaeology and experimental archaeology, in their arsenal of approaches

to attack the central problem of explaining cultural process. [Willey and Sabloff

1980:246]

We need to do as other professions and make the analysis of the effectiveness of

our methods, and the sources of variance within our data, a routine part of our

practice. [Jordan 2009:87]

The above quote from the 1980 Second Edition of *A History of American Archaeology*,

by Gordon R. Willey and Jeremy A. Sabloff, illustrates the unbridled optimism amongst

processualists that the past really is knowable in a scientifically true and objective sense,

but only if we had the right middle-range theory to get there. Underlying the opinion

that historical archaeology could become a viable middle-range theory, just like

ethnoarchaeology or experimental archaeology, was a simple principle borrowed from

geology, uniformitarianism, which presumes that the same laws and processes in

operation now were also in operation in the past. It was thought that because the dating

of historical archaeological data can be made with great accuracy it could be used to test

the theoretical assumptions and methods employed by all archaeologists in a verifiable historically controlled context so as to better understand and generalize about the underlying processes of culture change (Deetz 1977; South 1977; Willey and Sabloff 1980). As the above quote by Jordan (2009) illustrates, however, archaeological geophysicists have for too long neglected trends of information feedback via ground-truthing (Hargrave 2006; Jordan 2009), quantitative attribute analysis (Zhao et al. 2013, 2015), statistics (Kvamme 2006a, 2007; Ernenwein 20008, 2009), and experimentation (Isaacson et al. 1999; Hildebrand et al. 2002), which can be used to test the replicability of geophysical methods and create uniformitarian principles for archaeological prospection. Applying and incorporating statistical and quantitative methods into geophysical prospecting at historical archaeology sites in order to create testable hypotheses as to interpretations is the key to creating and refining a knowledge base with which *generalize* about physical processes in the near-surface, and then and only then to begin to examine cultural processes with archaeological geophysics data alone.

Archaeological geophysics, like much of archaeological science, remains in an awkward adolescence (Killick 2015). I would argue one of the main reason for this is analogous to the developmental trajectory of archaeological method and theory in general (Johnson 2010; O'Brien et al. 2005; Trigger 2006). Processual research oriented at asking question about cultural processes were largely impossible before the Culture History approach had firmly established chronological control principles via seriation classifications of artifacts. Similarly, until rigorous quantitative methods are incorporated into our practices to feedback into interpretation to aid our ability to

111

classify and generalize about subsurface physical responses, more abstract questions about cultural processes will remain out of reach.

In sum, three case studies are presented that aimed at increasing the accuracy and predictive capabilities of archaeological geophysics interpretations in three key ways: (1) with experimental tests and georectification models; (2) quantitative attribute analysis and PPA autocorrelation spatial statistics; and (3) via the reflexive use of ground-truthing to provide feedback to iteratively improve future interpretations.

Experimental Tests and Historic Models

In Chapter II an experimental test was conducted at the Tran controlled archaeological test site. It was determined that the Geonics EM-63 transient controlled source time-domain EMI instrument can be used to accurately detect and predict the location of subsurface metal artifacts. EMI data is also potentially a better method than magnetometry because it has a more compact spatial signature. The experimental test proved the viability of the method, which could prove to be a long-term cost efficient research strategy.

In Chapter IV historical maps were used to create 2D and 3D georectification models. These models were tested against physical GPR data in order to first test their accuracy and then to iteratively improve the models by re-referencing them based upon the GPR data. This can then be extrapolated to entire island for future testing without excavation, which keep in line with the focus on long term preservation archaeology.

Quantitative Attribute Analysis and Statistics

In Chapter IV I present the results of a quantitative attribute analysis of GPR data from Alcatraz Island, California. Using these advanced processing methods helped to more accurately locate and provided clues as to the extent and integrity of the earthwork fortification figures from an important period in the islands history. This research provides a strong basis for the public dissemination of significant archaeological research when presented with the 3D model and TLS data.

In Chapter's II and III PPA spatial autocorrelation statistics were used to distinguish between non-significant noise and significant anomalous patterns in EMI data sets because they quantified the odds of error and compacted the spatial signature of the EMI data. Using PPA spatial statistics to examine EMI data has applications to statistics, UXO remediation, geotechnical engineering, ore deposit exploration, and historic archaeological battlefield research – amongst others. These methods provide a site specific feedback mechanism to classify archaeological features based upon their quantitative geophysical signature. This classification can then be used to create generalized hypotheses (models) to test against similar phenomena at other archaeological sites, as with the middle range use of the Tran controlled experimental test site. This research is time and labor efficient and promotes the long term ethic of preservation archaeology.

Reflexive Ground-Truthing: Real and Virtual

In Chapter III I present the results of systematic archaeological excavations, real ground-truthing, at the Paint Rock sites in west-central Texas. These excavations revealed no evidence of a possible historic battle between the Texas Rangers and Comanche in 1842/6. The excavations indicates the U.S. military presence at Paint Rock dates to between approximately 1854 and 1875, which coincides well with the local forts that date from 1852-1875. The spatial extent and structure of the mid-nineteenth century military presence at Paint Rock indicates heavy use of the areas around the springs and the road near the fords on first terrace of the Concho River. My use of EMI and PPA spatial statistics accurately located and allowed for a classification of the archaeological data, which greatly increased the efficiency of the excavation strategy. The results of the excavation proved the efficacy of the method and can possibly contribute to reduced excavations in the future at other historic archaeological sites.

In Chapter IV I present data from a virtual ground-truthing of the military fortification beneath the recreation yard at Alcatraz Island, California. The quantitative attribute analysis of GRP data increased the information content of amplitude attributes of the data related to physical properties of the subsurface. When combined with TLS data the visualization, localization, and interpretation of subsurface archaeological features at Alcatraz Island was greatly improved. The use of georectification of historical maps to creating testable models as to the subsurface structure of historical

archaeological sites allowed for an iterative virtual ground-truth of the site without the need for excavation.

The results of the research presented herein are modest contributions; however, the long term goals of this approach are much greater than the sum of their parts. The research presented herein promote an archaeological geophysics research program aimed at advanced quantitative data analysis, visualization, experimentation, and reflexive use of excavation. The immediate goal is to increase the information content of geophysical data so as to increase the accuracy of archaeological interpretation. More accurate interpretations will allow for a generalized classification of anomalies based upon their physical signatures, which can be further refined by hypothesis testing and ground-truth excavations. Once the groundwork is lain, as with the culture history analogy, archaeological geophysics will be ready to tackle fundamental anthropological research questions about social organization, human behavior, and culture change through time. This research approach promotes the conservation ethic in archaeological geophysics, as remote sensing data can be used as standalone methods to study cultural phenomena, or as a complement to focused excavations, thereby decreasing the scale of archaeological excavations to preserve these nonrenewable resources for future generations by answering the most anthropological research questions with the least amount of costly and destructive excavation.

REFERENCES

Abidi, H.
    2007   Bonferroni and Sidak corrections for multiple comparisons. In *Encyclopedia of Measurement and Statistics*, edited by N.J. Salkind, pp. 103-107. Sage Publications, Inc., Thousand Oaks, California.

Abrams, J. J.
    2012   *Alcatraz*. Warner Bros. Television.

Affleck, D.
    1911   The Battle Lost to History, San Antonio Ex-Ranger fought Comanches with Jack Hays at Enchanted Rock. *San Antonio Express*, September 24, 1911.

Agapiou, Athos and Vasiliki Lysandrou
    2015   Remote sensing archaeology: Tracking and mapping evolution in European scientific literature from 1999 to 2015. *Journal of Archaeological Science: Reports* 4:192-200.

Aldstadt, J., D.M. Chen, and A. Getis
    2002   PPA: point pattern analysis (version 1.0a), www.nku.edu/~longa/cgibin/cgi-tcl-examples/generic/ppa/ppa.cgi, accessed 2011/2012.

Al-kheder, Sharaf, Yahya Al-shawabkh, and Norbert Haala
    2009   Developing a documentation system for desert palaces in Jordan using 3D laser scanning and digital photogrammetry. *Journal of Archaeological Science* 36:537-546.

Altunas, Cihan, Ferruh Yildiz, and Marco Scaioni
    2016   Laser scanning and data integration for three-dimensional digital recording of complex historical structures: The case of Mevlana museum. *International Journal of Geo-Information* 5(18).

Anderson, Gary Clayton
    2005   *The Conquest of Texas: Ethnic Cleansing in the Promised Land, 1820-1875*. University of Oklahoma Press, Norman.

Anselin, Luc
    1995   Local indicators of spatial association – LISA. *Geographic Analysis* 27: 93-115.

116

Ashmore, Tom
    2010   Archeological investigations: Paint Rock 1800s historic camp sites (41CC01), Concho County, Texas. *Occasional Papers of the Concho Valley Archeological Society*.

Barrow, J. D., and S. P. Bhavsar
    1987   Filaments-what the astronomer's eye tells the astronomer's brain. *Quarterly Journal of the Royal Astronomical Society* 28:109-128.

Bay, M.
    1996   *The Rock*. Hollywood Pictures.

Beard, L.P., W.E. Doll, T.J. Gamey, J.S. Holladay, J.L.C. Lee, N.W. Eklund, J.R. Sheehan, and J. Norton
    2008   Comparison of performance of airborne magnetic and transient electromagnetic systems for ordnance detection and mapping. *Journal of Environmental and Engineering Geophysics* 13: 291-305.

Beck, Robin A. Jr., Douglas J. Bolender, James A. Brown, and Timothy K. Earle
    2007   Eventful archaeology: The place of space in structural transformations. *Current Anthropology* 48:833-860.

Benavides, A. and M.E. Everett
    2005   Target signal enhancement in near-surface controlled-source electromagnetic data. *Geophysics* 70: G59-G67.

Benavides. A., M.E. Everett, and C. Pierce
    2009   Unexploded ordnance discrimination using time domain electromagnetic induction and self-organizing maps. *Stochastic Environmental Research Risk Assessment* 23:169-179.

Bevan B.W.
    2006   Geophysical exploration for buried buildings. *Historical Archaeology* 40:27-50.

Böniger, U. and J. Tronicke
    2010a   Improving the interpretability of 3D GPT data using target-specific attributes: application to tomb detection. *Journal of Archaeological Science* 37(2):360-367.

    2010b   Integrated data analysis at an archaeological site: A case study using 3D GPR, magnetic, and high-resolution topographic data. *Geophysics* 75 (4):B169-B176.

Bourdieu, P.

    1977   *Outline of a Theory of Practice*. Cambridge University Press, London.

    1984   *Distinction: A Social Critique of the Judgment of Taste*. Harvard University Press, Cambridge, Massachusetts.

Boatwright, Mary T. Daniel J. Gargola, and Richard J.A. Talbert

    2004   *The Romans From Village to Empire: A History of Ancient Rome from the Earliest Times to Constantine*. Oxford University Press, New York.

Brown, John Henry

    1983   *History of Texas from 1685-1892, Volume 1 and 2*. L.E. Daniell, St. Louis.

Butler, D.K.

    2004   Report on a workshop on electromagnetic induction methods for UXO detection and discrimination. *The Leading Edge* 23:776-770.

Calloway, Colin G.

    2003   *One Vast Winter Count: The Native American West Before Lewis and Clark*. University of Nebraska Press, Lincoln.

Campbell, B. J.

    1964   *Escape from Alcatraz: A farewell to the rock*. Hammond.

Campbell, Randolph B.

    1989   *An Empire for Slavery: The Peculiar Institution in Texas, 1821-1865*. Louisiana State University Press, Baton Rouge.

    1993   *Sam Houston and the American Southwest*. Harper Collins, New York.

    2003   *Gone To Texas: A History of the Lone Star State*. Oxford University Press, New York.

Castellazzi, Giovanni, Antonio Maria D'Altri, Gabriele Bitelli, Ilenia Selvaggi, and Alessandro Lambertini

    2015   From laser scanning to finite element analysis of complex building by using a semi-automated procedure. *Sensors* 15:18360-18380.

Ciminale, Marcello, Danilo Gallo, Rosa La Saponara, and Nicola Masini

    2009   A multiscale approach for reconstructing archaeological landscapes: Applications in Northern Apulia (Italy). *Archaeological Prospection* 16: 143-153.

Clifton, R.P.

    1970   *Barbs, Prongs, Points, Prickers, and Stickers: A Complete and Illustrated Catalog of Antique Barbed Wire*. University of Oklahoma Press, Norman.

CLR

    2010   *Alcatraz Island National Historic Landmark: Cultural Landscape Report*. Mundus Bishop.

Connor, M., and D.D. Scott

    1998   Metal detector use in archaeology: An introduction. *Historical Archaeology* 32:76-85.

Constanzo, Antonio, Mario Minasi, Giuseppe Casula, Massimo Musacchio, and Maria Fabrizio Buongiorno

    2015   Combined use of terrestrial laser scanning and IR thermography applied to a historical building. *Sensors* 15(1):194-213.

Conyers, Lawrence B.

    2012   *Interpreting Ground-Penetrating Radar for Archaeology*. Left Coast Press, Walnut Creek, California.

    2013   *Ground-Penetrating Radar for Archaeology*, Third Edition (Geophysical Methods for Archaeology). AltaMira, Latham, Maryland.

    2015   Analysis and interpretation of GPR datasets for integrated archaeological mapping. *Near Surface Geophysics* 13:645-651.

    2016   *Ground-Penetrating Radar for Geoarchaeology* (New Analytical Methods in Earth and Environmental Science). Wiley-Blackwell.

Conyers, L.B., and J. Leckebusch

    2010   Geophysical archaeology research agendas for the future: some ground-penetrating radar examples. *Archaeological Prospection* 17: 117-123.

Creasman, P. P., Sassen, D., Koepnick, S., Doyle, N.

    2010   Ground-penetrating radar survey at the pyramid complex of Senwosret III At Dahshur, Egypt, 2008: search for the lost boat of a Pharaoh. *Journal of Archaeological Science* 37 (3):516-524.

Cressie, N. A. C.

    1993   *Statistics for Spatial Data*. Wiley-Interscience.

Cruse, J. Brett
     2008   *Battles of the Red River War: Archaeological Perspectives on the Indian Campaign of 1874*. Texas A&M University Press, College Station, Texas.

Cutrer, Thomas W.
     1993   *Ben McCulloch and the Frontier Military Tradition*. North Carolina University Press, Chapel Hill.

Deetz, J. F.
     1977   *In Small Things Forgotten: The Archaeology of Early American Life*. Anchor, New York.

DeLay, Brian
     2008   *War of a Thousand Deserts: Indian Raids and the U.S.-Mexican War*. Yale University Press, New Haven.

Diggle, P.J.
     2003   *Statistical Analysis of Spatial Point Patterns, 2nd Edition*. Hodder Arnold.

Doelle, William and Deborah Huntley
     2012   Teaching, research, and so much more through a preservation field school. *The SAA Archaeological Record* 36-38.

Domingo, Inés, Valentín Villaverde, Esther López-Montalvo, José Luis Lerma, and Miriam Cabrelles
     2013 Latest developments in rock art recording: towards an integral documentation of Levantine rock art sites combining 2D and 3D recording techniques: *Journal of Archaeological Science* 40(4):1879-1889.

Doll, W.E., J.R. Sheehan, T.J. Gamey, L.P. Beard, and J. Norton
     2008   Results of an airborne vertical magnetic gradient demonstration, New Mexico. *Journal of Environmental and Engineering Geophysics* 13:277-290.

Drennan, R.J.
     2010   *Statistics for Archaeologists: A Common Sense Approach, Second Edition*. Springer, New York.

Ernenwein, Eileen G.
>   2008   A geophysical view of Pueblo Escondito: Implications for the Pithouse to
>   Pueblo transition in the Jornada Mogollon. *Bulletin of the Texas
>   Archaeological Society* 79:125-145.

>   2009   Integration of multidimensional archaeogeophysical data using
>   supervised and unsupervised classification. *Near Surface Geophysics*
>   7:147-158.

Everett, Mark E.
>   2005   What do electromagnetic induction responses measure? *The
>   Leading Edge* 24:154-157.

>   2013   *Near-Surface Applied Geophysics*. Cambridge University Press,
>   Cambridge.

El-Hakim, S., L. Gonzo, F. Voltolini, S. Girardi, A. Rizzi, F. Remondino, and E.
Whiting
>   2007   Detailed 3D modelling of castles. *International Journal of Architectural
>   Computing* 02(05):221-236.

Entwistle, J.A., K.J.W. MCCaffrey, and P.W. Abrahams
>   2009   Three-dimensional (3D) visualization: the application of terrestrial laser
>   scanning in the investigation of historic Scottish farming townships.
>   *Journal of Archaeological Science* 36:860-866.

Ezzo, J.A.
>   1994   Zinc as a paleodietary indicator: an issue of theoretical validity in bone-
>   chemistry analysis. *American Antiquity* 59:606-621.

Field, R.
>   2011   *Forts of the American Frontier, 1776-1891: California, Oregon,
>   Washington, and Alaska*. Osprey Publishing.

Flannery, Kent V.
>   1982   The golden Marshalltown trowel: A parable for the archaeology of the
>   1980s. *American Anthropologist* 84(2):265-278.

Floyd, D. E.
>   2010   Coastal Defenses. In *A companion to American military History*, edited
>   by J.C. Bradford, pp. 662-680. Blackwell Publishing.

Frankenheimer, J.
    1962   *Birdman of Alcatraz*. United Artists.

Freeman, Douglas Southall
    1934   *R. E. Lee: A Biography, Volume I*. Charles Scribner's Sons, New York.

Gaffney C.
    2008   Detecting trends in the prediction of the buried past: a review of geophysical techniques in archaeology. *Archaeometry* 50(2):313-336.

Geonics Ltd.
    2002   *EM-63 full time domain electromagnetic UXO detector: Operating instructions*. Geonics Ltd., Missassauga, Canada.

Getis, A.
    1984 Interaction modeling using second-order analysis. *Environment and Planning A* 16:173-183.

Getis, A., and J.K. Ord
    1992   The analysis of spatial association by use of distance statistics. *Geographic Analysis* 24:189-206.

    1996   Local spatial statistics: an overview. In *Spatial Analysis: Modeling in a GIS Environment*, edited by P. Longley and M. Batty, 261-277. John Wiley & Sons, New York.

Giddens, Anthony
    1984   *The Constitution of Society: Outline of the Theory of Structuration*. University of California Press, Berkley.

Godden, Geoffrey A.
    1964   *Encyclopedia of British Pottery and Porcelain Marks*. Bonanza Books, New York.

Goodman, Dean and Salvatore Piro
    2013   *GPR Remote Sensing in Archaeology*. Springer, Heidelberg.

Hakonen, Aki, Jari-Matti Kuusela, Jari Okkonen
    2015   Assessing the application of laser scanning and 3D inspection in the study of prehistoric cairn sites: The case study of Tahkokangas, Northern Finland. *Journal of Archaeological Science: Reports* 2: 227–234

Hämäläinen, Pekka
       2008   *The Comanche Empire*. Yale University Press, New Haven.

Hanson, James
       1972   Upper Missouri arrow points. *Museum of the Fur Trade Quarterly* 8:2-8.

Hargrave, M. L.
       2006   Ground truthing the results of geophysical surveys. In *Remote sensing in archaeology: An explicitly North American perspective,* edited by J.K. Johnson, pp. 269-304. The University of Alabama Press, Tuscaloosa.

Hildebrand, J.A., S.M. Wiggins, P.C. Henkart, and L.B. Conyers
       2002   Comparison of seismic reflection and ground-penetrating radar imaging at the controlled archaeological test site, Champaign, Illinois. *Archaeological Prospection* 9(1):9-21.

Hill, Matthew G., David J. Rapson, Thomas J. Loebel, and Davis W. May
       2011   Site structure and activity organization at a Late Paleoindian base camp in western Nebraska. *American Antiquity* 76:752-772.

Isaacon, J., R.E. Hollinger, D. Grundrum, and J. Baird
       1999   A controlled archaeological test site facility in Illinois: training and research in archaeogeophysics. *Journal of Field Archaeology* 26:227-236.

Jacob, R.W. and T.M. Urban
       2015   Ground-penetrating radar velocity determination and precision estimates using common-midpoint (CMP) collection with hand-picking, semblance analysis and cross-correlation analysis: A case study and tutorial for archaeologists. *Archaeometry* DOI: 10.1111/arcm.12214.

Jaklič, Aleš, Miran Erič, Igor Mihajlović, Žiga Stopinšek, and Franc Solina
       2015   Volumetric models from 3D point clouds: The case study of sarcophagi cargo from a 2nd/3rd century AD Roman shipwreck near Sutivan on island Brač, Croatia. *Journal of Archaeological Science* 62:143-152.

Johnson, David M.
       2007   Apache Victory against the U.S. Dragoons, the Battle of Cieneguilla, New Mexico. In *Fields of Conflict: Battlefield Archaeology from the Roman Empire to the Korean War, Volume 2*, edited by Douglas Scott, Lawrence Babits, and Charles Haecker, pp. 235-254. Preager Security International, Westport, Connecticut.

Johnson, Jay K.

    2006   *Remote Sensing in Archaeology: An Explicitly North American Perspective*. The University of Alabama Press, Tuscaloosa.

Johnson, Matthew

    2010   *Archaeological Theory: An Introduction*. Second Edition. Blackwell, Oxford.

Johnson, Jay K. and Bryan S. Haley

    2006   A cost-benefit analysis of remote sensing application in cultural resource management archaeology. In *Remote Sensing in Archaeology: An Explicitly North American Perspective*, edited Jay K. Johnson, pp. 33-45. The University of Alabama Press, Tuscaloosa.

Jol, H.M.

    2009   *Ground Penetrating Radar: Theory and Applications*. Elsevier Science.

Jordan, David

    2009   How effective is a geophysical survey? A regional review. *Archaeological Prospection* 16(2):77-90.

Kaufmann, J. E., and H. W. Kaufmann

    2005   *Fortress America: The forts that defended America, 1600 to the Present*. Da Capo Press.

Khwanmuang, Wisarat and Suwimon Udphuay

    2012   Ground-penetrating radar attribute analysis for visualization of subsurface archaeological structures. *The Leading Edge* 31: 946-949.

Killick, David

    2015   The awkward adolescence of archaeological science. *Journal of Archaeological Science* 56:242-247.

Kirkland, Forest, and W. W. Newcomb Jr.

    1967   *The Rock Art of Texas Indians*. University of Texas Press, Austin.

Kluckhohn, Clyde, W.W. Hill, and Lucy W. Kluckhohn

    1971   *Navaho Material Culture*. The Belknap Press, Harvard University, Cambridge, Massachusetts.

Konstam, A.

    2003   *American Civil War Fortifications (1): Costal brick and stone forts*. Osprey Publishing.

Krige, D.G.

 1951 A statistical approach to some basic mine valuation problems on the Witwatersrand. *Journal of the Chemical, Metallurgical, and Mining Society of South Africa* 52:119-139.

Kvamme, Kenneth L.

 1990 Spatial autocorrelation and the Classic Maya collapse revisited. *Journal of Archaeological Science* 17:197-207.

 2006a Integrating multidimensional geophysics data. *Archaeological Prospection* 13:57-72.

 2006b Magnetometry: Nature's gift to archaeology. In *Remote Sensing in Archaeology: An Explicitly North American Perspective*, ed. J.K. Johnson, pp. 205-234. University of Alabama Press, Tuscaloosa.

 2007 Integrating Multiple Geophysical Datasets. In *Remote Sensing in Archaeology* (Interdisciplinary Contributions to Archaeology), Eds. J. Wiseman and F. El-Baz, pp. 345-374. Springer.

Leckebusch J.

 2003 Ground-penetrating radar: A modern three-dimensional prospection method. *Archaeological Prospection* 10: 213–240.

Lévi-Strauss, Claude

 1983 *The Raw and the Cooked (Mythologiques)*. Translated by John Weightman and Doreen Weightman. The University of Chicago Press, Chicago.

Lee,Wen-Hsiung, Paul D. Gader, and Joseph N. Wilson

 2007 Optimizing the area under a receiver operator characterization curve with application to landmine detection. *IEEE Transaction of Geoscience and remote Sensing* 45:389-397.

Linford, Neil

 2006 The application of geophysical methods to archaeological prospection. *Reports of Progress in Physics* 69:2205-2257.

Loo, T. and C. Strange

 2000 Rock prison of liberation: Alcatraz island and the American Imagination. *Radical History Review* 78:27-56.
  .

Lubowiecka, I., J. Armesto, P. Arias, and H. Lorenzo
    2009   Historic bridge modelling using laser scanning, ground penetrating radar
            and finite element methods in the context of structural dynamics:
            Engineering Structures 31:2667-2676.

Lubowiecka, I., P. Arias, B. Riveiro, M. Solla
    2011   Multidisciplinary approach to the assessment of historical structures
            based on the case of a masonry bridge in Galicia (Spain): *Computers and
            Structures* 89:1615-1627.

MacDonald, J.A., and M.J. Small
    2009   Statistical analysis of metallic anomaly patterns at former air force
            bombing ranges. *Stochastic Environmental Research Risk Assessment*
            23:203-214.

Martini, J. A.
    2004   *Fortress Alcatraz: Guardian of the Golden Gate*. Ten Speed Press.

Matheron, G.
    1963   Principles of geostastistics. *Economic Geology* 58:1246-1266.

Ord, J.K., and A. Getis
    1995   Local spatial autocorrelation statistics: distribution issues and an
            application. *Geographic Analysis* 27:286-306.

McCarthy, Cormac
    2010[1985]   *Blood Meridian: Or the Evening Redness in the West*. Modern
            Library, New York.

Miller, Myles R.
    2011   Estimating site structure and site occupation span using point pattern
            spatial analysis: Interpretations of surface artifact distributions at the El
            Arenal Site, El Paso County, Texas. *Bulletin of the Texas Archaeological
            Society* 82:193-222.

Neubauer, W., C. Gugl, M. Scholz, G. Verhoeven, I. Trinks, K. Löcker, M. Doneus, T.
Saey, and M. Van Meirvenne
    2014   The discovery of the school of gladiators at Carnuntum, Austria.
            Antiquity 88:173-190.

Núñez, M. Amparo, Felipe Buill, and Manel Edo
    2013   3D Model of the Sadurní cave. *Journal of Archaeological Science*
            40(12):4420-4428.

O'Brien, Michael, R. Lee Lyman, and Michael Brian Schiffer
    2005   *Archaeology as a Process: Processualism and Its Progeny*. The
            University of Utah Press, Salt Lake.

Ord, J.K., and A. Getis
    1995   Local spatial autocorrelation statistics: distribution issues and an
            application. *Geographic Analysis* 27:286-306.

Ostrouchov, G., W. E. Doll, D. A. Wolf, L. P. Beard, M. D. Morr, and D. K. Butler
    2003   *Spatial Statistical Models and Optimal Survey Design for Rapid
            Geophysical Characterization of UXO Sites*,
            http://www.dtic.mil/cgibin/GetTRDoc?AD=ADA481018, accessed 29
            May 2012.

Paasche, H., and D. Eberle
    2009   Rapid integration of large airborne geophysical data suites using a fuzzy
            partitioning cluster algorithm: A tool for geological mapping and mineral
            exploration. *Exploration Geophysics* 40:277–287.

    2011   Automated compilation of pseudolithology maps from geophysical data
            sets: A comparison of Gustafson-Kessel and fuzzy c-means cluster
            algorithms. *Exploration Geophysics* 42:275–285.

Pate, Ann
    2010   *Fort Chadbourne: A Military Post, A Family Heritage*. H.V. Chapman
            and Sons, Abilene.

Pavlidis, G., D. Tsiafakis, V. Tsioukas, A. Koutsoudis, F. Arnaoutoglou, and C.
Chamzas
    2007   Preservation of architectural heritage through 3D digitization:
            International Journal of Architectural Computing 02(05):221-236.

Pérez-Grarcia, V., J.O. Caselles, J. Clapés, G. Martinez, and R. Osorio
    2013   Non-destructive analysis in cultural heritage building: Evaluating the
            Mallorca cathedral supporting structures: *NDT & E International*
            59(3):40-47.

Perry, J. N., A. M. Liebhold, M. S. Rosenberg, J. Dungan, M. Miriti, A. Jakomulska, and
S. Citron-Pousty
    2002   Illustrations and guidelines for selecting statistical methods for
            quantifying spatial patterns in ecological data. *Ecography* 25:578–600.

Perttula, T.K., C.P. Walker, and T. C. Schultz
    2008 A Revolution in Caddo archaeology: the remote sensing and archaeological view from the Hill Farm site (41BW169) in Bowie County, Texas. *Southeastern Archaeology* 27:93-107.

Pétronille, M., J. Thiesson, F.X. Simon, and O. Buchsenschutz
    2010 Magnetic signal prospecting using multiparameter measurements: the case study of the Gallic site of Levroux. *Archaeological Prospection* 17:141-150.

Pincus, Jessie, Timothy S. de Smet, Yotam Tepper, and Matthew Adams
    2013 Ground penetrating radar and electromagnetic investigations at Legio, Israel. *Archaeological Prospection* 20:175-188.

Plisson, Hughes and Lydia V. Zotkina
    2015 From 2D to 3D at macro-and-microscopic scale in rock studies. *Digital Applications in Archaeology and Cultural Heritage* 2(2-3):102-119.

Premo, L.S.
    2004 Local spatial autocorrelation statistics quantify multi-scale patterns in distributional data: An example from the Maya lowlands. *Journal of Archaeological Science* 31:855-866.

Ramos, Raúl A.
    2008 *Beyond the Alamo: Forging Mexican Ethnicity in San Antonio, 1821-1861*. University of North Carolina Press, Chapel Hill.

Reynolds, John M.
    2011 *An Introduction to Applied and Environmental Geophysics*, Second Edition John Wiley & Sons, Oxford.

Ripley, B.D.
    1976 The second-order analysis of stationary point processes. *Journal of Applied Probability* 13:255–266.

    1977 Modelling spatial patterns. *Journal of the Royal Statistical Society* 2:172–212.

    1981 *Spatial Statistics*. John Wiley and Sons, New York.

Rister, Carl Coke
    1946 *Robert E. Lee in Texas*. University of Oklahoma Press, Norman.

Rogers, M. B.

    2014   Visualizing an integrated landscape using archaeogeophysical and 3D laser surveying. In S. D. Stull ed., *From West to East: Current Approaches in Medieval Archaeology*, pp. 6-19. Cambridge Scholars Publishing, Cambridge.

Saarenketo, Timo

    2009   NDT Transportation. In *Ground Penetrating Radar Theory and Applications*, edited by Harry M. Jol, pp. 395-444. Elsevier.

Schiffer, Michael B.

    1987   *Formation Processes of the Archaeological Record*. University of New Mexico Press, Albuquerque.

Schwarz, K.R. and J. Mount

    2006   Integrating spatial statistics into archaeological data modeling. In *GIS and Archaeological Site Location Modeling*, edited by M. Mehrer and K. Westcott, 167-189. CRC Press, Boca Raton, Florida.

Sewell, William H., Jr.

    1992   A Theory of Structure: Duality, Agency, and Transformation. *American Journal of Sociology* 98(1):1-29.

    2005   *The Logics of History: Social Theory and Social Transformation*. University of Chicago Press, Chicago.

Shennan, Stephen

    1997   *Quantifying Archaeology*. University of Iowa Press, Iowa City.

Šidàk, Z.

    1967   Rectangular confidence region for the means of multivariate normal distributions. *Journal of the American Statistical Association* 62:626–633.

Siegel, D.

    1979   *Escape from Alcatraz*. Paramount Pictures.

Simpson, D., M. van Meirvenne, T. Saey, H. van Meersch, J. Bourgeois, A. Le Houck, L. Cockx and U.W.A. Vitharana

    2009   Evaluating the multiple coil configurations of the EM38DD and DUALEM- 21S sensors to detect archaeological anomalies. *Archaeological Prospection* 16:91–102.

Smith, Thomas T.
        1999   *The U.S. Army and the Texas Frontier Economy, 1845-1900.* Texas A&M
                University Press, College Station.

South, Stanley
        1977   *Method and Theory in Historical Archaeology*. Academic Press, New
                York.

Stolt, R.H.
        1978   Migration by Fourier transform. *Geophysics* 43(1):23-48.

Strange, C. and T. Loo
        2001   Holding the rock: The "Indianization" of Alcatraz island, 1969-1999. *The
                Public Historian* 23(1):55-74.

Tapete, Deodato, Nicola Casagli, Guido Luzi, Riccardo Fanti, Giovanni Gigli, and
Davide Leva,
        2013   Integrating radar and laser-based remote sensing techniques for
                monitoring structural deformation of archaeological monuments. *Journal
                of Archaeological Science* 40(1):176-189.

Thiesson, Julien, Michel Dabas, and Sébastian Flageul
        2009   Detection of resistive features using towed slingram electromagnetic
                induction instruments. *Archaeological Prospection* 16:103-109.

Thompson, E.
        1979   *The Rock: A History of Alcatraz island, 1847-1972 (Historic
                Resource Study)*. National Parks Service.

Thompson, Jason Randal
        2015   *Anthropological Research Framing for Archaeological Geophysics:
                Material Signatures of Past Human Behavior*. Rowman & Littlefield,
                Lanham, Maryland.

Thompson, Marc
        1980   A survey of aboriginal metal points from the Apacheria. *The Artifact*
                18:1-10.

Trigger, Bruce
        2006   *A History of Archaeological Thought*, Second Edition. Cambridge
                University Press, Cambridge.

Turpin, Solveig, Larry Riemenschneider, and David G. Robinson
    2002   Archeological investigations, Paint Rock, Concho County, Texas. *Current Archeology in Texas* 4:8-19.

Udphuay, Suwimon, Vivian L. Paul, Mark E. Everett, and Robert B. Warden
    2010   Ground penetrating radar imaging of Twelfth Century Romanesque foundations beneath the Thirteenth Century Gothic Abbey Church of Valmagne, France: *Archaeological Prospection* 17:199-212.

Urban, T. M., Rowan, Y. M., Kersel, M. M.
    2014   Ground-penetrating radar investigations at Marj Rabba, a Chalcolithic site in the lower Galilee of Israel. *Journal of Archaeological Science* 46:96-106.

Verdonck, Lieven, Devi Taelman, Frank Vermeulen, and Roald Docter
    2015   The impact of spatial sampling and migration on the interpretation of complex archaeological ground-penetrating radar data. *Archaeological Prospection* 22:91-103.

Wallace, Ernest, and E. Adamson Hoebel
    1986[1952] *The Comanches: Lords of the South Plains*. University of Oklahoma Press, Norman.

Ward, D. and G. Kassebaum
    2009   *Alcatraz: The gangster years*. University of California Press, Berkeley.

Watters, M. S., and S. Wilkes
    2014   Integrating 3D surface and sub-surface data for heritage preservation and planning. *LiDAR Magazine* **3**(4).

Wellman, G. L.
    2008   *A History of Alcatraz Island 1853-2008, Images of America*. Arcadia Publishing, Charleston, SC.

West, Elliott
    1995   *The Way to the West: Essays on the Central Plains*. University of New Mexico Press, Albuquerque.

Whitley, D.S., and W.A.V. Clark
    1985   Spatial autocorrelation tests and the Classic Maya collapse: methods and inferences. *Journal of Archaeological Science* 12:377-395.

Wilbarger, John Wesly
    1889   *Indian Depredations in Texas*. Hutchings Printing House, Austin.

Willey, Gordon R. and Jeremy A. Sabloff
      1980   *A History of American Archaeology*, Second Edition. London, Thames & Hudson, London.

Wooster, Ralph A.
      1995   *Texas and Texans in the Civil War*. Eakin Press, Austin.

Yang, Hao, Xiangyang Xu, and Ingo Neumann
      2014   The benefits of 3D laser scanning technology in the generation and calibration of FEM models for health assessment of concrete structures. *Sensors* 14:21889-21904.

Yarovoy, Alenxander
      2009   Landmine and Unexploded Ordnance Detection and Classification with Ground Penetrating Radar. In *Ground Penetrating Radar Theory and Applications*, edited by Harry M. Jol, pp. 445-478. Elsevier.

Yilmaz, O.
      2001   *Seismic Data Analysis: Processing, Inversion, and Interpretation of Seismic Data*. SEG Investigations in Geophysics No. 10, Tulsa, Oklahoma.

Zhao, Wen-Ke, Tian Gang, Wang Bang-Bang, Shi Zhan-Jie, and Lin Jin-Xin
      2012   Application of 3D GPR attribute technology in archaeological investigations. *Applied Geophysics* 9(3):261-269.

Zhao, W., Forte, E., Pipan, M., Tian, G.
      2013a Ground penetrating radar (GPR) attribute analysis for archaeological prospection. *Journal of Applied Geophysics* 97: 107-117.

Zhao, W., Tian, G., Wang, B., Forte, E., Pipan, M., Lin, J., Shi, Z., Li, X.
      2013b 2D and 3D imaging of a buried prehistoric canoe using GPR attributes: a case study. *Near Surface Geophysics* 11 (4): 457-464.

Zhao, W., Forte, E., Levi, S. T., Pipan, M., Tian, G.
      2015a Improved high-resolution GPR imaging and characterization of prehistoric archaeological features by means of attribute analysis. *Journal of Archaeological Science* 54: 77-85.

Zhao, Wenke, Gang Tian, Emanuele Forte, Michele Pipan, Yimin Wang, Xuejing Li, Zhanjie Shi, and Haiyan Liu
      2015b Advances in GPR data acquisition and analysis for archaeology. *Geophysics Journal International* 202:62-71.